NUCLEAR INSTRUMENTS & METHODS

A JOURNAL ON ACCELERATORS, INSTRUMENTATION
AND TECHNIQUES IN NUCLEAR PHYSICS

EDITOR: K. SIEGBAHN - UPPSALA

VOLUME 6

DECEMBER 1959 — MARCH 1960

NORTH-HOLLAND PUBLISHING COMPANY — AMSTERDAM

PRINTED IN THE NETHERLANDS
DRUKKERIJ MEIJER N.V. — WORMERVEER AND AMSTERDAM

64-06908

NUCLEAR INSTRUMENTS AND METHODS

Per.
QC
786
N883
v.6-7

EDITORIAL BOARD:

J. B. ADAMS (CERN)
F. A. ALSINA (Buenos Aires)
E. AMALDI (Rome)
H. L. ANDERSON (Chicago)
K. T. BAINBRIDGE (Cambridge, Mass.)
C. J. BAKKER (CERN)
P. R. BELL (Oak Ridge)
R. E. BELL (Montreal)
A. BERTHELOT (Saclay)
H. BRINKMAN (Groningen)
E. H. COOKE–YARBOROUGH (Harwell)
S. DE BENEDETTI (Pittsburgh)
M. DE HEMPTINNE (Louvain)
A. DE-SHALIT (Rehovoth)
M. DEUTSCH (Cambridge, Mass.)
S. DU TOIT (Pretoria)
B. S. DŽELEPOV (Leningrad)
W. GENTNER (CERN)
P. C. GUGELOT (Amsterdam)
H. HALBAN (Paris)
O. HAXEL (Heidelberg)
P. HUBER (Basel)
D. J. HUGHES (Brookhaven)
S. KIKUCHI (Tokyo)
J. KOCH (Copenhagen)
M. S. KOZODAEV (Moscow)
S. LIVINGSTON (Cambridge, Mass.)
E. M. MCMILLAN (Berkeley)
M. G. MEŠČERJAKOV (Moscow)
P. B. MOON (Birmingham)
M. L. OLIPHANT (Canberra)
W. PAUL (Bonn)
A. S. RAO (Bombay)
G. SALVINI (Rome)
P. SAVIĆ (Belgrade)
P. SCHERRER (Zürich)
CH. SCHMELZER (CERN)
H. W. B. SKINNER (Liverpool)
R. TANGEN (Oslo)
D. TAYLOR (Northampton)
V. I. VEKSLER (Moscow)
O. WERNHOLM (Stockholm)
G. VON DARDEL (CERN)
R. R. WILSON (Cornell)
S. D. WINTER (Saclay)

DECEMBER 1959 VOLUME 6 (1959) No. 1

GREGG M. SINCLAIR LIBRARY
UNIVERSITY OF HAWAII
8-7-63

NUCLEAR INSTRUMENTS & METHODS

A JOURNAL ON ACCELERATORS, INSTRUMENTATION AND TECHNIQUES IN NUCLEAR PHYSICS

EDITOR: K. SIEGBAHN - UPPSALA

CONTENTS

R. S. LIVINGSTON and F. T. HOWARD, The Oak Ridge relativistic isochronous cyclotron . . . 1
D. A. TRAGESER, Engineering methods for electron-beam processing 26
PAUL V. C. HOUGH, Performance of a nuclear emulsion scanner 33
E. KOLTAY, Elektronenoptische Konstruktion von inhomogenen Beschleunigungsröhren . . 45
S. ABID HUSAIN and A. A. JAFFE, The proportional counter as a charged particle spectrometer 50
C. H. VINCENT and W. G. KING, A pulse to direct current voltage comparator 57
H. MORINAGA and T. KUROYANAGI, Internal target for a betatron 66
JAGADISH B. GARG, A fast neutron time-of-flight spectrometer 72
P. DELATTRE, Deux piles atomiques considérées comme instruments de physique 83
R. F. STETSON and S. BERKO, A directional scintillation counter for neutrons 94
HOWARD L. ANDREWS, Accelerators in biology and medicine 96
EDWARD, J. BURGE, Statistical errors in particle polarization measurements (Letter to the Editor) 101
Book Reviews 103
Erratum 104

NORTH-HOLLAND PUBLISHING COMPANY - AMSTERDAM

NUCLEAR INSTRUMENTS AND METHODS

A journal on accelerators, instrumentation and techniques in nuclear physics

EDITOR: K. SIEGBAHN, UPPSALA

EDITORIAL BOARD:

J. B. ADAMS (CERN)
F. A. ALSINA (Buenos Aires)
E. AMALDI (Rome)
H. L. ANDERSON (Chicago)
K. T. BAINBRIDGE (Cambridge, Mass.)
C. J. BAKKER (CERN)
P. R. BELL (Oak Ridge)
R. E. BELL (Montreal)
A. BERTHELOT (Saclay)
H. BRINKMAN (Groningen)
E. H. COOKE–YARBOROUGH (Harwell)
S. DE BENEDETTI (Pittsburgh)
M. DE HEMPTINNE (Louvain)
A. DE-SHALIT (Rehovoth)
M. DEUTSCH (Cambridge, Mass.)
S. DU TOIT (Pretoria)
B. S. DŽELEPOV (Leningrad)
W. GENTNER (Heidelberg)
P. C. GUGELOT (Amsterdam)
H. HALBAN (Paris)
O. HAXEL (Heidelberg)
P. HUBER (Basel)
D. J. HUGHES (Brookhaven)
S. KIKUCHI (Tokyo)
J. KOCH (Copenhagen)
M. S. KOZODAEV (Moscow)
S. LIVINGSTON (Cambridge, Mass.)
E. M. MCMILLAN (Berkeley)
M. G. MEŠČERJAKOV (Moscow)
P. B. MOON (Birmingham)
M. L. OLIPHANT (Canberra)
W. PAUL (Bonn)
A. S. RAO (Bombay)
G. SALVANI (Rome)
P. SAVIČ (Belgrade)
P. SCHERRER (Zürich)
CH. SCHMELZER (CERN)
H. W. B. SKINNER (Liverpool)
R. TANGEN (Oslo)
D. TAYLOR (Northampton)
V. I. VEKSLER (Moscow)
O. WERNHOLM (Stockholm)
G. VON DARDEL (CERN)
R. R. WILSON (Cornell)
S. D. WINTER (Saclay)

INSTRUCTIONS FOR CONTRIBUTORS

Contributions may be sent to the Editor, Professor K. Siegbahn, Institute of Physics, University of Uppsala, Sweden, either directly or through the intermediation of one of the members of the Editorial Board. Contributions may be written in English, French or German but should always, except for very short papers, be supplied with a brief abstract in English. Figures should be in inked original drawings or glossy prints and they should be sufficiently large. Contributors should make sure that important details in drawings and photographs will show up clearly in the diminished copy used by the publisher.

Books for review should be sent to Professor Siegbahn.

Objective and descriptive material on endeavours and product developments from the industry for the section "Spotlight on Industry" should be sent directly to the publishers, North-Holland Publishing Company, P.O. Box 103, Amsterdam.

Nuclear Instruments and Methods is published monthly. The subscription price of a volume of 360 pages is $ 17.00 (130 s), postage free.

Subscription should be sent to the publishers, North-Holland Publishing Company. P.O. Box 103. Amsterdam or to any subscription-agent.

No part of this issue may be reproduced in any form, by print, photoprint, microfilm or any other means without written permission from the publisher. Reprints, photoprints or microfilms are obtainable at cost from the publisher.

PHILIPS

equipment for Nuclear Physics and Atomic Energy

Transistorized
Pocket Radiation Monitor
type PW 4014

- Civil defence instruments.
- Linear electron accelerators.
- Generators for very high d.c. voltages.
- Synchro-cyclotrons for various final energies.
- Cockcroft-Walton accelerators.
- Radiation measuring and detection equipment.
- Area monitoring instrumentation.
- Reactor control instrumentation.
- Geiger counter tubes.
- Radio-active isotopes.
- Air liquefiers.

Outstanding features such as:
- Lowest measuring range: 0-3 mr/h (Ra- γ)
- Provision for connecting separate G.M. Probes and earphone
- Low power consumption
- Printed wiring
- Tropic and waterproof construction

make this new all-transistorized pocket radiation monitor-incorporating the rugged Philips Geiger Müller counter tube type 18503 - the ideal instrument for measuring and locating radioactivity.

PHILIPS

Nuclear Equipment

For further information please apply to one of the following addresses:

N.V. PHILIPS' GLOEILAMPENFABRIEKEN, Scientific Equipment Department, Eindhoven-Holland
PHILIPS ELECTRICAL LTD., Research and Control Instruments Division, Shaftesbury Avenue, London W.C. 2
PHILIPS ELECTRONICS INC., Instruments Division, 750. South Fulton Avenue, Mount Vernon N.Y. U.S.A.

COMPACT 100 CHANNEL PULSE HEIGHT ANALYZER

The C.D.C. KICKSORTER

developed by Atomic Energy of Canada and manufactured by Computing Devices of Canada Limited

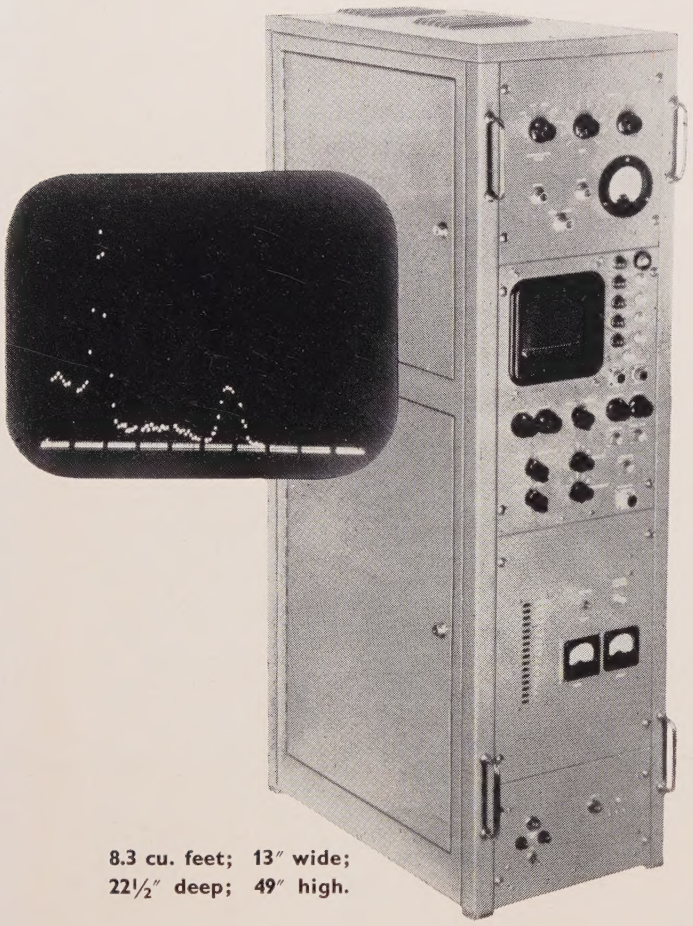

8.3 cu. feet; 13″ wide; 22½″ deep; 49″ high.

88% Transistorized

- Printed Circuitry
- Low Maintenance—High Reliability
- Compact—Semiportable
- Low Power Consumption—120 watts
- No Ventilation or Cooling problems

Highly Versatile

- Oscilloscope display
- Binary manual count readout allows the count on any channel to be displayed in digital form
- Accessory readout devices: photo recording camera, strip chart recorder, punch tape
- Magnetic core memory—65,535 counts can be stored per channel
- Permanent count storage—sixteen magnetic cores for each of the 100 channels

Bendix International

The "Chalk River Kicksorter", recently developed and based on designs and specifications prepared by Atomic Energy of Canada Ltd. is an extremely fast, accurate and versatile instrument.

The "Kicksorter" is designed to span random pulses of various amplitudes and shapes, sort them out according to amplitude into 100 channels, and store a record of the counted pulses in a magnetic core memory. A simple computer with its magnetic core memory and versatile data display system make it possible to observe the pulse amplitude spectrum as it accumulates or after it has accumulated.

In addition to its wide use in gamma spectroscopy, it has many applications in the fields of medical research, neutron time-of-flight studies, radioactive fallout studies, shielding studies, oil well and uranium logging, neutron activation analyses, measuring of radioactivity in humans and other uses.

The analyzer is designed so that information accumulated may be displayed or read out in various ways. Data may be observed on the oscilloscope, or information already accumulated in the memory core may be displayed on the screen, plotted on a strip chart recorder, or printed out in decimal form on an automatic printer.

Since the unit is highly versatile, it can be modified to accommodate most applications which require additional features.

For additional information, wire or write to:

Bendix International

DIVISION OF BENDIX AVIATION CORPORATION

205 E. 42ND ST., NEW YORK 17, N.Y., U.S.A. Cable Address: "BENDIXINT"

Sales Representatives for Great Britain

NUCLEAR ENTERPRISES (G.B.) LTD.

BANKHEAD MEDWAY, SIGHTHILL; EDINBURGH 11, SCOTLAND

256 THE TMC 256-CHANNEL PULSE ANALYSIS SYSTEM

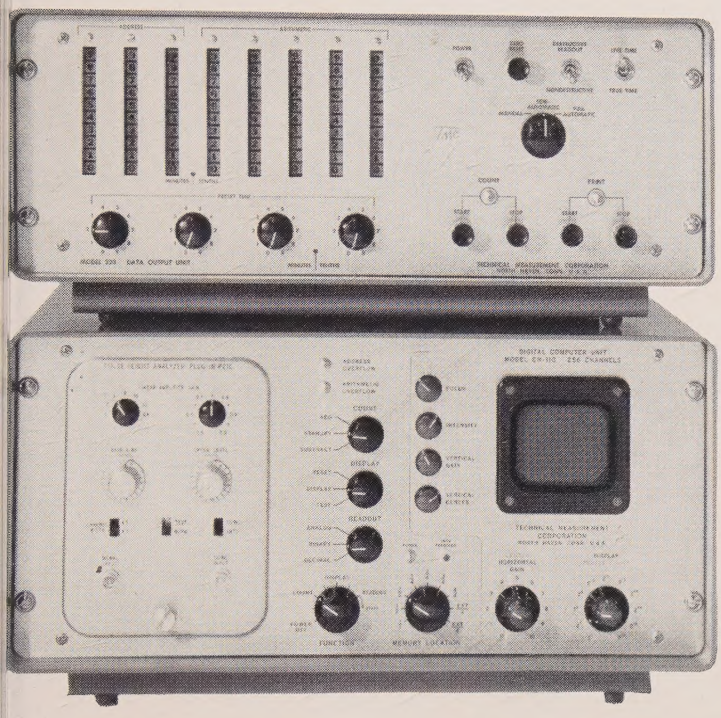

#220 DATA HANDLING UNIT usable as an active timer, event counter and readout device ... effective or actual counting times may be selected from 0.1 to 999.9 minutes in 0.1 min. steps ... manual, semi- or fully automatic operation, destructive and non-destructive readout.

PULSE HEIGHT ANALYSIS — #210 plug-in ... built-in linear amplifier, pulse generator ... 10-74 μs. dead time ... ±0.5% linearity

The Model CN-110 digital computer assembly ... only 8¾" high ... weighs 30 lbs. with plug-in ... operates on 25 watts

TIME-OF-FLIGHT MEASUREMENT #211 plug-in ... built-in delay of 0, 1, 2, 3 times address cycle ... choice of 9 channel lengths from 0.25 to 64 μs. ... automatic channel advance

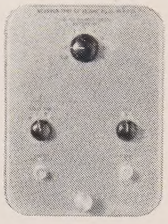

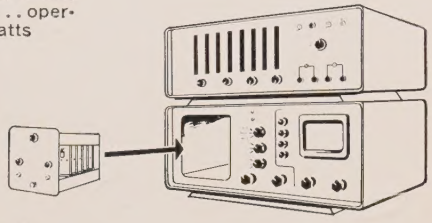

ONE BENCH-TOP INSTRUMENT...

Becomes a different pulse analyzer every time you change the logic

PULSED NEUTRON MEASUREMENT — #212 plug-in ... analysis channel lengths from 10 to 2560 μs. ... 10 μs. storage time ... (a high speed arithmetic scaler is supplied with the CN-110 at no extra charge when the 212 unit is purchased with it)

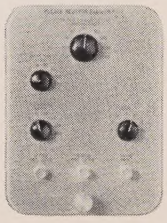

With just one CN-110 in your laboratory you have 256 channels of the pulse analysis you need – whether it's pulse height, time-of-flight, pulsed neutron or a special program. When you plug in the logic network, the instrument becomes a ready-to-use analysis system for that program. And you can change them in the time it takes to loosen a thumbscrew. Total weight is only 30 lbs., all circuits are transistorized – making this today's most versatile, compact pulse analyzer for research, field work or regular laboratory use. *They are now in production and deliveries are being made.*

THE BASIC UNIT IS A COMPLETE DIGITAL COMPUTER with all the circuitry for a 256-channel magnetic core memory and has the advantages of completely enclosed, plug-in memory ... choice of memory sub-groups ... pushbutton data transfer ... instantly selected analog, binary or digital readout.

FOR DATA HANDLING, a readout instrument has been designed specifically for use with the CN-110. The compact #220 data handling unit can be used as a live-timer during data gathering and as a readout system afterward. The #220 can be used with various types of paper tape printing and punching instruments.

Other readout devices that you can use with the CN-110 include strip chart and X-Y recorders, magnetic computer tape, punched paper cards.

Write for the new 6-page bulletin which contains complete details of the CN-110 and all accessories.

TECHNICAL MEASUREMENT CORPORATION TMC 441 WASHINGTON AVE., NORTH HAVEN, CONN.

for nuclear engineering and experimental work

A MULTI-CHANNEL COINCIDENCE UNIT

with a time resolution of 3 millimicroseconds

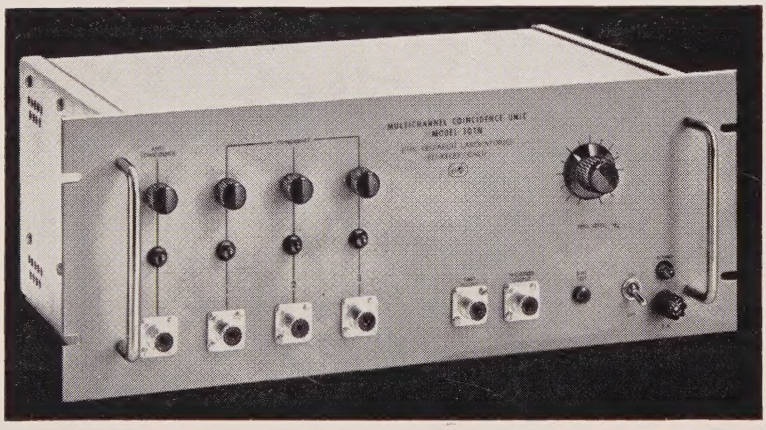

F.O.B. Oakland, Calif. **$725**

Flexible, as well as fast, this E•H Model 101 N functions as a pulse coincidence-anticoincidence analyser over *four channels.*

This unit generates two output pulses—one a microsecond trigger pulse, the other a prompt pulse derived directly. Exceptional reliability is provided over a wide range of input pulse shapes and amplitudes. With the E•H 101 N, photomultiplier tubes (including those having transit time spreads in the millimicrosecond region) may be tied directly to the inputs.

E•H MULTICHANNEL COINCIDENCE UNIT SPECIFICATIONS

INPUT

Minimum pulse amplitude, negative 2 volts. Minimum pulse width, 5 x 10^{-9} sec. Maximum input rate, 5% duty factor. Input impedance, 125 ohms (other impedances supplied at no additional cost).

FAST OUTPUT

5 ma. current pulse delivered from plate of triode on coincidence. Time delay from inputs less than 5 x 10^{-9} sec. Width same as input pulses, or 2 x length of clipping line, if used.

TRIGGERED OUTPUT

Positive 10 volts, 1 μsec. pulse on coincidence. Maximum rate, 100 kc.

ULTIMATE RESOLUTION

3 x 10^{-9} sec.

CONNECTORS

UHF type 83. (Other types may be specified at nominal additional cost.)

TRIGGER LEVEL

Amplitude selection of coincidence pulses for operating trigger circuitry.

POWER REQUIREMENTS

105-130 volts 50/60 cps. 75 watts.

E-H instruments are designed to meet the critical requirements of advanced work. Thanks to superior engineering and the finest components, these instruments have a remarkable record for stable performance.

Write or wire E-H for additional information

E-H RESEARCH LABORATORIES, INC.

1922 PARK BLVD. • GLENCOURT 2-1314 • OAKLAND 6, CALIFORNIA

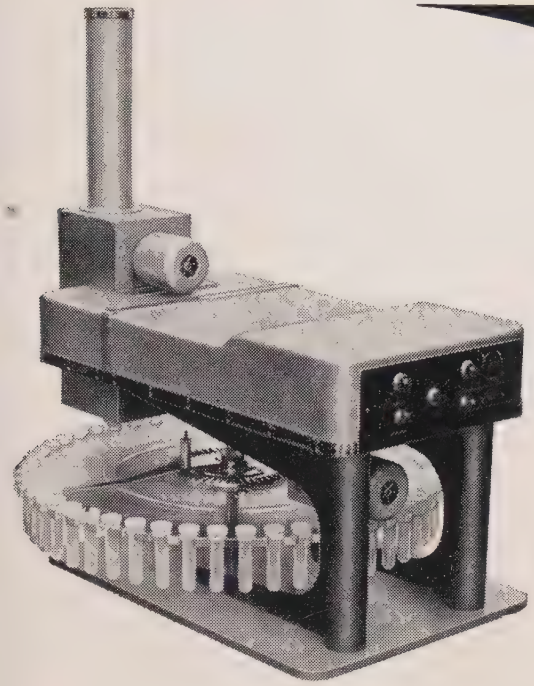

EKAF type RSC-1 Automatic Sample Changer

The EKAF type RSC-1 is an automatic changer for liquid samples, developed by Prof. Dr. H. de Waard, Natuurkundig Laboratorium, Rijksuniversiteit, Groningen.
The instrument holds max. 50 samples in tubes of 9/16" diam. The tubes are lowered one after another in the well of a well-type scintillation detector (EKAF type 50302). Counting starts automatically when sample is in proper position in the detector. Counting stops when preset count or preset time level is reached.

Brief specifications:

Loading capacity: *50 tubes, polythene, 9/16" diam.*

Programming unit: *possibility to start operations at any preselected starting point and to stop changing at a preset sample number. When stopped at preset sample number the rotating disk moves on to position "1" and restarts operating.*
Measuring cycle is ended by means of a "make" signal from counter, hereafter changer provides "stop" and "reset" signals for counter.

Sample changing time: *interval between 2 counting periods is 25 seconds.*

Power requirements: *input 220 V - 50 cycles*
or 110 V - 60 cycles (optional)

Dimensions: *Height (overall): 63 cm (± 25 ins)*
Width : 48 cm (± 19 ins)
Depth : 60 cm (± 23½ ins)

EKAF

ELEKTRONISCH-KERNFYSISCHE APPARATENFABRIEK N.V.

Hartogstraat 5a
The Hague, Holland
Phone: 070-113959

Sales office: **N.V. NENIMIJ**
Laan Copes van Cattenburch 74
The Hague, Holland
Phone: 070-630977

a new approach to time interval measurement

0.25 milli microsecond measurements

WITH THE

Eldorado

MODEL TH-300

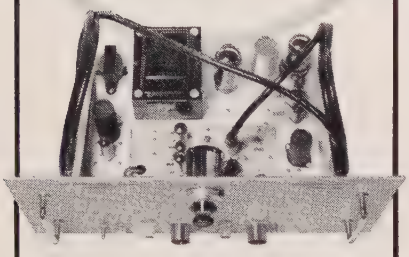

TIME-TO-PULSE HEIGHT CONVERTER

applications

- *Neutron time-of-flight measurements*
- *Half-life determinations of short lived isotopes*
- *Determination of short-time decay in isomeric states*
- *Fast coincidence studies*
- *Delay line calibration*
- *Energy determinations*
- *Transient time studies*

An analog-to-analog converter which transforms time to amplitude over the time range of 1 to 3000 milli microseconds, the TH-300 provides an output pulse whose amplitude is proportional to time. The output can be measured with a pulse height analyzer or scope.

KEY SPECIFICATIONS Three time ranges – 300, 1000, and 3000 milli microsecond full scale. Input, pulse start channel, amplitude of 2 – 100 v negative, duration of 0.01 – 0.10 microseconds; stop channel, amplitude 15 – 150 v negative, duration of 0.01 – 1.00 microseconds. Output, negative ramp, 8 v full scale. Domestic price $795. Immediate delivery.

For complete technical and sales information, call your nearest Eldorado Engineering Representative or write directly to Dept. H12

Eldorado Electronics

2821 Tenth Street
Phone THornwall 1-4613
Berkeley 10, California

SCINTILLATION SPECTROMETRY

NON-OVERLOADING LINEAR PULSE AMPLIFIER NE 5202:

with 5 microsecond recovery for 100 times overload. Designed for scintillation spectrometry and pulse height analysis studies, this amplifier features high gain (50,000), high gain stability (better than 0.25% per week), good linearity, low noise (less than 40 microvolts at input), excellent overload characteristics, and operation at high duty cycles. Rise time 0.2 microseconds and integral linearity 0.15%. Preamplifier NE 5202A also available. Based on the double delay line differentiated Fairstein system, it consists of three high gain feedback groups and a White cathode follower output.

Resolving time 1.2 microsecs; 3–140 volts operating range with energy zero drift less than 0.05 volts per day; 0 to 10 volt gate width with less than 0.01 volts per day drift; maximum counting rate, 2×10^6 c.p.s.

SINGLE CHANNEL PULSE HEIGHT SELECTOR NE 5102:

E.H.T. SUPPLY UNIT NE 5302:

with minimum of noise and ripple; output stability 0.01%; low noise and ripple—less than 1 mV RMS; output voltage continuously variable from 500–1,800 V; output current 5mA.

E.H.T. SUPPLY UNIT NE 5303:

As NE 5302, but with output voltage range from 1000–5000V.

containing white cathode follower preamplifiers with noise level of 25 microvolts; photomultipliers of 1" or 2" can be accommodated; for general use or for C14 and Tritium investigations with special rotary light locking device.

SHIELDED SCINTILLATION HEAD UNITS NE 5501 & 5502:

Other Units available:

Precision Ratemeter NE 5401 with eight ranges and six time constants n.p. Scanning scintillation spectrometer NE 8601.
Multi-channel scintillation spectrometer NE 8201 for industrial tracer investigations.
Scintillometers for geophysical exploration.

(C14 and H3) counting unit NE 8301. Moisture and density gauge NE 8401.

Exclusive concessionaire for C.D.C./Bendix 100-channel Transistorized Kicksorter in Great Britain.

Sole agent for Harshaw Sodium Iodide Crystals in the United Kingdom.

Write for Bulletins and New Illustrated price list
For full details of the above and of our SCINTILLATION PHOSPHOR PRODUCTS (plastics, liquids, loaded liquids, crystals, gels, neutron detectors, and chemicals) write to

NUCLEAR ENTERPRISES (G.B.) LTD.

SIGHTHILL, EDINBURGH, 11, SCOTLAND — TEL.: CRA 5262

Associate Company: Nuclear Enterprises Ltd.
1750 Pembina Highway, Winnipeg, Canada

Visit Stand No. 2 at The Physical Society Exhibition.

From Detection to Analysis
RCL NUCLEAR DATA PROCESSING EQUIPMENT

AVAILABLE SOON:

Two New Small Instrument Lines

1. TRANSISTORIZED
- Scaler
- Power Supply
- Rate Meter
- Amplifier
- Single Channel Analyzer

2. LOW COST
- Scaler
- Rate Meters

Magnetic Tape Auxiliary Memory for Multi-Channel Analyzers

AVAILABLE NOW:

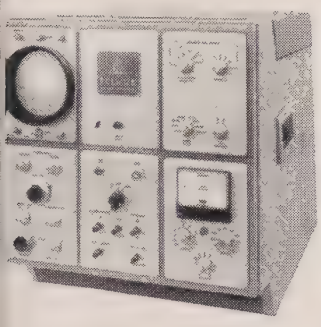

RCLiac 128. Transistorized RCLiac 128 is a unique, new type of nuclear instrument. It is both a 128 channel analyzer and a 125 channel scaler. Both digital number and curve CRT display . . . Six plug-in modules: Display, Memory, Adder, ADC, Control and Power Supply . . . Portable (138 lbs.) . . . "Live Time" — 0.19 second to 28 hours . . . Split memory . . . Preset time, preset count.

MULTI-CHANNEL ANALYZERS. New RCL 256 Channel Analyzer, Model 20613, features pre-selected automatic programming. Any function may be included or excluded from the analyzer cycle including digital printer, strip chart recorder, data shift, background subtraction, quartered or halved memory, etc. For example: Stored background can be automatically subtracted without manual intervention. Six modes of readout: Magnetic tape, punched paper tape, digital printer, X-Y plotter, strip chart recorder and CRT display. Also available: 512, 1024, and 2048 channel pulse height analyzers, 1024 Channel Neutron Time of Flight Analyzer, Single Channel Analyzers and Recording Spectrogammeometers.

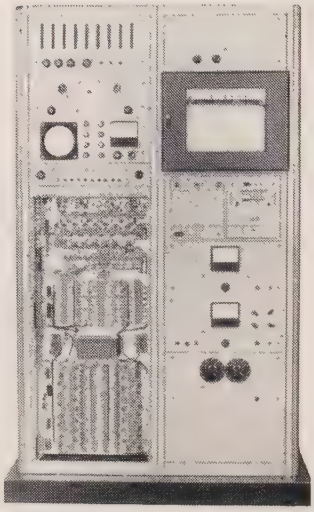

DETECTORS. RCL's non-corrosive halogen quenched geiger counters are non-photosensitive . . . 100% gas efficient . . . Infinite life (3 x 10^{10} counts) . . . —50°C to 220°C operation . . . 1-2% Avg. Plateau Slope. RCL also has a complete line of cosmic ray, scintillation, neutron and gas flow detectors.

SURVEY METERS. RCL's New Fast-Slow Neutron Survey Meter, Model 20810, is a portable, battery operated, transistorized instrument with printed circuitry and low power consumption. Fast and slow neutrons are measured independently. Weight: Less than 10 lbs. Dimensions: 21½" x 6" x 6". Individual fast or slow neutron survey meters also available.

ACCESSORIES. RCL keeps a continuous supply of radiation shields, sample holders, sources, safety equipment and clothing, timers, glassware, scintillation crystals, sample preparation and handling equipment, etc.

LIQUID SCINTILLATION COUNTERS. Liquid scintillation counters are now available in any size up to whole body human counters.

NUCLEAR GAUGES. A complete line of nuclear thickness and density gauges and all necessary controls are available from RCL.

RADIATION COUNTER LABORATORIES, Inc.

5121 W. GROVE ST. ORchard 3-8700
SKOKIE, ILLINOIS, U.S.A.

Write RCL Dept. B for catalogs, brochures and product specifications.

INTERNATIONAL

advertise

YOUR NUCLEAR PRODUCTS IN

sell

YOUR NUCLEAR PRODUCTS

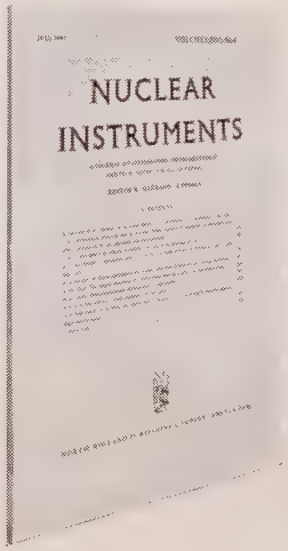

reap

YOUR NUCLEAR SALES
REWARDS

world wide

KEY NUCLEAR MANAGEMENT
NUCLEAR SCIENTISTS
NUCLEAR ENGINEERS
NUCLEAR PRODUCTION
PERSONNEL

SUBSCRIBE TO

you reach

THE WHOLE
NUCLEAR SALES WORLD IN

Entirely international in scope Nuclear Instruments and Methods is the one nuclear scientific journal that has an established subscription clientele throughout the whole world-where-ever nuclear men are at work—they want your nuclear products—they need your nuclear products—advertise in Nuclear Instruments and tell them WHAT – HOW – WHERE they can get your nuclear products

GO INTERNATIONAL WITH YOUR SALES PROGRAM TODAY WRITE

WILLIAM F. BAARS - ADVERTISING MANAGER NORTH-HOLLAND PUBLISHING COMPANY

P.O. BOX 103 – AMSTERDAM, HOLLAND

INTERNATIONAL

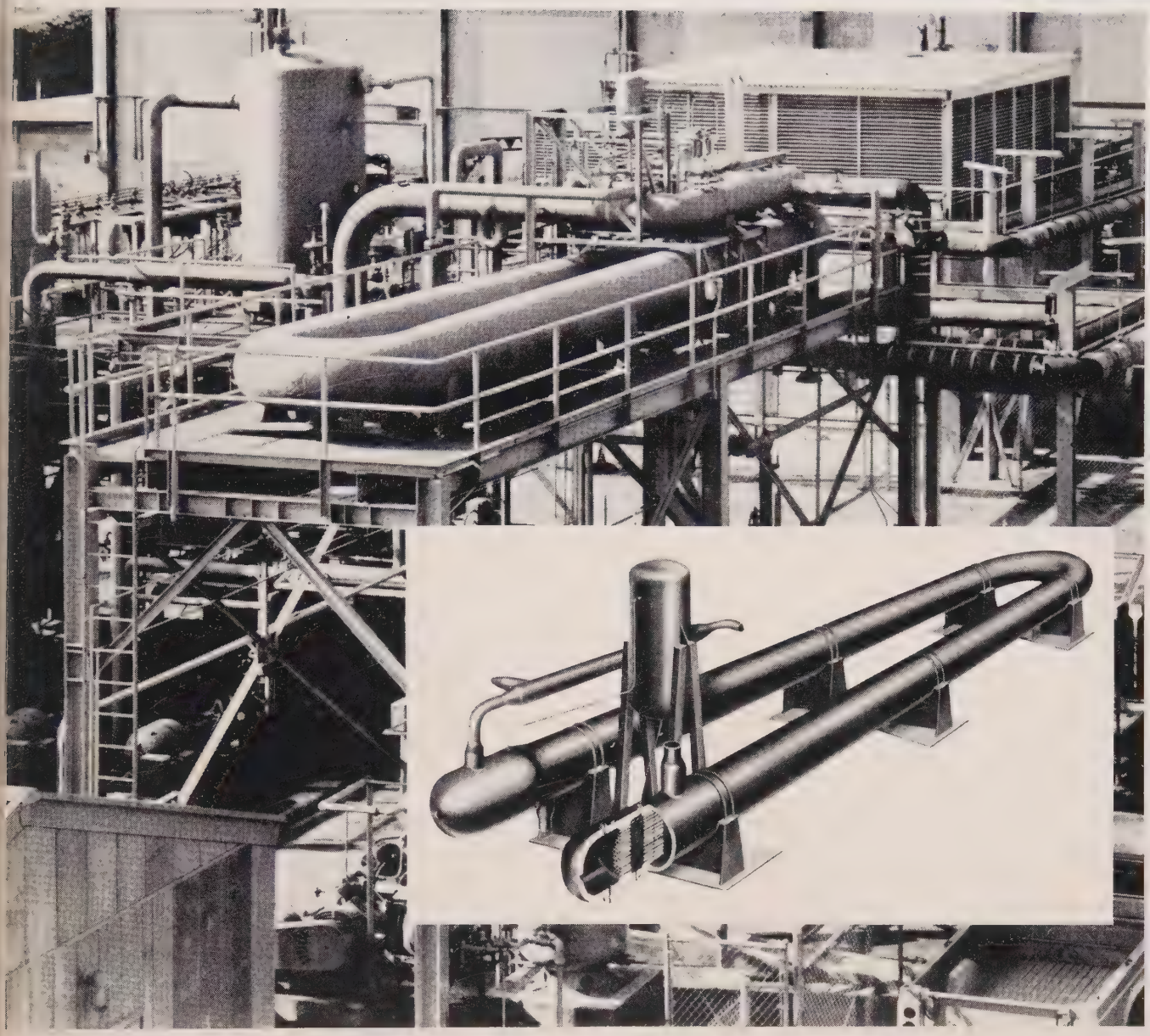

Southern California Edison's electric power station utilizing SRE heat energy, located northwest of Los Angeles in the Santa Susana Mountains.

"PEACEFUL CO-EXISTENCE"—(of sodium & water)—

AT SANTA SUSANA

Everyone knows sodium and water do not mix—peacefully. Therefore, in addition to normal functional requirements, the Sodium Reactor Experiment demands a Steam Generator which minimizes the possibility of these two liquids coming into contact.

To solve this problem The Babcock & Wilcox Company designed and manufactured a tube-within-a-tube steam generator. A mercury-filled annulus between the tubes assures continuous separation of the sodium and water. The success of B&W's design has been amply demonstrated as SRE goes into its third year of operation.

Successful resolution of unusual problems in the steam generating field has become synonymous with B&W. Perhaps we can help you. The Babcock & Wilcox Company, Export Department, 161 East 42nd Street, New York 17, N. Y., U. S. A.

B&W

THE BABCOCK & WILCOX COMPANY

NC-108-E

NUCLEAR ENERGY EQUIPMENT

Complete nuclear systems, cores, components, fuel elements, nuclear research and development

The place of the Particle Accelerator in Basic Research...

Atomic Displacement by High-energy Particles-VI

Research on the interaction of high-energy particles with atoms in the solid phase has received new impetus with the availability of controlled beams of electrons, positive ions, and monoenergetic neutrons from Van de Graaff accelerators. Investigations in this important field of solid-state physics and chemistry have been the subject of several recent surveys and books. [1, 2, 3.]

Determination of Displacement Threshold

Of great interest has been the determination of the threshold for displacement in semi-conductors, by measurements that can be made with electrons of several hundred Kev. Increasing the energy above the threshold value causes the atom to recoil with sufficiently high kinetic energy to cause further displacements in collisions with neighbouring atoms. Electrons cannot transfer large amounts of energy to these recoil atoms because of the large mass difference, but changes can be effected by heavy particles if they have sufficient kinetic energy. Although high-energy protons and deutrons have been used for solid-state studies, these particles do not provide the best results because they lose energy to the lattice electrons and, at low energies, have a limited range.

Neutrons can be produced with a Van de Graaff accelerator by bombardment of targets such as Li^7 and H^3 with protons or deutrons. The resulting neutron beam is monoenergetic, with a high flux, making it ideal for displacement studies. It does not suffer from the broad energy spectrum of pile-produced neutrons and has relatively low gamma background.

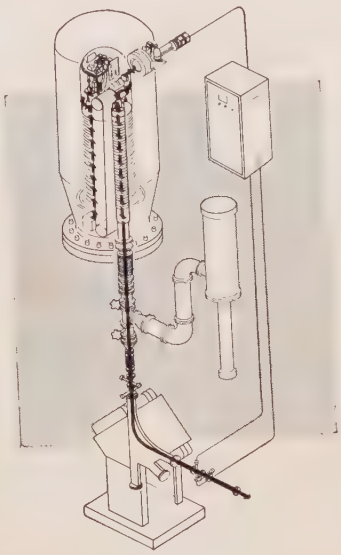

2-Mev positive-ion Van de Graaff with analyzing system.

Thermal Spike

In general the monoenergetic neutrons produced by particle accelerators have energies above the displacement threshold. Their interaction with the atomic nuclei can be described by classical hard-sphere collisions and the subsequent recoil atom energy is sufficient to produce electronic excitation of neighbouring atoms. This phenomenon, originally described in 1923[3], is generally known as a thermal or displacement spike. It is one of the most difficult and yet most interesting phenomena in solid-state radiation reactions.

Seitz, in describing the theory of the high-temperature spike[2], has made an estimate of the volume affected and of the temperature and pressure produced in this region by transfer of incident energy to a lattice atom. Using assumptions deduced from rather meager experimental evidence, it can be shown that the affected volume has a radius approximately ten times the atomic radius. In this volume, the temperature is above the melting points of most solids and the pressure due to the high local temperature is of the order of 10^7 dynes per cm.^{2} Although these conditions last for only about 10^{-11} seconds, which is brief in comparison with most chemical reactions, they could be useful for certain selected systems.

One of the exciting possibilities of such local thermal spikes is the use of the extremely high temperatures and pressures for chemical solid-state reactions. Little has been done in this field because of the difficulty of analyzing the results. With the availability of low-energy monoenergetic neutrons from a Van de Graaff, without the complication of Coulomb encounters with the lattice atoms, there appears hope that this promising field will attract more attention.

References.
1. Radiation Effects in Solids, D. J. Dienes, G. H. Vineyard, Interscience Publishers Inc., New York, 1957
2. Solid State Physics, F. Seitz, D. Turnbull, Editors, Vol. 2, Academic Press Inc., New York, 1956
3. J. A. Brinkman, Journal of Applied Physics, 25, 961, 1954
4. F. Desauer, Z. Physik, 38, 12, 1923.

Write for a copy of our new particle accelerator bulletin.

HIGH VOLTAGE ENGINEERING CORPORATION

BURLINGTON MASSACHUSETTS

High Voltage Servicing Company, Ltd.
London, England

High Voltage Engineering (Europa) N.V.
Amersfoort, The Netherlands

NUCLEAR INSTRUMENTS AND METHODS 6 (1960) 1–25; NORTH-HOLLAND PUBLISHING CO.

THE OAK RIDGE RELATIVISTIC ISOCHRONOUS CYCLOTRON

Compiled and Edited by

R. S. LIVINGSTON and F. T. HOWARD

Oak Ridge National Laboratory†, Oak Ridge, Tennessee

Received 1 October 1959

This document was originally submitted to the United States Atomic Energy Commission in support of a proposal for the design and construction of the cyclotron described herein. The proposal has since been approved and the machine is now being constructed. The document has been revised and, for convenience in publication, reorganized into three parts, as follows:

I. Development of the Isochronous Cyclotron
II. Magnetic Field Design for the Isochronous Cyclotron
III. Analyses of Ion Orbits in the Isochronous Cyclotron

PART I. DEVELOPMENT OF THE ISOCHRONOUS CYCLOTRON††

A variable-energy cyclotron of unusual versatility is described. In this cyclotron a spatially varying magnetic field provides for both focusing and isochronous orbits. This azimuthally varying field has three-fold symmetry and gives an estimated maximum energy of 75 MeV for protons, 100 MeV for N^{4+}. Flexibility in energy and choice of particle to be accelerated are achieved with a resonant system tunable between 22.5 and 7.5 Mc/s and with 21 sets of magnet coils which can be adjusted individually to control the magnetic field configuration. Background information on the development of this type of cyclotron is included.

1. Introduction

During the first decade after Lawrence's introduction of the cyclotron, this nuclear research instrument underwent rapid development to the stage best represented by the classic 60-inch cyclotron. This latter design has been adapted over the years to the needs of many research institutions throughout the world. In the drive toward ever higher energies, attention was subsequently centered on the development of frequency-modulated cyclotrons and, more recently, on proton synchrotrons. For precision work in the region of lower energies the Van de Graaff machine has been developed to a high state of perfection.

Recently there has been an increasing interest in more precise work in the intermediate energy field. Attention is now focused on the improvement of the fixed-frequency cyclotron. Efforts have been directed especially toward overcoming the limitations of energy imposed by the relativity effect, on providing greater flexibility both in the choice of energy and the choice of the particle to be accelerated, on improving the energy definition, and on increasing the beam current and stability.

A number of novel accelerator features have been developed and, in some cases, applied individually to cyclotrons to increase their level of performance, their reliability, and their versatility. Several of these new features have

† Operated for the USAEC by Union Carbide Corporation.

†† Part I represents a summary of the combined efforts of many individuals. Those who were largely responsible for the experimental, theoretical, and design work reported here and for the preparation of the manuscript are: R. S. Bender, H. G. Blosser, B. L. Cohen, E. D. Hudson, R. J. Jones, R. S. Lord, J. A. Martin, E. G. Richardson, Jr., W. R. Smith, T. A. Welton, R. E. Worsham and A. Zucker.

been incorporated in the Oak Ridge Relativistic Isochronous Cyclotron (ORIC) to provide the greatly enlarged research potential which now appears practical for a fixed frequency cyclotron in the intermediate energy field. Among these novel features are the use of (1) an azimuthally varying magnetic field (AVF) to provide axial and radial focusing, (2) an average magnetic field increasing with radius in a manner to keep the accelerated particle approximately synchronous, thus to minimize the threshold voltage required, (3) an oscillator adjustable through an extended range, 3:1, of fixed frequencies, (4) harmonic acceleration to provide additional bands of frequencies, (5) auxiliary coils of various types to control the magnetic field configuration within a wide range of average field strengths, (6) defining grids near the center to eliminate components of the beam with radial oscillations of large amplitude, and (7) the use of r-f amplitude control to reduce the energy spread in the beam. The purpose of this report is to describe the ORIC and to review some recent studies which have led to the choice of certain design features.

1.1. THE AZIMUTHALLY-VARYING-FIELD (AVF) CYCLOTRON CONCEPT

The basic dilemma of the cyclotron mechanism lies in the contradictory demands which focusing and resonance requirements place on the circularly symmetric magnetic field of the classical cyclotron. In 1938, L. H. Thomas[1]) pointed out a solution to this dilemma based on the introduction of azimuthal variations into the magnetic field in a fashion so as to provide both focusing and synchronous acceleration. The technology of this type of machine was explored in theoretical and model studies at the University of California[2,3]) in the years 1950–52. At this time studies were also being made for the conversion of the ORNL 86-Inch Cyclotron to a three-sector Thomas cyclotron, but after the very satisfactory operation of this machine the plan was dropped. The principles involved were explored independently by the Midwestern University Research Association, and attention was called to the important effect of spiral[4]). MURA applied these principles first to their concept of a spiral-ridge synchrotron and subsequently to fixed-frequency machines.

In February 1959 active interest in the sector-focused cyclotron was indicated by the 29 laboratories represented at an international conference[5]) at Sea Island, Georgia. The Los Alamos Scientific Laboratory[6]) has been using three-sector Thomas shims for some time to improve the performance of a conventional cyclotron. In 1958 a four-sector isochronous machine was put in operation at Delft[7]). Recently, the operation of six-sector 14-MeV deuteron machine at Dubna[8]) was reported. Other machines are under construction at the Universities of California, Colorado, and Illinois, at the University of Birmingham, and at Oak Ridge.

Various studies have indicated the feasibility of the azimuthally-varying-field, fixed-frequency cyclotron as an instrument for obtaining relativistic particles. New methods have been worked out for straightforwardly obtaining the complex magnetic field shapes required. These methods, in conjunction with presently available techniques for the use of pole-face windings as current shims, should make it possible to design a magnet which will give the proper field shape over a considerable range of field strengths, thereby allowing the acceleration of various ions to a wide range of energies.

Active interest in the construction of an azimuthally-varying-field cyclotron was renewed at the Oak Ridge National Laboratory in late

[1]) L. H. Thomas, Phys. Rev. **54** (1938) 580.

[2]) D. L. Judd, Phys. Rev. **100** (1955) 1804.

[3]) E. L. Kelly, R. V. Pyle, R. L. Thornton, J. R. Richardson and B. T. Wright, Rev. Sci. Instr. **27** (1956) 492.

[4]) K. R. Symon, D. W. Kerst, L. W. Jones, L. J. Laslett, and K. M. Terwilliger, Phys. Rev. **103** (1956) 1837.

[5]) F. T. Howard, Editor, Sector Focused Cyclotrons, Proceedings of the Conference on Sector-Focused Cyclotrons, Sea Island, Georgia, Feb. 2–4, 1959, Nuclear Science Series Report Number 26 and National Academy of Science-National Research Council Publication 656, in press.

[6]) K. Boyer, in ref. [5]).

[7]) F. A. Heyn and K. K. Tat, Rev. Sci. Instr. **29** (1958) 662.

[8]) D. P. Vasilenskaya *et al.*, Atomnaya Energia **6**, No. 6 (1959) 657.

1954, and an extensive theoretical study of the properties of machines of this type was begun. It soon became apparent that analytical studies of these devices were hardly adequate, and so, at an early stage, numerical integration procedures were devised and coded for the digital computer so that orbit behavior in complex fields could be studied in detail. These integration routines and their subsequent refinements have since been the major tool in both theoretical explorations and detailed design of devices. The progress achieved in the development of the AVF cyclotron in the past half decade is due in large measure to the availability of the digital computer.

Théoretical studies[5]) have included studies of the fundamental acceleration process, the focusing properties of the fields, the effects of nonlinearities and resonance difficulties, the effects of factors which determine beam quality, and details of deflection systems appropriate for such devices.

In addition to these theoretical studies, an operating relativistic AVF cyclotron has been constructed for the purpose of experimentally verifying of the computational results. This device[9]), known as the Cyclotron Analogue I, accelerates electrons to a velocity of 0.7 c (in units of velocity of light) and to a radial focusing frequency of 2 (in units of the orbital frequency). The magnetic field in the Analogue is of a four-sector radial configuration; the field is obtained from a precisely fabricated set of air-cored coils, the detailed performance of which was accurately precalculated. In operation, the Analogue has verified the design calculations of isochronism and focusing strength and has yielded useful information on performance near resonances.

A second analogue[10]) having a spiral magnetic field configuration is presently under construction for studying in more detail the performance of a proposed 850-MeV f-f cyclotron.

1.2. VARIABLE ENERGY CYCLOTRONS

Because of the interrelationships of the maximum energy, the magnetic field strength, and the frequency of rotation of the particle being accelerated, any variation of energy means that the accelerating system of the cyclotron must tune over some range of frequencies. The high dee voltage required in cyclotrons can be achieved for practical driving power only by using a high-Q resonant circuit; high Q means that the energy storages is large relative to the power loss per cycle.

The frequencies at which cyclotrons operate make it possible to use transmission line elements as components of the circuit. Thus, the resonant system, the dees, and their stems form a quarter-wave resonant circuit foreshortened by the dee capacity. To tune such a system, three variables are available:

(1) C, the dee capacity

(2) l, the length of the dee stems

(3) Z_0, the characteristic impedance of the dee stems.

On most cyclotrons, the dee capacitance can be changed but a small amount and is used only for fine tuning of the accelerating frequency. The resonant frequency varies nearly inversely with the square root of the capacity. Therefore, a change in the frequency of 2:1 would require a maximum to minimum capacity ratio of 4. The large capacity of the dees is nearly fixed, however, by the area of the dee surfaces parallel to the magnet pole face. Normally it is the capacity along the edge of the dee which can be varied, and this quantity is relatively small. The spacing between the dees and the dee liner next to the magnet poles is set to the minimum required for voltage breakdown between the dees and liner. The designers of the 90-Inch Cyclotron at Livermore[11]) made use of the fact that the threshold voltage varied with the energy of the particle such that the highest voltage is required at the highest frequency. Therefore, they have designed a movable liner

[9]) H. G. Blosser *et al.*, Four-Sector Azimuthally Varying Field Cyclotron, Rev. Sci. Instr. **29** (1958) 819.

[10]) J. A. Martin, Paper presented at International Conference on High Energy Accelerators and Instrumentation at CERN, Geneva, September 14–19, 1959.

[11]) B. H. Smith, in ref. [5]); C. J. Taylor, in ref. [5]); J. M. Peterson, in ref. [5]).

which allows the voltage to be greater than threshold at each frequency, but which allows tuning over the range from 4 to 6.2 or 6.2 to 9.5 Mc/s; the two ranges correspond to two shorting-bar positions.

The second method, variation of the length of the dee stems by moving the shorting bar along the stems, allows a wide variation of frequency. It also requires long stems and movement at the joint through which the current is highest in the machine. The cyclotrons at Rochester[12]) and Los Alamos, and the machine under construction at Illinois all use this method. For good contact the connection to the shorting bar requires great pressure. If bolts are used long delays are encountered in resetting the frequency. The connection can also be remotely controlled with hydraulic or pneumatic pistons, a faster method.

The dee stems must present an inductive reactance equal to the dee capacitive reactance for resonance. In addition to, or instead of, tuning this inductive reactance by varying the length of the dee stems, the characteristic impedance of the stems may be varied. The properties of lines with non-uniform characteristic impedance has been studied by Donaldson[13]). Cyclotron tuning schemes using this method, or some modification, have been considered at Colorado; Berkeley, and UCLA. A "barn door" method considered at Colorado involved movement of the dee-stem liner surface; because of quite low Q at low frequencies the system was abandoned. A variation which consists of making the stem and lines like long enmeshed capacitor plates has been considered at UCLA[14]) and Berkeley[15]). Since the surface area of the lines can be large this system shows promise for a low-loss, wide-range tuning scheme.

[12]) H. W. Fulbright, in ref. [5]).

[13]) M. R. Donaldson, An Investigation of Resonant Properties of Short Exponentially and Linearly Tapered Lines, ORNL-2260 (May, 1958).

[14]) K. R. MacKenzie, in ref. [5]).

[15]) R. H. Smith, in ref. [5]).

[16]) R. S. Livingston, The Oak Ridge 86-Inch Cyclotron, Nature **170** (1952) 221.

[17]) J. A. Martin *et al.*, Radioisotope Production Rates in a 22-MeV Cyclotron, Nucleonics **13** (1955) 28–32.

1.3. CYCLOTRONS IN OPERATION AT ORNL

The Oak Ridge Relativistic Isochronous Cyclotron is an outgrowth of the research and development programs associated with the two unusual cyclotrons built at Oak Ridge, the ORNL 86-Inch and the ORNL 63-Inch Cyclotrons. In subsequent paragraphs the origin, characteristics, and performance of these two machines are reviewed. In addition to these, a 44-in. proton cyclotron is operated at 2 to 5 MeV for cyclotron development work.

The ORNL 86-Inch Cyclotron

The 86-inch cyclotron[16]) produced its first proton beam in November, 1950 after a construction period lasting a little more than a year. This machine, which now provides both internal and external 22-MeV proton beams, has been an effective tool both for basic nuclear physics research and for applied uses such as isotope production and neutron production for biological research. The versatility of the machine was enhanced in 1956 by the addition of a deflector system and beam room facilities. The 86-inch cyclotron is believed to have the highest production rates for isotopes[17]) of any existing cyclotron.

The machine incorporates several innovations in cyclotron design. The median plane is vertical rather than horizontal; the magnet yoke is U-shaped with the top open to permit the easy transfer of large cyclotron components with an overhead crane. The high dee-to-dee potential, 300 to 500 kV, needed to accelerate protons to 22 MeV is provided by a self-excited, grounded-grid, single-tube oscillator. Ion loading, which often impedes oscillation in self-excited oscillator systems, is eliminated by maintaining the whole dee structure at a negative potential of one kilovolt.

The deflector is unique in several ways. Electric deflection is produced wholly by the r-f dee potential—no d-c potential is used. The septum, or beam-splitter, is a grid of water-cooled aluminum tubes and is mounted in a fixed position on the dees; the beam is positioned by introducing a controlled first harmonic in

the magnetic field. (The same result was previously obtained in conventional machines by a complicated mechanical arrangement which moves the dees and septum.) The beam passes from the electrostatic deflector through a magnetic channel which sharply reduces the magnetic field and permits the beam to cross the fringing magnetic field easily. Focusing of the deflected beam is accomplished by a set of 2-in.-aperture quadrupole magnets. For nuclear physics experiments the beam is piped a distance of 40 ft to the reaction room.

At present the 86-inch cyclotron is operated 16 hours a day, five days a week. In routine operation the beam on an internal target is 2000 to 3000 μA, with the peak at 4000 μA.

The ORNL 63-Inch Cyclotron

The 63-inch cyclotron[18]) was the first such machine specifically designed to accelerate heavy ions, i.e., ions with masses greater than helium. It was originally built as a test machine to determine the feasibility of accelerating heavy ions and to explore in a preliminary way the possibilities for nuclear research. The heavy-particle nuclear physics field is now well established[19]); heavy ions are now being accelerated by seven machines in the world, and several other heavy-ion accelerators are in various stages of development or construction.

The new heavy-particle cyclotron was built largely of existing components formerly used in the electromagnetic separation of uranium isotopes. An existing magnet gap was reduced to six-inch clearance and shimmed to operate at a field of 15 000 gauss. Ion sources[20]) were developed which produce copious quantities of N^{3+} and N^{4+} ions. A new dee system and oscillator were designed and built to operate at the prescribed frequency of 5 Mc/sec. Existing power supplies were modified to provide high voltage for the oscillator tube and the deflector. The time schedule was approximately as follows: The idea was proposed in October, 1950, construction of the machine was authorized in April, 1951, and an internal beam was obtained in May, 1952. Experiments were performed with the internal beam until the spring of 1953. Then, the magnetic field was reshimmed and a beam deflector system was installed. A satisfactory deflected beam was obtained in November, 1953, and has since been used for atomic and nuclear physics experiments.

At present the cyclotron operates twelve hours a day, five days a week. The circulating beam of N^{3+} ions is about 100 μA; the deflected beam is about 2 μA at an energy of about 28 MeV. The machine operates in an unshielded area.

2. The New Isochronous Cyclotron

Construction of a new cyclotron was proposed by the Laboratory to free the heavy-particle experimental program from the handicaps of the physical environment of the 63-inch cyclotron and, by increasing the particle energy, to open up the upper two-thirds of the periodical table as possible experimental territory. The Laboratory first proposed that a replacement cyclotron be constructed to permit heavy-ion physics to continue under somewhat improved circumstances in an existing building. The Commission (USAEC) approved this proposal in 1957 and the project, originally designated the 48-in. cyclotron, was begun. Engineering designs were prepared an orders were placed for the magnet steel and aluminum.

Meanwhile advances in technology continued at an unanticipated rate. Studies of properties of ion orbits (for high-energy particles) have shown the superior performance possible with alternating strong and weak sectors in the magnetic field. Accelerating protons to 75 MeV in a fixed-frequency cyclotron, previously impossible, thus becomes relatively straightforward. New systems for varying the radio frequency offer the possibility for continuous variation of the energy. New ideas for control of

[18]) R. S. Livingston, Acceleration of Partially Stripped Heavy Ions, Nature **173** (1954) 54.

[19]) A. Zucker, R. S. Livingston and F. T. Howard (Editors), Proceedings of the Conference on Reactions Between Complex Nuclei, Gatlinburg, Tennessee, May 5–7, 1958–ORNL-2606.

[20]) R. J. Jones and A. Zucker, Two Ion Sources for the Production of Multiply Charged Nitrogen Ions, Rev. Sci. Instr. **25** (1954) 562–566.

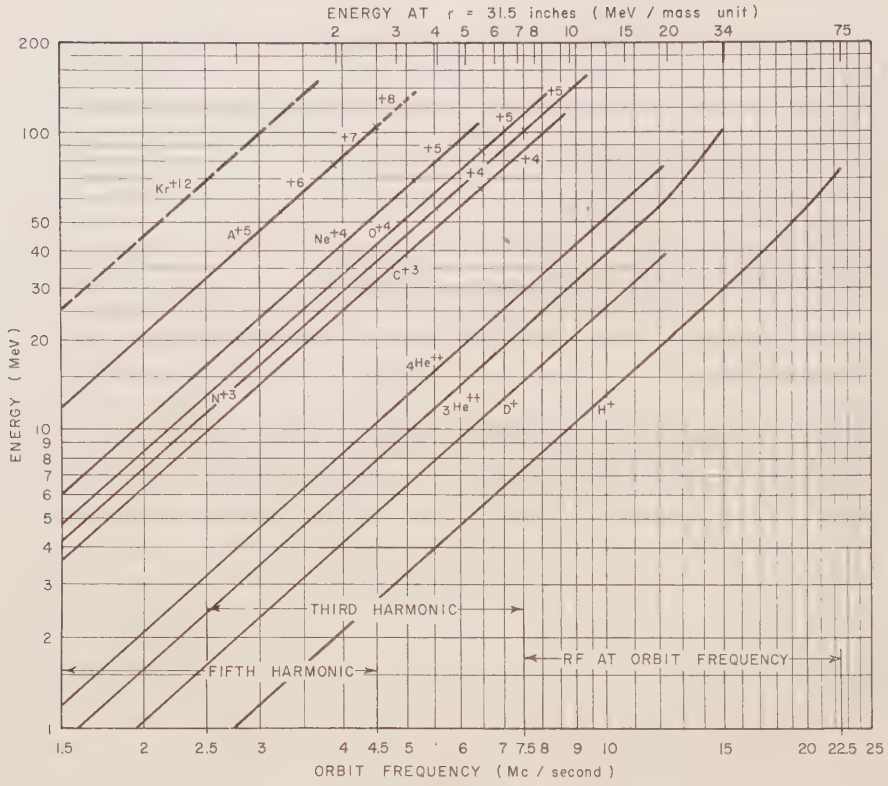

Fig. 1. Particles accelerated and energies available.

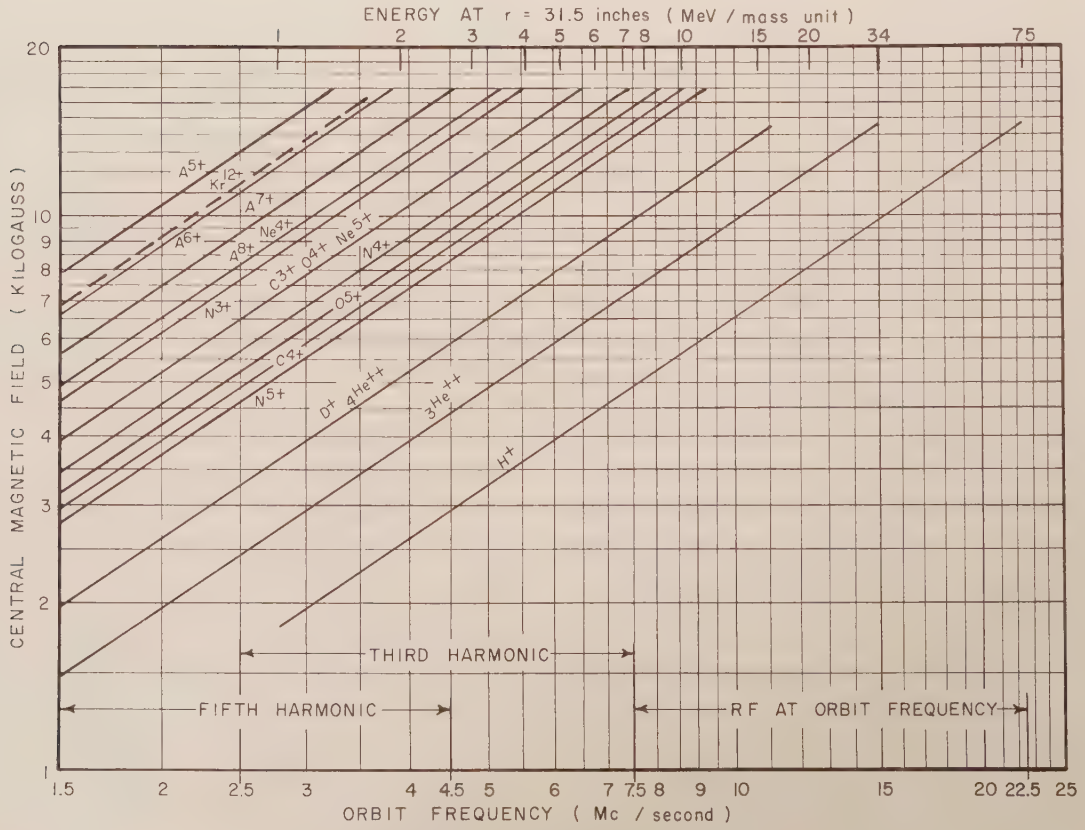

Fig. 2. Resonance conditions for various ions.

TABLE 1

Maximum energy and resonance conditions for various ions

	Charge state	Max energy (MeV)	Energy per nucleon (MeV)	Orbital frequency (Mc/sec)	Central magnetic field (kilogauss)
Proton	+ 1	75	75	22.5	14.8
Deuteron	+ 1	39	19.5	12.3	14.5
Helium-3	+ 2	100	34	15	14.7
Alpha	+ 2	78	19.5	12.3	14.5
Carbon-12	+ 4	115	9.5	8.6	17
Nitrogen-14	+ 4	100	7.3	7.5	17
Oxygen-16	+ 4	88	5.7	6.5	17
Neon-20	+ 5	108	5.7	6.5	17
Argon-40	+ 7	103	2.8	4.6	17
Krypton-84	+ 12	145	1.8	3.7	17

radial oscillations and r-f amplitude indicate beams of much finer definition are possible.

In the face of these technological developments it was decided that a more modern and versatile cyclotron should be sought. The new concept was advanced as a replacement for both the 86-inch and the 63-inch cyclotrons, and as an alternate to the 48-inch machine then under construction. The new machine which evolved, the ORIC, is described below in terms of the anticipated performance and the design features. Subsequently, studies which led to choice of certain design features will be described.

2.1. DESIGN PERFORMANCE

The ORIC is a variable-energy, azimuthally-varying-field, 76-inch, fixed-frequency cyclotron designed to accelerate various particles with e/m ratios from 1 to 0.125 over a wide range of energies, up to 145 MeV. The machine is designed to accomodate large ion currents, with a beam power up to 75 kW (one milliampere of protons at 75 MeV). The conditions associated with the acceleration of various particles to their maximum respective energies are shown in table 1 and presented graphically in figs. 1 and 2.

2.2. DESIGN CHARACTERISTICS

The most conspicuous features of the ORIC are shown in a photograph of the model, fig. 3. The three-sector magnet pole, with slight spiral, is shown at the left. An earlier concept for the wide-range, variable, radio-frequency system is at the right. The most important design characteristics are summarized in table 2.

TABLE 2

Design characteristics of ORIC

Magnet Data	
Magnet field configuration	3 sector
Magnet core dia	76 in.
Magnet pole tip dia	76 in.
Beam radius, average max	31.5 in.
Magnet gap, hill	7.5 in.
Magnet gap, valley	28.5 in.
Central magnetic field, max ave	17 kgauss
Magnet field rise with radius (max)	8%
Magnet excitation	1.23×10^6 amp-turns
Magnet weight	200 tons steel 9 tons aluminum
R-F System	
Dee diameter	71 in.
Dee aperture	1.87 in.
Dee-to-dee gap	2 in.
Oscillator tube	RCA 6949
Oscillator input power	650 kW max
Oscillator output power	500 kW max
Frequency	22.5 to 7.5 Mc/sec
As 3rd and 5th harmonics	7.5 to 1.5 Mc/sec
Miscellaneous	
Beam extraction type	Regenerative
Ion Source	Hot cathode
Shielding	7 ft ordinary concrete, 8 ft locally
Beam power	75 kW (1 mA protons at 75 MeV, other ions comparable)

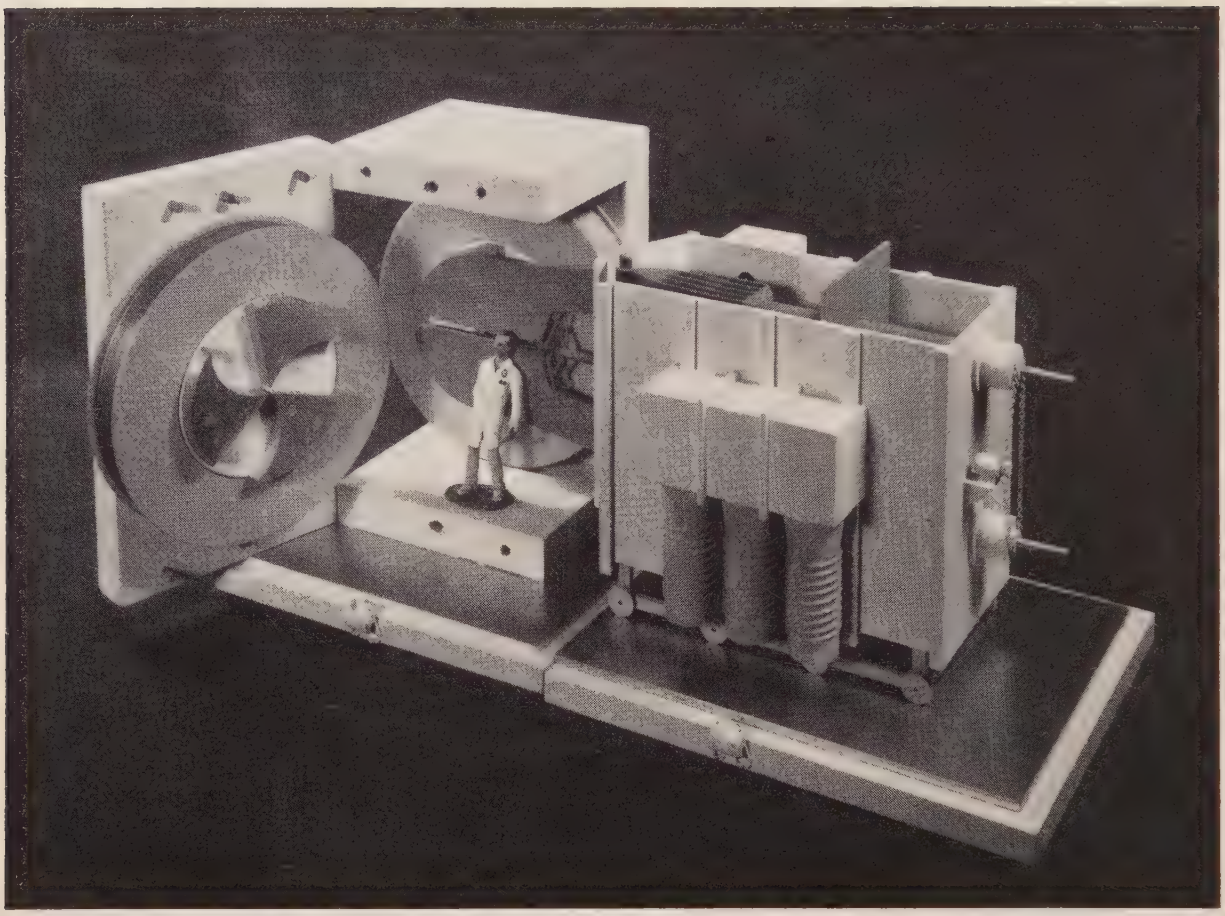

Fig. 3. Model of ORIC showing three-sector pole tips and one of the earlier F-R systems studied.

In subsequent sections of this report, the work on the preliminary design of the magnetic field and of the radio-frequency system is described; background material on the genesis of the ORIC design, on the intended research applications, and on other design features is included. Part II will describe design studies basic to specifications for magnetic fields with azimuthal variations. Analyses of ion orbits, resonances, and deflection problems will be summarized in Part III.

3. The Magnet

Since the specifications for a cyclotron magnet involve relations between many dependent parameters, it is necessary to make both successive approximations and compromises in the preparation of firm specifications. The process of selecting the specifications involves the determination of the following parameters: (1) basic criteria, (2) ampere-turns, (3) operating power, (4) choice of conductor material, (5) specification of the conductor material, (6) coil design, (7) yoke specifications, (8) yoke design, and (9) the design of auxiliary coils for the AVF feature of the ORIC.

The magnetic field requirements for a variable-energy, variable-particle cyclotron are, of course, much more complex than for a conventional machine. The unusual field configuarations in the ORIC will be generated partly by fixed iron poles energized with conventional main coils mounted outside the vacuum tank and partly by auxiliary coils mounted in the vacuum tank, see fig. 4. Forty-six coils are to be used: two main coils, six valley coils, eighteen harmonic

coils also mounted in the valleys, and twenty circular trimming coils. These coils will be current-regulated so that current variations in

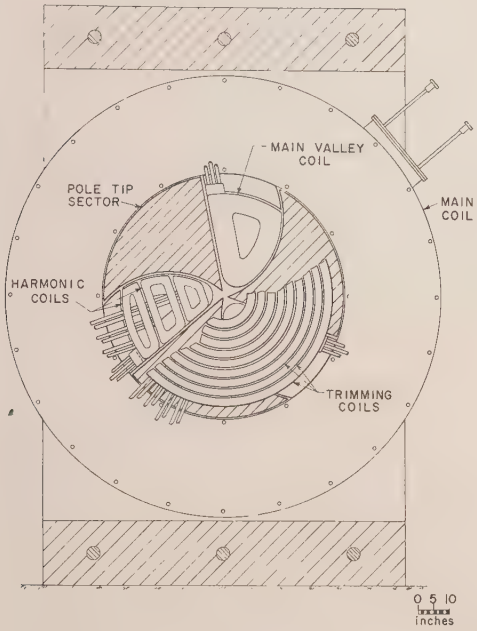

Fig. 4. Magnet section showing sector shape and arrangement of auxiliary coils.

any coil produces short time changes of no more than 1 part in 10 000 in the magnetic field. All coils in the vacuum tank with the exception of the circular trimming coils will be in sealed containers to minimize vacuum difficulties.

The basic design criteria for a cyclotron magnet evolves from a consideration of the $H\rho$ and beam aperture required for the transmission of the desired ion currents to a given maximum energy. These criteria are usually selected by a suitable compromise between desired maximum energies and currents and those obtainable practically, at a reasonable cost. The design latitude of the ORIC magnet was slightly, but not seriously, restricted by the availability and usefulness of existing equipment obtained for the earlier 48-in. machine. Thus, after a review of previous calculations and model work, an energy of 75 MeV for protons, a maximum beam radius of 31.5 in., a pole diameter of 76 in., and a minimum gap of 7.5 in. were chosen. A horizontal section through the magnet is shown in fig. 5.

3.1. MAGNET EXCITATION

The number of ampere-turns required to obtain the magnetic field specified by the basic criteria was determined by model magnet measurements. First, an estimate of the ampere-turns was obtained by assuming a magnet with an efficiency of 60% and substituting in the relationship

$$NI = \frac{2.02\, Hg}{\eta}$$

where NI is the ampere-turns, H the magnetic field strength in kilogauss, g the magnetic gap in inches, and η the efficiency.

With this estimate, a $\frac{1}{9}$-scale model was constructed for use in investigating field shapes

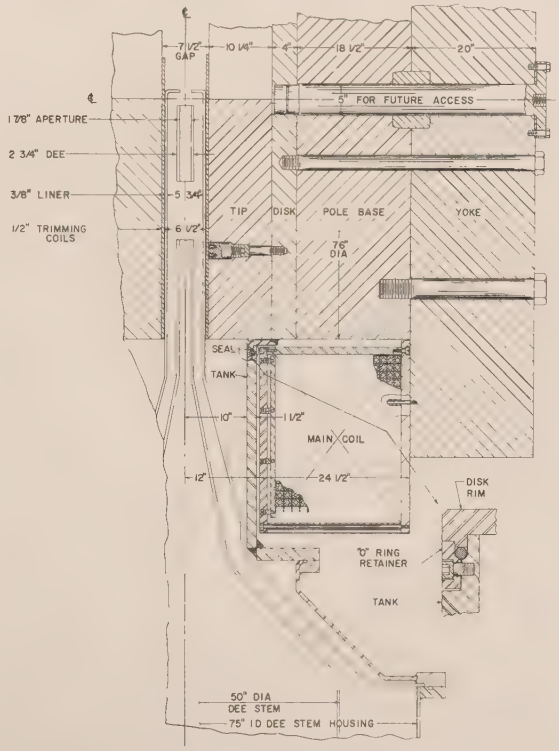

Fig. 5. Horizontal section through magnet showing dimensions and details of design.

and for determining a reliable value for ampere-turns. The value obtained was 1.09×10^6 ampere-turns at an efficiency of 52.4%. This

value was adjusted for possible errors, which were all assumed to be in the direction to increase the ampere-turns required, as follows:

Items	% As estimated	As % of total current
Iron (μ)	1.5	1.0
Current measurement error	0.2	0.2
Winding end effects	0.1	0.1
Dimensional errors of model	1 to 2.0	6.0
Field measurement errors	1.0	3.0
Contingencies	1.0	3.0
		13.3%

With this 13% adjustment for errors the value for use in subsequent calculations became 1.23×10^6 ampere-turns.

The operating power level for the magnet was selected to provide the minimum-cost magnet that meets the basic criteria. The choice of operating power level is related to the amortization time of initial costs. This time was arbitrarily chosen as 10 years, and a range of practical power levels was selected. The initial cost plus cost of operation for 10 years was then calculated for each of the various power levels until a minimum cost design was found. The initial cost estimates did not have a high degree of accuracy; however, the total estimated cost passed through a broad minimum. In this manner the power level was established at approximately 1000 kW.

3.2. CONDUCTOR FOR MAGNET WINDING

For practical reasons the only suitable conductor materials are copper and aluminum; a choice between these two materials becomes a matter of cost and reliability. To the first approximation, in magnets of the same power and ampere-turns, the weight ratio of the aluminum to copper is 0.5; this follows directly from the ratios of density and conductivity.

This rough approximation would require copper to cost half as much per ton as aluminum to be competitive. Of course, other factors were considered. The use of aluminum would require more yoke steel because of the larger coils. For a magnet the size of the ORIC (200 tons) this would amount to an increase of 10 tons or an approximate cost of $ 4400.00. Also, because of the greater volume of aluminum, the coil windings are displaced radially outward where they are magnetically less effective.

In making a choice of these conductor materials several studies were made of various coil and yoke configurations operating at different current densities and power levels. Complete magnets with both copper and aluminum were calculated for several cases of interest. At the market price for these metals at the time these studies were made, a substantial saving was indicated for aluminum.

A rating of reliability of the two conductor materials could only be estimated for particular designs. A possible difficulty with aluminum would result from corrosion or deposits in the cooling water passage. Difficulty with copper would be most likely to occur in connection with the several hundred brazed joints. These joints are necessitated by the limitation in copper extrusion technology for producing long conductors at practical costs. In view of all these considerations aluminum was chosen for the conductor material.

Conductor Corrosion Test. Since an adequate degree of reliability of aluminum had been assumed, it was felt that a test for corrosion and deposit under operating conditions would be desirable.

Test sections of aluminum were obtained from Aluminium Limited Sales, Inc. The test was made in the water system used in cooling the r-f components of the ORNL 86-Inch Cyclotron. Two test pieces of conductor 24-in. long were separated from ground and from each other by 30-in. lengths of rubber hose. The unit was inserted in the circulating water system of the cyclotron in which the water is demineralized and filtered but not deaerated. The total capacity of the system is 15 000 gal, and the make-up is supplied by a central demineralization plant. Analysis of the water in the system showed a pH of 7, small amounts of carbonates,

and approximately 4.2 mg of solids/liter of solution. The latter is in collodial suspension and gives the water a brown color. The total iron content was 3.3 ppm with 0.3 ppm of iron dissolved. The conductivity of the water was 6.5×10^{-6} mhos per cm^3. The piping in the system contains seamless mild steel pipe, admiralty brass tubes in the heat exchangers, copper tubing, and a small amount of aluminum in the cyclotron deflector. The average summer temperature of the water is 75° F; the average winter temperature is not available but can be presumed to be in the vicinity of 34–40° F.

A simulated operating potential was applied to the test sections, with one piece of aluminum conductor at 175 volts positive and the other piece at 175 volts negative to ground. Upon termination of the test after 6900 hours, it was found that the specimen at negative potential had gained 5 g (0.57%) and the positive 3 g (0.34%). There was more deposit at the ends of the negative section; this was a relative loose material. There was very little pitting at the tips of the negative section; pitting at the tips of the positive section was heavier, averaging about 60 mils. As would be expected, the heaviest deposits and deepest corrosion occurred at the ends of the specimens facing one another where the effective potential was 350 volts. All significant changes in the aluminum test sections appeared within 0.5 in. of the ends; there was only a very thin layer of brown deposit beyond the ends.

The test was reassuring in that it indicated that no serious problems should be enountered in using aluminum conductors with a demineralized water system. A replaceable section is provided, however, at the entrance and exit of each strand of conductor.

Specifications for Aluminum Conductor. The specifications for the aluminum conductor were as follows:

The material to be EC (Electrical Conductivity) aluminum, ASTMB0236-56T, each strand (1170 ft) to be one continuous extrusion from one or more billets.

The tensile strength to be adequate to meet a hydraulic pressure test of 300 psi, the outside dimensions not to exceed the required tolerance of $\pm$ 0.010 in. during the test.

The cross section of the conductor to be 1.137 $\pm$ 0.010 in. square, with the radius of corners not to exceed $\frac{3}{64}$ in., and with a center hole of 0.700 $\pm$ 0.010 in. diameter. The maximum allowable eccentricity to be 0.0218 in., with the wall no thinner than 0.186 in. at any point.

A piece removed from each end of the conductor in the $\frac{1}{4}$-hard maximum temper at shipment to be capable of being bent cold 90 deg around a 2.5-in. radius mandrel with-out cracking. Buckling, distortion, and the reduction in area of the 0.7-in. dia opening to be considered within tolerance if the buckling is undetectable by eye, if the bending decreases the outside edge by no more than 10%, and if the area of the 0.7-in. diameter opening is decreased by no more than 10%. (This test was made to determine the properties of the aluminum; the conductor would not be subjected to this extreme bending.)

A chemical analysis was not requested; however, an analysis furnished with the conductor gave the following: Cu 0.007, Fe 0.29, Mn 0.003, Si 0.08, Ti 0.004, V 0.010, B 0.003, and Ga 0.017, all in percent. All specifications were satisfactorily within tolerances.

3.3. MAGNET YOKE

The magnet yoke is made from forged low carbon steel and is of the conventional closed-yoke design with a 1:1 ratio of pole base to yoke cross section. The forgings result in homogeneous steel, and the H-type construction provides a very rugged mechanical structure. The finished magnet, less coils, weighs approximately 200 tons and is 180 in. high with base dimensions of 113 $\times$ 113 in. The four 20-in. thick yoke pieces are bolted together with through bolts. The pole bases are attached with two bolts each and the tank disks are each attached with nine bolts.

Magnet Steel Specifications. A most important and difficult specification to determine is the

composition of the steel. Several types of high permeability alloy steels were considered. Most of the superior steel alloys do not maintain their superiority of relatively high permeability at magnetic fields above 20 000 gauss. The best alloys have objectionable components for a high neutron flux (e.g. cobalt) and give rather little gain in magnetic field at large costs. The choice made in this case was low carbon steel. The precise content of carbon and impurities was a compromise to permit feasibility of forging (see below); however the adverse effects due to the compromises are small. At high magnetic fields the effect of low impurities on the permeability of steel is small, but some investigations have found the effect of carbon at low values to be completely negligible. In the ORIC model magnet, with a permeability of approximately 90, it is estimated that a 1% decrease of permeability would result in a decrease of 0.21% in flux in the magnetic gap.

A steel known as Cyclotron Analysis Steel was chosen. It has the following composition:

	% Max
C	0.15
Mn	0.50
P	0.04
S	0.05
Si	0.20
Ni	0.08

A comparison was made of yoke structures fabricated of forgings and of laminations. The loading on the yoke structure due to magnetic and vacuum forces was calculated as being 1 050 000 lbs and 60 000 lbs, respectively. Since the size of each yoke member was well within the range of readily obtainable forgings, it was desirable to use the latter if the cost was not prohibitive. A study indicated that the over-all cost of the forgings was well within the acceptable range as compared with the laminations; so forging was chosen.

The following fabrication procedures were specified:

The material to be open hearth killed steel with both pole bases from a single heat and with the two ingots of the same size and shape and forged in the same manner.

Sufficient discard to be made from each ingot to secure freedom from piping and undue segregation, and the forgings to be made from ingots having at least two times the cross sectional area. All sections to be tested ultrasonically.

All mating surfaces to be machined to a finish of 125 micro-inches, and all other surfaces to 250 micro-inches.

The mating surfaces of pole bases and yoke pieces to be planes within $\pm$ 0.005 in. T.I.R. (total indicator run-out) and parallel to within 0.005 in., as measured around the periphery.

The finished magnet forgings satisfactorily met these sepcifications. The chemical check analysis of the steel, well within our specifications, was:

	%
C	0.110
Mn	0.330
P	0.010
S	0.030
Si	0.015
Ni	0.060

3.4. DESIGN AND FABRICATION OF MAIN COILS

Each of the two main coils is made of eight double pancakes of conductor wound successively onto the coil bobbin. The double pancake construction was chosen so that all water and electrical connections would be made at the outside of the coils. The sixteen electrical circuits thus formed are connected in series-parallel, arranged so that corresponding coils across the gap carry the same current to preserve symmetry. The total resistance of the circuit, 0.07 ohms, was selected to match the existing generator being used as the magnet power supply. As originally designed, each double pancake was to be wound from a single extruded strand of conductor 1170 ft long. It was found, however, that the conductor strands contained faults at the midpoint where the two

billets used in the extrusion failed to bond satisfactorily. Several feet of conductor around the fault was cut out of each strand, and the conductor was then d-c arc-welded together with a tungsten electrode in an argon atmosphere. X-ray pictures were used in inspecting each weld.

Paper insulation 0.020 in. thick and a laminated insulation consisting of a layer of 0.010 in. paper on each side of a layer of 0.001 in. "Mylar" polyester film were used throughout the coil. The paper was chosen because of its resistance to compressive forces and to abrasion encountered in the coil winding operation. The laminated insulation has these same mechanical qualities with the additional feature of maintaining its insulation property even when wet. Four layers of paper plus two layers of laminated insulation are used between adjacent pancakes, and one layer of paper tape and one layer of laminated tape are used between radially adjacent turns. An air drying alkyd resin was used to coat the insulation as it was placed in the coils. The form factor resulting from the insulation and water passage is 0.60. The conductor is secured by clamps inside the coil case and the entire assembly bolted to the magnet yoke.

As shown in fig. 6, the double pancakes were each wound from a single strand of conductor by first storing one half of the strand on top of the bobbin and then starting the winding at the midpoint. The turn table was then reversed for winding the second half of each strand, fig. 7. Fig. 8 shows the finished coils being attached to the yoke in the temporary installation being

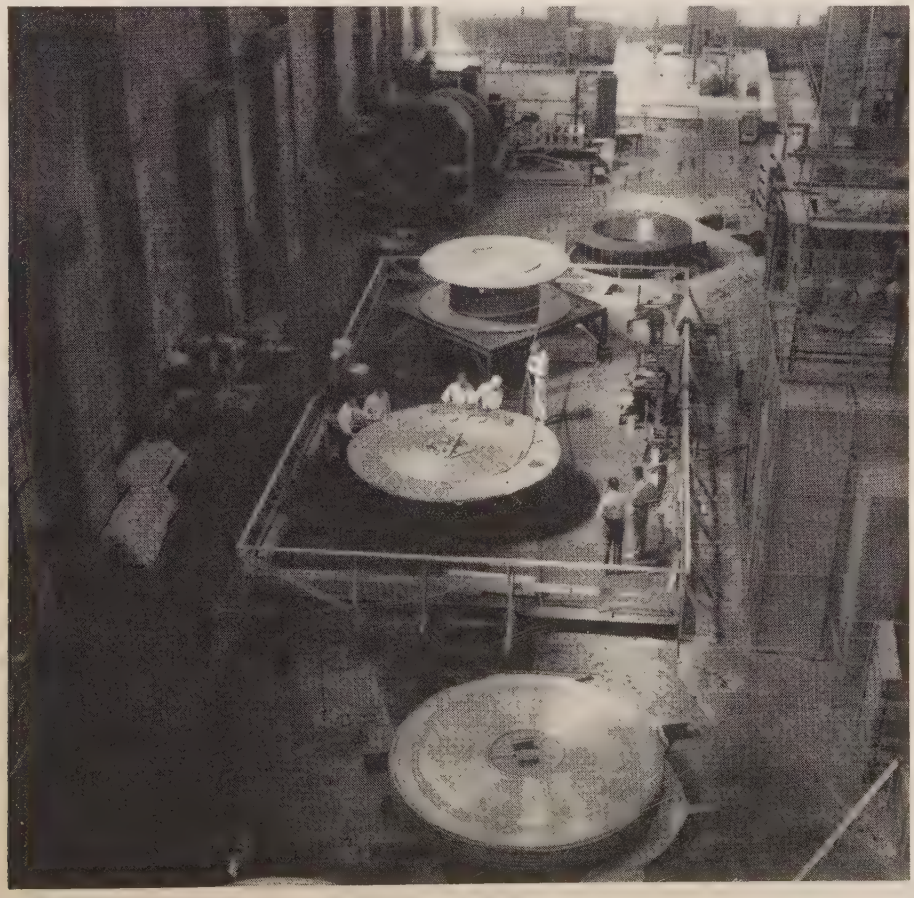

Fig. 6. Shop arrangement for winding main coils. Winding begins at the midpoint of each 1170 ft strand. Conductor shipment in foreground; second bobbin beyond winding area.

Fig. 7. Winding second half of sixth strand. Conductor enters from the left, varnished insulating tape from foreground.

used for magnetic field measurements. Some of the characteristics of the coils are given in table 3.

TABLE 3

Characteristics of main magnet coils

Total power	1034 kW
Ampere-turns	1.23×10^6
Total current	3838 amps
Current density	2113 amps/in.^{2}
Total turns	640
Form factor	0.60
Turns, axial/coil	16
Turns, radial/coil	20
Total resistance	0.07 ohms
Coolant ΔP	166 lb/in.^{2}
Inlet temp, max	100° F
Coolant, ΔT	60° F

3.5. POLE-TIP WINDINGS

In addition to the main magnet coils there will be three sets of coils on the pole tips, as shown in fig. 9. They are the AVF valley coils, the harmonic coils, and the pole-face circular trimming coils. The power supplies for all coils will be reversible, widely variable, and regulated to $\pm$ 0.01%.

The valley coils will be water-cooled copper, sealed in stainless steel containers and mounted in the valleys of the pole tips. The valley coils will oppose the existing magnetic field in the valleys, thereby increasing the magnetic field ratio between hill and valley, and thus increase the axial focusing forces on the ions. The six

valley coils will be energized, in series, from a separate motor-generator set.

The harmonic coils will be small water-cooled coils also palced in the valleys, toward the median plane from the valley coils. These coils will be used to compensate for undesired harmonics in the field. Each of the nine pairs of harmonic coils will have a separate power supply.

The pole-face circular trimming coils will be water-cooled copper windings mounted on the face of each pole. Ten concentric coils one conductor thick will be attached to each pole face. These coils will be used to obtain the isochronous field for various ions and to provide for some control over the magnetic median plane. Each of the ten pairs of trimming

Fig. 8. Placing completed coils in yoke, for temporary installation.

coils will also have a separate power supply.

Final specifications for the pole-tip windings will be made after further magnetic field measurements with the quarter-scale model magnet and with the full-scale magnet.

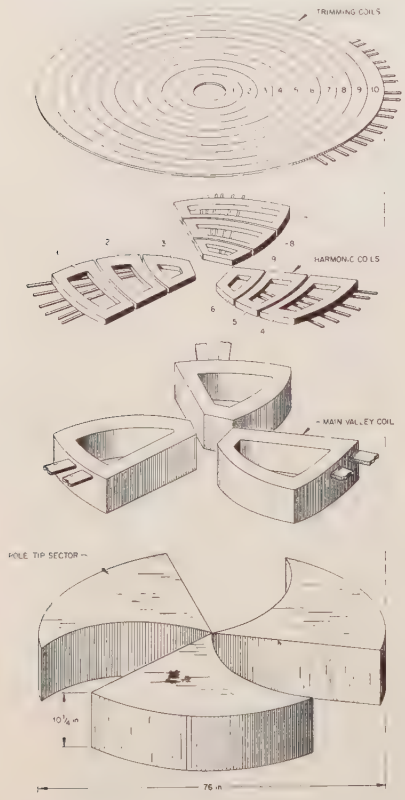

Fig. 9. Exploded schematic view of pole tip coils.

4. The Radio-Frequency System

4.1. REQUIREMENTS AND SPECIFICATIONS

A continuous frequency range is, of course, required of the radio-frequency accelerating system to provide a continuous energy range. Since it is possible to use harmonics to accelerate particles with the radio frequency at certain multiples of the ion rotation frequency, the frequency range actually required is considerably reduced. In the case of 180-deg dees, operation of the dees in the out-of-phase (or push-pull) mode makes possible the use of the first and all odd harmonics. Thus, the r-f system need tune only over a 3:1 range. Use of the in-phase (or push-push) mode on the dees would allow acceleration of the particles on even harmonics if the dees have an angular width less than 180 degrees. The required tuning range would then be only 2:1.

A 3:1 tuning range with the dees operating in the push-pull mode appears to be most satisfactory. The specified range is from 7.5 to 22.5 Mc/s. Operating with the r-f at the third and fifth harmonic of the orbit frequency would, in effect, bring the lower limit of the orbit frequency range down to 2.5 and 1.5 Mc/s, respectively.

The maximum energy gain/turn for this machine was originally set at 400 keV. Thus, with two 180-deg dees, a dee-to-ground voltage of 100 kV peak would be required. This requires a dee-to-liner spacing of 1.5 in., see fig. 5.

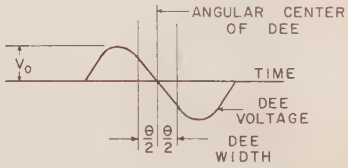

Fig. 10. Effect of angular width of dee.

A particle gains the maximum energy when it passes through the center of a dee, of angular width θ, when the dee voltage is zero, see fig. 10. Thus, for particles of the same frequency as the r-f, the maximum voltage gain/dee is $V_d = 2V_0 \sin\theta/2$. For particles rotating on sub-harmonics of the dee frequency, the angular width of the dee is $n\theta$ to the particle where n is the order of the sub-harmonic, and the energy gain is $2V_0 \sin n\theta/2$. Where $n = 3$ even a 15-deg wedge removed from the dee lip would cut the voltage gain/turn of heavy particles by 30%. Therefore, a dee width of 180 degrees was specified.

4.2. RESONATOR DESIGN STUDIES

Variable Characteristic Impedance. To achieve reliability and ease of tuning the resonator, one of the early goals in design was to avoid sliding contacts having a high current density. This consideration led to the so-called "barn-door" method of tuning. In this scheme, the liner surrounding the dee stems is moved toward or

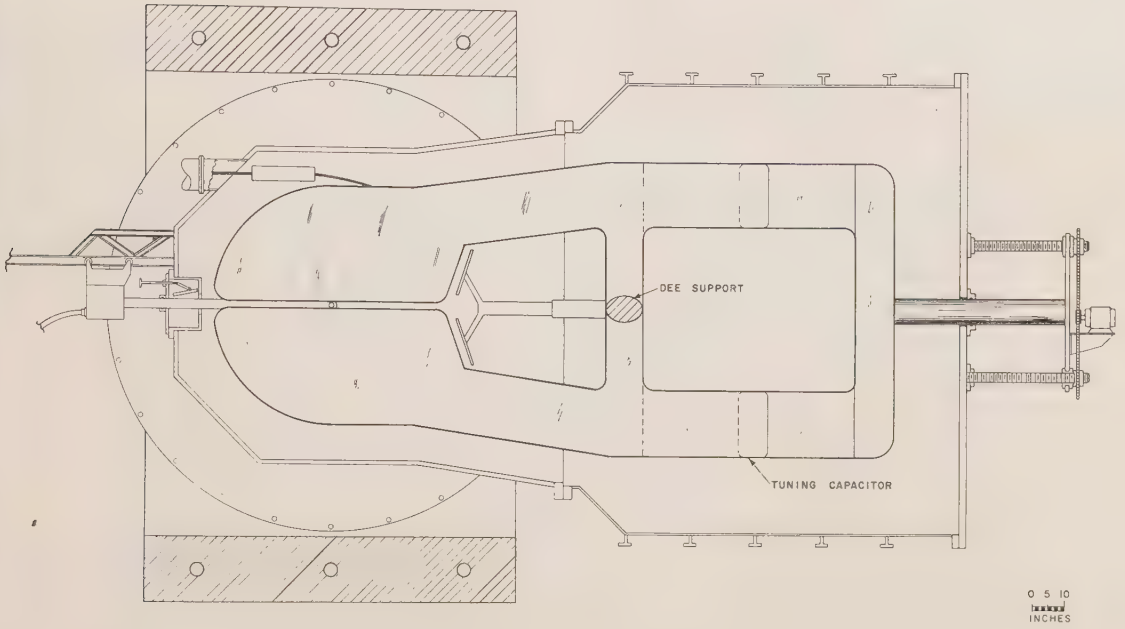

Fig. 11. A resonant system with fixed mutual inductance.

away from the stems to change their characteristic impedance and, hence, the resonant frequency. Within the limitations imposed by available space in the magnet, it was not possible to get the 3:1 frequency range without the addition of a movable shorting plane.

Coupled-Line Resonator. Another method of tuning which has no movable contacts and might be applicable to the ORIC case is the three-quarter wave system used on some synchrocyclotrons[21]). A resonator of this type is shown in fig. 11. This circuit configuration may be considered as two coupled circuits. The mutual inductance coupling the circuits is the central stem which physically supports the dees and dee stems. The tuning is accomplished by adjusting the large outer circuit and leaving the inner, or dee, circuit fixed. The natural resonant frequencies of two coupled lumped circuits are given in fig. 12. The circuit shown has a fixed value of mutual inductance so that the system may be tuned only along two of the lines of constant k. Therefore, it is impossible to tune to the region around $f = f_{01}$. In ORIC's case f_{01}, the self-resonant frequency of the dee circuits necessarily falls in the 7.5 to 22.5 Mc/s range; a

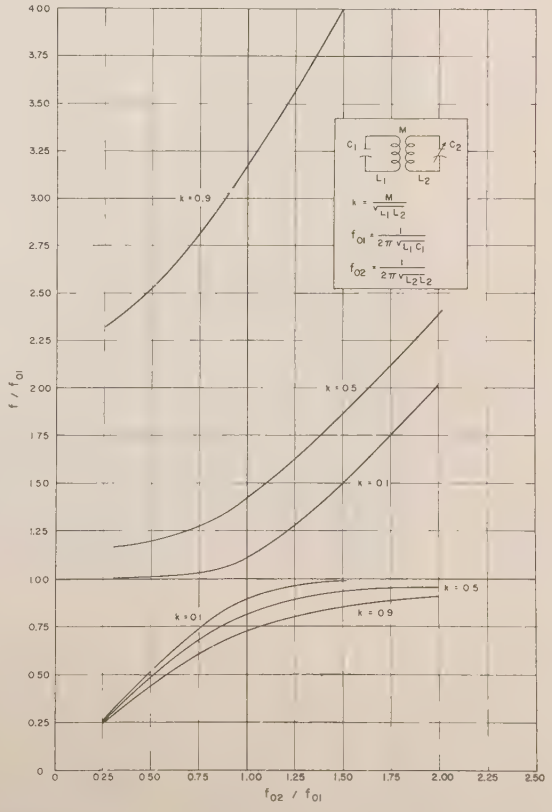

Fig. 12. Natural frequencies for two coupled circuits

[21]) K. R. MacKenzie, Preliminary Report on the "Three-Quarter-Wave" R-F System for Frequency Modulated Cyclotrons, AECD-1860 (Sept. 12, 1947).

fixed mutual inductance would mean leaving out a portion of the frequency spectrum. Although the resonator does not have lumped inductive and capacitive elements, the behavior of the system is, of course, quite similar to that shown in fig. 12.

A quarter-scale r-f model was built along the lines shown in the resonator of fig. 13. With variable mutual inductance the system could be tuned to all frequencies over a range greater than 3:1. To get a peak dee voltage of 100 kV and keep the r-f excitation power less than about 400–500 kW a coefficient of coupling of nearly unity must be achieved in the coupled transmission line region. It was not possible, however, to get tight coupling in this model; only a 30-kV peak dee-to-liner voltage could be obtained within the power limitation[22]). A second model of improved design is under construction.

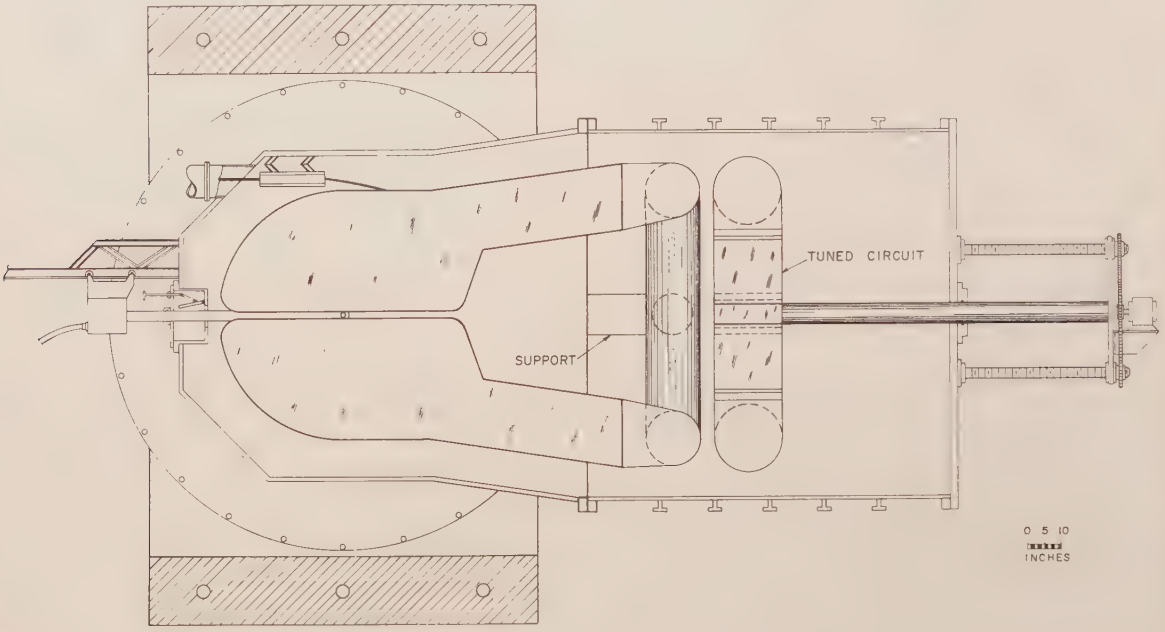

Fig. 13. A resonant system with variable mutual inductance.

Single 180°-Dee Resonator. Further investigation of the required threshold r-f voltage has allowed a reduction from the originally planned 400 keV/turn to 200 keV/turn. This can be provided with a single 180-deg dee. Unfortunately, it is essential to use movable contacts on the shorting plane to achieve the wide frequency range. A quarter-scale model of this type of r-f system was constructed, as shown in fig. 14. Tests with the model have suggested certain modifications. The modified full-scale system will have characteristics listed in table 4. The dee will be coupled to the driver tube through a capacitor and transmission line. The frequency is to be servo-controlled to better than 1 part in 10^5.

[22]) R. E. Worsham, in ref. [5]).

Table 4

Characteristics of R-F system with single 180-degree Dee

Frequency range	7.5 to 22.5 Mc/s
Dee voltage, max	100 kV
Voltage variation at dee lip, center to edge	+ 2%
Dee diameter	70 in.
Dee-stem diameter	50 in.
Shorting-plane travel	130 in.
Shorting-plane current density, peak	83 amps/in.
Excitation power	≈ 250 kW
Dee-stem characteristics impedance near Dee	11.9 Ω
Dee-stem characteristics impedance near forward shorting position	5.0 Ω

To achieve a stable external beam, it will be necessary to control the applied r-f potential to about 1 part in 10^3, thus insuring sufficiently identical paths for all particles as they are accelerated in the machine. The method proposed is identical with a system being installed for tests in the ORNL 86-Inch Cyclotron. The oscillator will operate with its plate at d-c ground. A series regulator tube will be placed in the positive lead of the high voltage power supply. The series regulator tube which controls the oscillator plate voltage will then be controlled by a signal from the r-f voltmeter at the dee.

Fig. 14. Quarter-scale model of the single 180-deg Dee system.

4.3. ENGINEERING DESIGN

A conceptual design of the single 180-deg dee resonant system and vacuum chamber has been

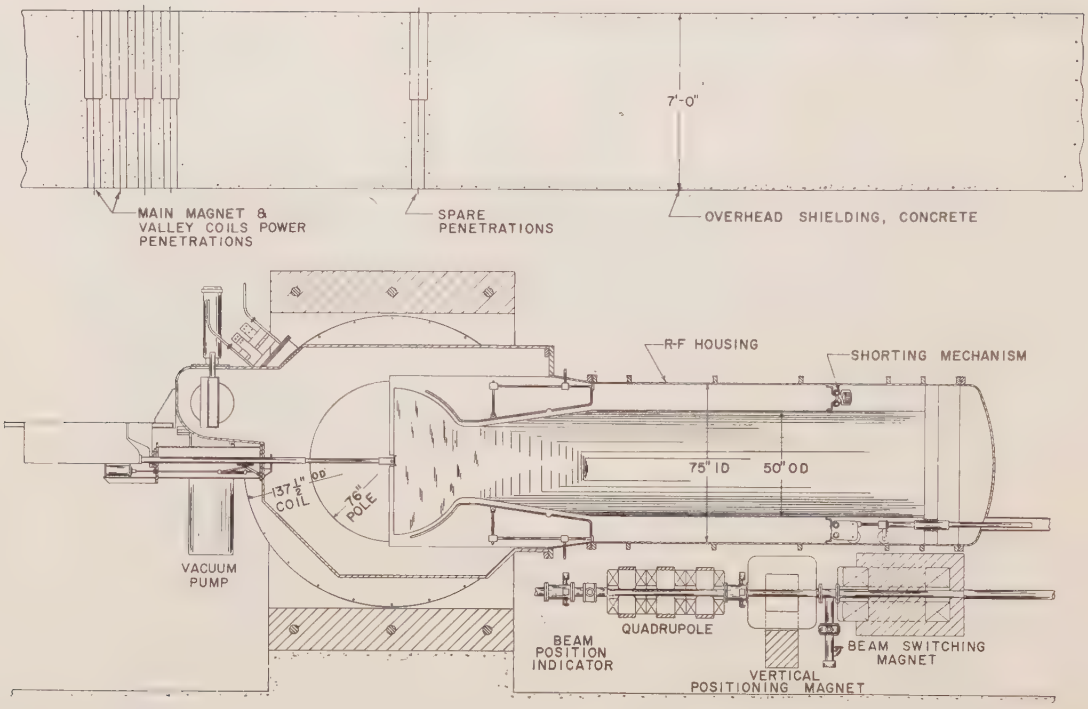

Fig. 15. Section through ORIC showing features of R-F system.

completed, fig. 15, and engineering details are being worked out. The r-f housing and dee stem will be constructed of either silver- or copper-clad stainless or carbon steel. The dee and the transition section extending out to the 50-in. diameter stem will be constructed of copper sheet.

The system will be tuned by means of a shorting bar, or "spider", which makes knife-edge, high-loading contact with the peripheral surfaces of the dee stem and the liner wall. It will consist of 48 pneumatic units of the type shown in fig. 16; each unit operates independently. In use, the knife edges are held against the dee stem and the liner wall by the bellows shown. This bellows is designed to produce a loading of 100 lbs/linear inch of contact surface when operated at maximum pressure. When it is required to move the spider, the pressure is released and the bellows are collapsed by spring action withdrawing the knife edges from the stem and liner wall.

It is expected that the design will accomodate an out of roundness of stem and tank of approximately $\pm \frac{5}{8}$ inch. This is an important factor since the cost of machining the inside of such a large tank is somewhat prohibitive.

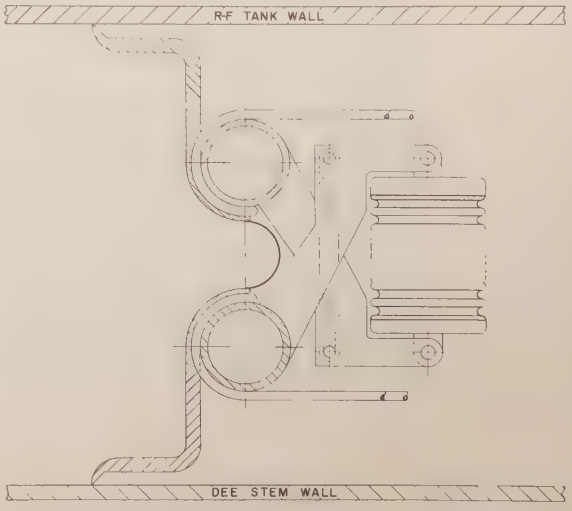

Fig. 16. Pneumatically operated shorting mechanism, one of 48 units.

In operation the spider will be positioned along the dee stem by use of three telescoping screws driven by a chain system behind the dee-stem

support structure. To meet the requirement of the r-f tuning of the machine the spider must be capable of being positioned to within less than $\pm \frac{1}{4}$ inch of any desired position. The fine tuning will then be done by moving the trimming capacitors.

The dee-stem structure will be cantilivered from the dee-stem house at the r-f ground end, and the spider will be positioned forward of this point. An auxiliary vacuum pump will be attached to the dee-stem house to pump directly on the volume restricted by the spider. The entire resonant system will be mounted in or attached to the dee-stem house and will be portable, probably mounted on a transporter.

The ion source and beam probe are also shown in fig. 15. They will be mounted on carriages suspended from overhead rails. The entire system will be motorized so that the source-probe unit can be brought outside the shield wall of the cyclotron room for repairs and returned to the machine remotely.

The ion source for the ORIC will be of the hot cathode type developed and used in other cyclotrons at ORNL. The 3-mA proton currents obtained from the 86-inch cyclotron indicates fully adequate beam current for low-mass ions. The ion species higher than plus 4 (for nitrogen) have not yet been measured due to lack of resolving power; however the ion currents of 10 mA for N^{3+} and 2.6 mA for N^{4+} already obtained in ion source tests lead one to expect satisfactory results for high order species. A new test system is planned to search for the higher ion states, although the basic cyclotron design does not depend on them.

5. Scientific Motivation

The following is a broad and rather general survey of the areas of research open to a cyclotron of the type described above. Some specific fields are indicated which at this juncture seem manifestly worth investigating. It can be seen that a flexible program of research will proft extensively from the availability of different bombarding particles, from a continuously variable energy, and from intense non-pulsed beams.

Nuclear Spectroscopy. The location of nuclear energy levels and the determinations of their properties, such as spin, parity, width and electric and magnetic moments is perhaps the most important source of information on nuclear structure. Many new techniques for these studies are made available by the use of medium-energy nuclear reactions. The utility of deuteron stripping as a well-known example. Experimental evidence obtained at this laboratory and elsewhere indicate that (p,d) reactions as well as (d,p) reactions strongly excite single particle states. These reactions are, therefore, powerful tools in nuclear spectroscopy, especially when both reactions can be explored in the same laboratory to determine the locations of filled and unfilled neutron levels. The availability of other particle types might open up an exploration of proton bound states also, through (t, α) or (d, He^3) reactions for example. As other nuclear reactions are studied and become understood, there is every reason to believe that new spectroscopy techniques will evolve from them. Precision spectroscopy requires large, high quality beams of variable energy.

Nuclear Reactions. A most important source of information on nuclear interactions is the study of mechanisms for nuclear reactions and scattering. The work on heavy-particle transfer reactions at this laboratory provides an excellent example of this. Nuclear reaction studies become most interesting in the energy region between 10 and 100 MeV, which is just the region covered by the ORIC. The availability of a large variety of energetic ions is a most important asset in this work. Since coincidence techniques will be necessary in most of these studies, a cyclotron with its essentially continuous beam possesses great advantages over machines which provide only pulsed beams.

Coulomb Excitation. Since electric interaction is well known and understood, Coulomb excitation provides a unique opportunity for studies of nuclear structure. While extensive work in this field has been done with protons and alpha particles, work with heavy ions is still in its infancy. A variable energy would be of great

advantage in these studies because experience with heavy-ion linear accelerators has shown that energy reduction with absorbers introduces very serious backgrond difficulties.

Polarized Particles. Investigations with polarized particles are gaining in importance. The primary requirement for the production of such particles is a high intensity beam. It is interesting to note here that polarized protons may be produced in two ways: from p-He^4 scattering and from the equivalent α-H scattering. The latter is preferable in many cases because it gives higher yields. For example, the production of 20-MeV polarized protons gives about fifty times higher yields from the α-H scattering than from the p-He^4 scattering. This case represents the highest energy proton for which polarization calculations have been made. Of course the investigation of polarization of, say, p-He^4 scattering at higher energies is a promising field in itself. Here again, variable energy is of great importance.

Solid State Physics. There should be many applications for the accelerator in the field of solid state physics. The study of radiation damage is facilitated by the high power output of the beam. The 75 kW of beam available will, in general, be more than can be dissipated in the target. As a consequence, the time required for a given effect will not be determined by the accelerator but by the maximum temperature allowable in the target. The range of 75- MeV protons in aluminum is about 2 cm; this permits the use of relatively thick targets and a study of the effect of charged particles in the interior of the target material. With the acceleration of heavy ions to 100 MeV the surface effects of irradiation can be studied. Also, high-energy heavy ions can be used to simulate the effect of fission fragments without the high radiation background of a reactor. The use of protons or deuterons may be a major advantage over the use of reactor neutrons in that all the charged-particle energy is dissipated in the target.

Atomic Physics. The range-energy relations and the dependence of the ionic charge on the velocity have long been of interest to physicists. The field is still inadequately explored experimentally and theoretically. Different particles with variable energy provide an excellent tool for studies of this sort.

Obviously, research will not be performed at the same time in all the fields enumerated above. It is evident, however, that the great flexibility of the machine will make its use possible in any field which appears most interesting at the time. The flexibility also guarantees, as much as can be done for any accelerator, that it will not become obsolete. As long as there is interest in the structure and properties of the atomic nucleus, the ORIC will be a useful machine.

6. Experimental Facilities

It is clear that massive walls will be required to keep the radiation level safe; provisions for flexibility of operation must be built in from the beginning. With the varied and complex type of experiments to be done with the ORIC, the experimental facilities must be carefully planned to provide for efficient use of the machine. Ever increasing demands are made on the experimental nuclear physicist which involve both higher precision and the measurement of more complicated phenomena. It is essential that one have enough time to set up and thoroughly test the apparatus before taking data. Since the equipment may include such itmes as 20-ton analyzing magnets, 6-ft dia scattering chambers, and complicated electronics, this testing must be done in the same room and position where the actual data will be taken. at least two separate rooms are needed so that while data is being taken in one room, the radiation level is low enough in the other room to permit the preparation of apparatus for the next experiment.

6.1. SHIELDING

The design of the shielding and the experimental layout requires a reliable estimate of neutron yield. The shielding thickness determined by the fast neutron flux is more than adequate to

reduce the thermal neutron and gamma ray flux to a safe level. The experimental data of Crandall and Milburn[23]) indicate a yield of about one neutron for four 75-MeV protons hitting a thick target of high atomic number. Thus, a one-milliampere beam of 75-MeV protons would produce a point source of 10^{15} neutrons per second.

The most practical shield, in view of cost and general utility, is ordinary concrete. The thickness of such concrete to reduce fast fission spectrum neutrons to one tenth the intensity is 11.8 inches. If we assume that the effective neutron source is 20 ft from the shielding wall, the flux is $\sim 2 \times 10^8$ neutrons/cm^2–sec. A 7-ft thick concrete wall will reduce the flux to 16 neutrons/cm^2-sec; this is well within the allowed level.

There are several assumptions made which in certain unfavorable cases could increase the radiation level. For example, the distribution of neutrons from a target will not be isotropic but peaked in the forward direction. Furthermore, the energy spectrum will certainly contain neutrons of higher energy than fission neutrons, and the effective source (where the cyclotron beam is stopped) may be closer to the wall than 20 feet. In these cases, it will be easier and more practical to place small quantities of additional shielding in the vicinity of the target. For local shielding it would be possible to use special shields of more complicated construction, such as layers of iron and concrete, for those cases where an unusually high yield of neutrons is involved. Since for many applications the beam power will be lower or the particles used will produce a much smaller neutron yield, the occasional need of assembling a one or two foot thick shield around the target will not be a serious disadvantage.

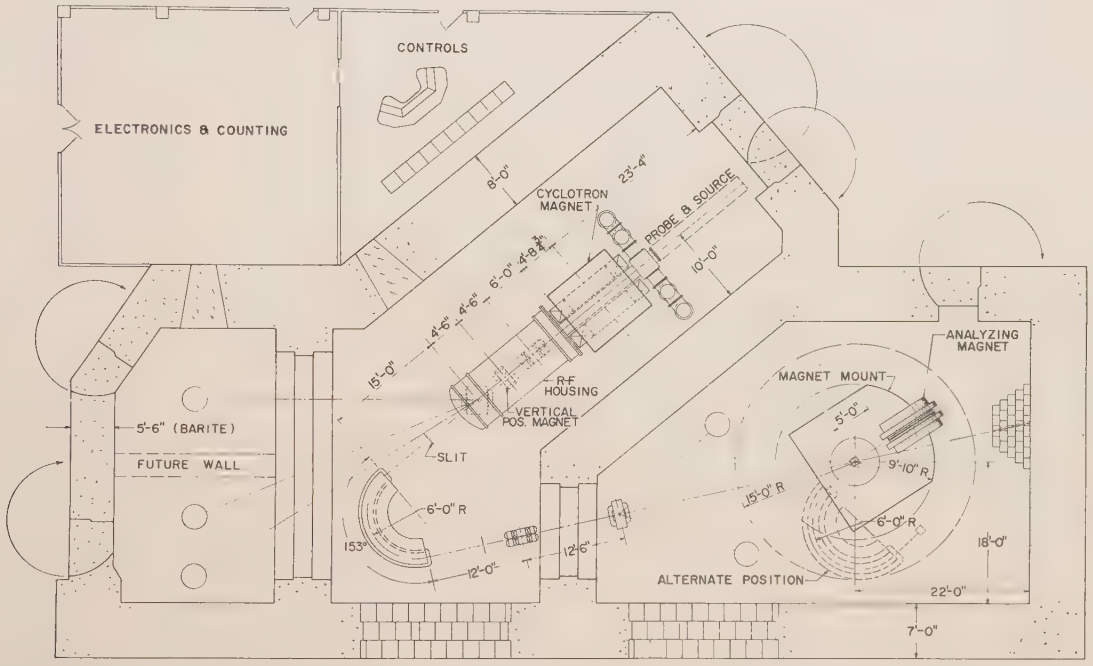

Fig. 17. Shielded cyclotron room and experimental areas.

6.2. EXPERIMENT ROOMS

The plan for the shielding structure, fig. 17, provides for two experimental areas in addition to the cyclotron room. The external beam of the cyclotron passes through a magnetic quadrupole

[23]) W. Crandall and G. P. Millburn, Neutron Production at High Energies, J. App. Phys. **29** (1958) 698.

lens for focusing and then through a beam switching magnet. The cyclotron operator can, by adjusting the field of the switching magnet, direct the beam to any one of several places in the smaller experimental area. A slot in the concrete to pass several evacuated pipes will allow adjustment so that the beam can be directed to the several different experimental setups. The slot in the concrete can be filled with water or blocks to minimize leakage of radiation from the cyclotron. If the pipes do not point in the direction of a source of radiation, it should be safe to work in the room while experiments are being done elsewhere. This area is large enough that it can be partitioned into two rooms by adding a shielding wall at small cost, if the demand for separate experimental facilities requires it. The magnet for switching the beam will also have sufficient energy resolution for it to be used to determine the energy and the energy spread of the beam. Experiments which do not require high-energy resolution, such as statistical theories of nuclear behavior, production of transuranic and new isotopes, polarization scattering effects, and cross-section measurements can well be done in this smaller room. The second experimental area is quite large to permit minimum background and controlled energy conditions.

For certain types of experiments high energy resolution is necessary. The density of energy levels increases with excitation energy and atomic weight of the target. Furthermore, the number of nuclear reactions leading to different ourgoing particles increases rapidly. High energy resolution is needed to resolve discrete levels or, if the level density it too great, to examine fine structure in the spectrum. Also, one can usually distinguish the outgoing particle, and quite often the mass of the recoil nucleus, by measuring the energy of the outgoing particle as a function of angle of scattering. The energy depends on the mass, and sufficient precision of measurement is then a valuable tool. In addition to precise magnetic analysis of the beam striking the target and of the outgoing charged particles from the target, an increasingly useful technique is time of flight. This requires a large room, both in order to have sufficient time intervals and to reduce background produced by radiation scattered from the walls.

Two large analyzing magnets have been designed with a dispersive power of 20 keV per millimeter for 75-MeV protons. To limit the physical size to a reasonable value they have nonuniform, double-focusing fields with $(r/B)\ (\mathrm{d}B/\mathrm{d}r) = \frac{1}{2}$. The problem of shaping the magnetic field is small compared with the doubling in size required to obtain the same dispersive power with a uniform field magnet. By using slits one millimeter wide and a thin target, an energy resolution of 50 keV for 75-MeV protons becomes possible. Where less resolution is adequate, the slits can be increased, a thicker target used, and a larger solid angle of detection is possible, reducing by a major factor the time needed to get adequate statistics. One can thus adjust to optimum value the amount of beam, energy, and energy spread of the beam.

If a large amount of beam were to be stopped by slits placed in the experimental area, the background would be very high. Furthermore, thick slits are required to stop 75-MeV protons. If the thickness of the slit is greater than the slit opening, an appreciable fraction of the beam will be scattered by the slit edges and would strike a nearby target. The slit is placed, therefore, inside the cyclotron enclosure, and a magnetic quadrupole lens is used to focus the desired beam through the slits onto a target placed in the center of the large experimental area.

A second magnetic analyzer similar to the previous one is used to analyze the outgoing charged particles from the target. This analyzer can be rotated about the target to cover an angular range of 160 deg in the laboratory system. To reduce background further, provision is made for a quadrupole lens to focus the beam which passes through the target into a shielded area in the wall.

The recent progress in solid-state barrier detectors makes it possible to use a large number of narrow detectors placed side by side. In this case a magnet which focuses over a large spread

of energies possesses many desirable features. With sufficiently complicated electronics, it is feasible to take precise data over a wide energy interval in a relatively short time. One is no longer limited, as in photographic emulsions, to measuring after the experiment is over but can see the results and can immediately correct for maladjustment or more detailed investigation of possible anomalies. In addition, coincidence techniques can be used. Plans are in progress to install a magnet of this type also on the magnet mount.

Part II will describe the magnet studies basic to the design of the azimuthally varying field.

NUCLEAR INSTRUMENTS AND METHODS 6 (1960) 26–32; NORTH-HOLLAND PUBLISHING CO.

ENGINEERING METHODS FOR ELECTRON-BEAM PROCESSING

D. A. TRAGESER

High Voltage Engineering Corp.

Received 24 August 1959

Improved economics for electron processing depend upon the development of new accelerators and better engineering methods for their use. The scope of future processing accelerators embraces a range of 0.5 MeV to 15 MeV in energy, and 1 kW to 1000 kW in power. New developments include (1) accelerators in the 0.5 to 2 MeV range, with power outputs of 10 to 100 kW, and (2) a series of linear accelerators in the 3 to 9 MeV range at about 5 kW, with flexibility of energy adjustment at maximum power. Longer-lived components are also under development.

The shielding for a processing installation can be minimized by the use of a shallow pit with local shielding around the point of beam use. Examples of this design are shown for processing film or wire, and for conveyorized materials. The cost of a facility for a 1.5 MeV, 2.5 kW installation has been estimated at $ 9000.

Magnetic systems can be used to change beam geometry external to the accelerator. A beam inverter has been developed so that a product can be bombarded from both sides simultaneously with one accelerator.

An intermittent filter has also been tested. The efficiency of double bombardment is thereby increased to about 80%, because the uniformity of dose is greatly improved. The optimum filter for a 2 MeV beam is about 0.25 g/sq. cm thick used in 331% interruption of the beam.

The availability of new metal alloys in the form of thin sheets and thinwalled tubes makes possible the development of new techniques for irradiating fluids under elevated pressure and temperature in continuous flow. Scanned electron beams at 1 or 2 MeV can treat liquids in flanged reactors with thin windows.

This will permit pressures up to about 40 atmospheres, with a 90% beam-use efficiency. Tubular reactors permit pressures of 75 atmospheres with a 50% efficiency.

1. Introduction

The immediate importance of electron processing as an industrial tool depends significantly on the uniqueness of the process achievement, because the engineering methods for its use revealed to date are somewhat restrictive in comparison with conventional processes, and the economics are typical of a beginning industry. Achieving process uniqueness, which is primarily the concern of the potential process user, not only demands the utmost skill in the direction taken in applied research, but also imposes considerable inventiveness in product development. Improved economics and the unleashing of better engineering methods demand considerable ingenuity, too, on the part of the equipment manufacturer.

Three areas of engineering development which will bring nearer a more general use of electron processing will be described. These areas concern (1) the accelerator itself, (2) the facility used to house it, and (3) various techniques for its industrial use.

2. Processing Accelerators

While it is speculative from the machine manufacturer's viewpoint to pinpoint the changes that can take place in the cost of accelerators over as long a period as that for which projections about isotope costs are made, general assurance can be given that significant economic improvement is likely, as stimulated by the development of applications. The detailed pattern to be taken by applications development is unknown now but will nevertheless be important. In our minds, the scope of future processing accelerators embraces a range of 0.5 MeV to 15 MeV in energy, and 1 kW to 1000 kW in power. Many energy-power combinations are possible within this range. We are already developing some of these combinations which are not covered by existing accelerators. For example constant-potential accelerators in the 0.5 to 2 MeV range with beam currents of 20 to 50 milliamperes, and hence with power outputs of 10 to 100 kW, look promising. Prototypes of three different designs which will

operate at about 1 MeV are now under construction at High Voltage.

We have also developed a series of linear accelerators, in the range of 3 to 9 MeV. Power ratings vary from 6 kW at the lower end of the energy range to 4 kW at the higher end. Simplification of design was a major objective in this program, so that all of the components, except the acceleration tube, are identical for all accelerators in the series. New power tubes at higher ratings have also become available. They can be incorporated in the same accelerator at a small incremental cost. This design also provide the flexibility for the user of changing from one energy to another in this range, as dictated by process needs, with only minor modification to the equipment.

In addition, we are placing great emphasis on the development of longer-lived components for all acclerators. Statistical methods are being used to isolate each component's effect from the complex inter-relationship among the many elements of the whole accelerator. Our aim is to achieve the same degree of performance from the processing accelerator as is realized by conventional industrial equipment.

The significant economic factor for industrial use, after all, is the cost per kilowatthour. Thus, the elements of both operating and capital cost are being attacked simultaneously. The extent of our accelerator-development program on both these "fronts" indicates our confidence that further stimulus will be provided by those applications which can take advantage of new packaging methods and product or process improvement. We are furthermore convinced that, in general, accelerators will increase their already large margin of economic advantage over the by-products or waste products of nuclear power reactors, even in a mature, nuclear-power economy.

3. Processing Facilities

Considerable ingenuity is possible in the design of installations for electron processes. Research installations do not furnish a pattern for the design of processing facilities. Therefore, cost extrapolations from them are not reliable.

The ideal for minimum cost can be achieved by minimizing the volume of built-up shielding surrounding the accelerator and the process material. A minimum shielding perimeter around the point of beam use would accomplish this objective. The use of local shielding, "tight" to the beam-tube extension is compromised, however, by the need for access to the tube's window and to the process material underneath it. Therefore, part of the local shielding should be removable without undue expense.

One way to obtain local shielding relatively cheaply is to excavate a shallow pit for the process line. Shallowness should be emphasized, because there is undoubtedly an optimum point of excavation beyond which its expense equals or even exceeds the saving in built-up walls. Another factor which adds to excavation cost is that of conveying process material from the grade level to the pit under the beam.

One design which includes a shallow pit is shown in fig. 1. Movable dollies in the pit on either side of the scanner are used as platforms for poured concrete, or for blocks, to provide most of the shielding along one axis, while the pit walls themselves act as shields in the other directions.

Wheels for the dolly platforms ride on rails built into the pit floor. Platform legs are high enough for the process material to pass underneath. The personnel entryway to the facility is relatively simple.

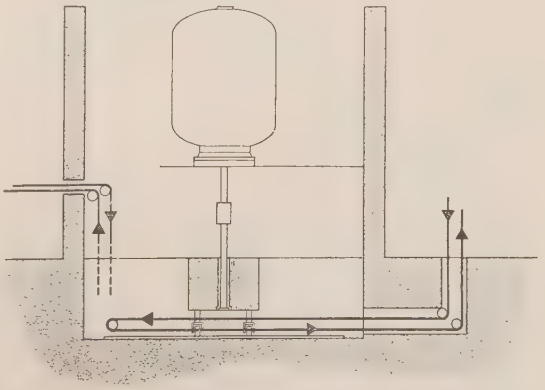

Fig. 1. Product entries for pit installation.

Costs based on this design have been estimated in detail by an engineering architect for the housing of a 1.5 MeV, 2.5 kW accelerator. They enters and leaves the facility through one small opening, which is separated from the large personnel entryway. The opening is placed out

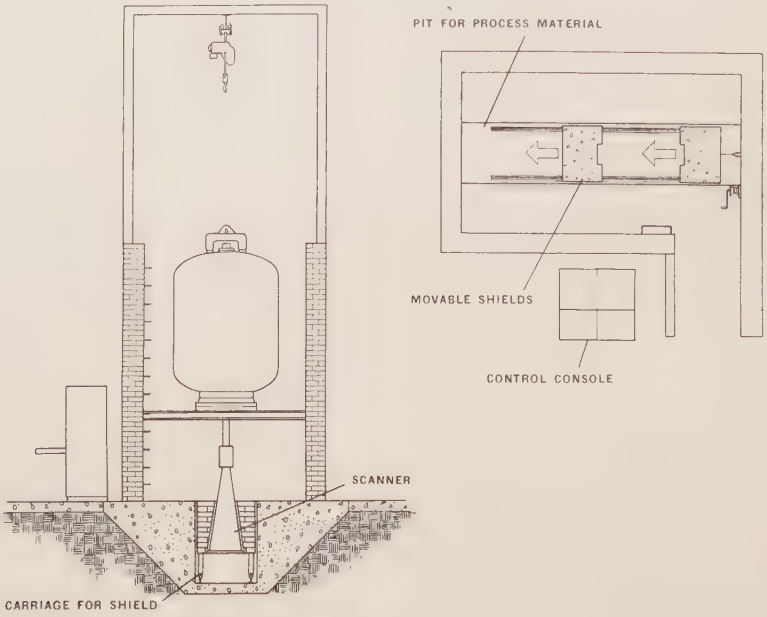

Fig. 2. Processing facility with pit.

total $ 9,000, given existing floor space and adequate overhead room in a factory building. This does not include allowance for product entry and removal.

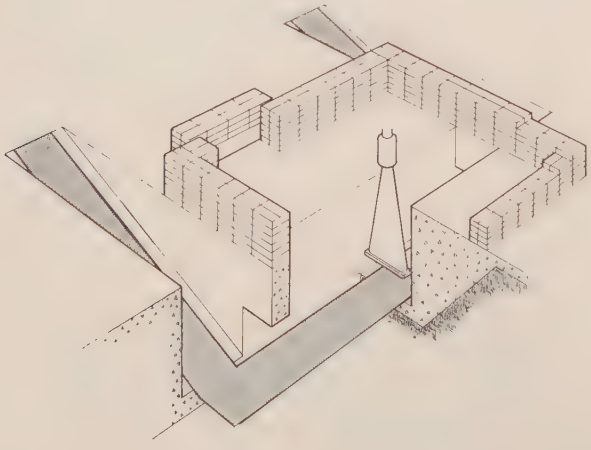

Fig. 3. "U" Shaped conveyor line for pit installation.

Two methods of handling non-conveyorized materials are shown in fig. 2. In either case, flexible process material, such as film or wire, of direct view of the unshielded beam, so that a least one scatter from a wall surface occurs before electrons or X-rays emerge to the operating area. Radiation survey measurements in our Burlington Processing Facility show that, in such a case, X-radiation from a 1.5 MeV, 2.5 kW beam is reduced below tolerance outside within a few feet from the opening in the wall.

Sloping aprons are needed when conveyors are used. A U-shaped handling system is shown in fig. 3. A straight-line apron system might also be used.

Many modifications of this idea are possible according to the nature of the material processed and the size of accelerator used. Therefore, although the example shown here is not a universal model for processing, it indicates that surprisingly low facility costs can be achieved.

4. Industrial Techniques

Another area of potential economic gain is that of increasing the efficiency of beam use, or of applying it to a wider variety of materials.

Many mechanical methods have already been used experimentally for unusual product geometries or thicknesses. Among them are the roll treatment of film; the spinning of fluids in tubes; the bombardment of wire insulation from each side continuously; the rotation of wire on its axis while moving continuously under the beam; the rotation of spherical objects while under the beam; and the treatment of solids at inclined angles. In addition, there is a large potential area of application which can be realized by modification of the beam itself. Greater scan widths than our present standard of 15 inches are under development. There are also many possible ways that other magnetic systems can be used, external to the basic accelerator, to change its characteristic geometry.

One of the magnetic systems will be discussed here, along with several other techniques. Each method involves relatively inexpensive equipment. Further engineering development is of course necessary for use in specific processes.

4.1. BEAM INVERSION

The first technique is the magnetic inversion of a beam to give simultaneous double bombardment from one accelerator.

Rigid materials are commonly irradiated with an electron beam from only one side. Under these conditions, the optimum product thickness to use with a monoenergetic electron beam is about two-thirds of the total range of the beam. At this thickness, the efficiency, which is a combination of total energy absorption and dose uniformity, is at a maximum.

In general, double bombardment increases the efficiency because a greater percentage of the beams' range can be used, from each side, with the same overall uniformity of dose distribution as that obtained in the optimum case of single bombardment. The optimum thickness for double bombardment is about 2.4 times that of single-side treatment. This means, for example, that a 2-MeV electron beam used in a double bombardment process on an industrial product has a useful penetrating ability nearly equal to that of a 5-MeV beam applied to a single side of the same product.

Solid materials which are processed on a conveyor in boxes or trays can be turned over manually or automatically, to accomplish the double irradiation. However, this cannot be done when packaged fluids, such as liquid solutions of drugs, are treated, because the fluid will move between exposures. Also, other solid materials which are not treated on conveyors may sometimes be difficult to turn over between passes. For example, some electrical cables are too stiff to be wound around small pulleys to return past the beam for a second bombardment with the opposite side exposed. In all these cases, simultaneous bombardment from both sides is needed to gain the higher efficiency and increased penetrating ability of double bombardment. This can be done with the beam from a single accelerator.

We have developed a method in which two separate magnetic fields are used to bend each

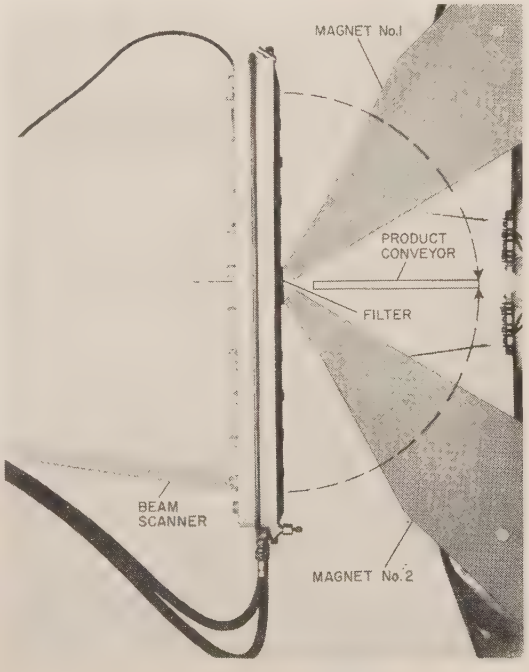

Fig. 4. Model of beam inverter.

half of a scanned beam through an arc of 90°. The two portions of the beam converge from opposite sides in a plane at right angles to the

original plane of the scanned beam. The general arrangement of this system is shown in fig. 4. This process can be used on products up to about 6 in. wide with 15-inch scanning. When tests are completed on a linear scanning system for 30 in., the useful width in the inversion process can be increased to about 12 in.

Tests made with a 2-MeV beam from a Van de Graaff accelerator show that the integrated dose a product receives in passing by the exit of the magnet-deflecting system is uniform within 10% over the entire scanned width. These tests also show that the amount of beam power lost by scatter in air to the magnet pole pieces is less than 10% of the available power entering the magnetic system. Thus, beam inversion can be made practical for industrial applications with existing accelerators.

4.2. INTERMITTENT FILTERS

Another technique concerns the use of special filters to increase the efficiency of double bombardment.

As mentioned previously, the efficient use of electron beam power depends on the fraction of the total energy which is intercepted and the acceptable uniformity of dose distribution. Since the characteristic absorption curve for monoenergetic electrons passes thru a maximum, uniformity of dose can be improved by inserting another absorber, such as a filter, between the beam and the product. If the filter is of a certain thickness, the efficiency for double bombardment can be increased to more than 70% despite the added loss in the filter, because the uniformity of dose is so greatly improved. Of course, the thickness of product at the maximum efficiency is not as large when a filter is used.

An intermittent filter achieves further gains in efficiency through increased uniformity. The energy absorbed in the product is the sum of the effects which would be achieved separately if the filter were permanently in, or permanently out, corrected for the proportion of time during which each condition exists. The net effect depends on both the filter thickness, and the percentage of the total time during which it is in the beam. The latter factor is called the per cent interruption.

The uniformity of dose and the fraction of

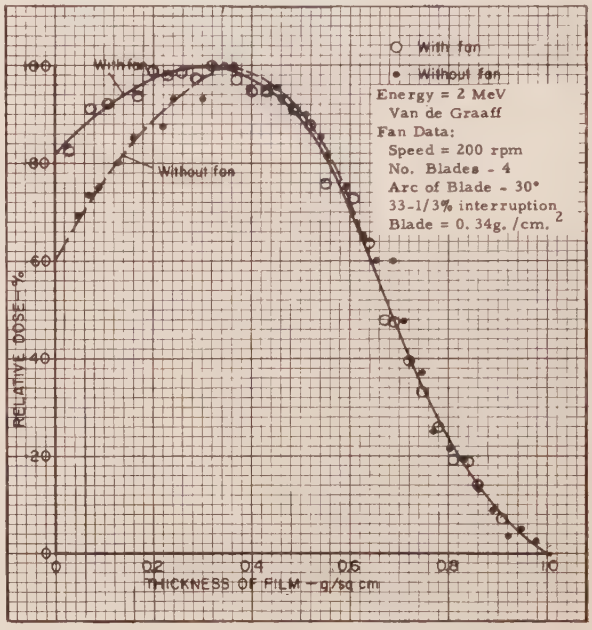

Fig. 5. Effect from rotating fan.

energy intercepted have been calculated for a number of intermittent-filter systems to find the optimum combination of filter thickness and per-cent interruption which would produce the highest net efficiency. The optimum filter for a monoenergetic 2-MeV beam is about 0.25 g/sq. cm thick used in $33\frac{1}{3}$% interruption of the beam. The depth efficiency calculated for this system is 84% in double bombardment.

Either a moving screen or a rotating fan can be used to interrupt the beam. In the experiments reported in fig. 5, a three-bladed fan rotating at 200 rpm was used with a 2-MeV Van de Graaff accelerator. The results confirm that use of the fan makes a significant change in the dose-depth curve.

This technique is easily adaptable to an industrial application where double bombardment is used, with or without a beam inverter. Only simple, mechanical equipment is needed to produce an efficiency of about 80%.

4.3. FLUIDS UNDER PRESSURE

A third technique is the application of electron beams to fluids in continuous flow under elevated pressure and temperature.

The availability of new alloys in the form of thin sheets and thin-walled tubes with high ratios of strength-to-weight, together with the development of new beam-handling techniques, makes this possible.

High efficiencies can be achieved if the design of the irradiation chamber takes ad van tage of electron beams which are scanned to a long length in one direction and yet are confined to a narrow width in the other direction. Several advantages are realized by aligning the reaction tube or narrow chamber with the direction of scan. First, a long path for mixing during the irradiation period is obtained. This insures that the irradiation dose is uniformly distributed in the fluid without requiring too high a velocity or incurring too large a pressure drop, and probably without the need of special baffles to eliminate "dead" spots which occur over short lengths of flow. Furthermore, large accelerator beam currents can be used without overheating the thin wall of the reaction chamber.

The best type of reaction chamber depends upon the pressure to be used. A welded, rectangular chamber with a flange for holding a thin, flat sheet seems best for pressures up to about 30 or 40 atmospheres. Its depth can be greater than the range of the energy used, which is about 0.2 inch of water for each MeV of monoenergetic beam. The optimum depth lies between that which makes the flow chamber so shallow that pressure drop becomes excessive, and that which is so much larger than the beam range that thorough mixing in the given reaction length is not obtained. The reactor can be reduced in size from the piping to which it is connected by appropriate Venturi sections, as shown in fig. 6.

Appropriate pressure-relief points should of course be provided in the pressurized system, to prevent failure of the reaction-chamber window.

Design data which have been calculated for one example of this type of reactor indicate that the beam-use efficiency is higher than 95% at 2 MeV, or higher than 90% at 1 MeV, for pressure up to 35 atmospheres. A minimum flow is needed to produce turbulence during passage under the scanned beam. The amount of radiation dosage which is delivered during each pass depends on the beam power. If the power available is too low, a recycle flow system with a reservoir should be arranged, to maintain a high enough flow rate for turbulence.

When fluids under pressure greater than 35 atmospheres are irradiated, it may be more convenient to use a tubular reactor in place of a flanged, welded chamber.

Titanium and aluminium tubes are both available with walls as thin as 0.005 in. so that reasonably high efficiencies can be obtained at substantial pressures, even with 1–3 MeV electron beams. Aluminium tubes sized from $\frac{1}{4}$ in. to 2 in. diameter would probably allow working pressures up to about 75 atmospheres at 70° F. Titanium, in sizes from $\frac{3}{16}$ in. to $1\frac{1}{8}$ in. diameter, would be most useful at pressures of 75 to 150 atmospheres at 70° F, or at one-half these pressures at 500° F. Hydrostatic bursting tests of titanium tubing have shown that the bursting pressure exceeds by 40% the allowable working

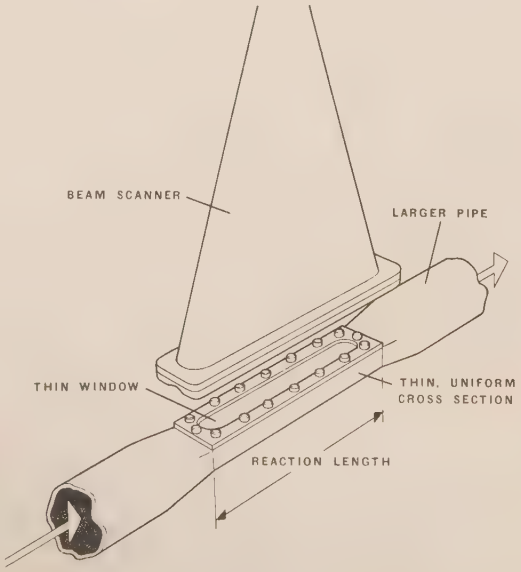

Fig. 6. Processing fluid in flow reactor.

pressure calculated from published values of yield strength. Nevertheless, more conservative values than even the yield strengths by a factor of two have been used in all calculations.

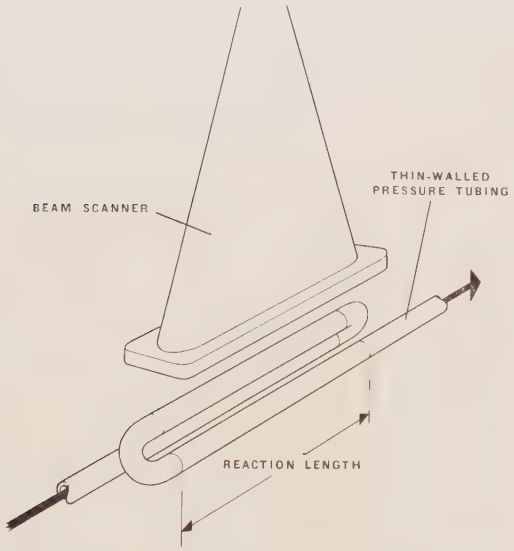

Fig. 7. Processing fluid in flow tube.

The diameter of the tube chosen for a reactor depends on the beam energy and the flow rate. One arrangement of tubes is shown in fig. 7. With a nest of tubes connected for series flow, it is merely necessary that enough tubes be used so that the entire envelope of the beam is intercepted. The width of the envelope varies with the distance from the accelerator. Indeed, the distance can be increased by adding more tubes, in order to reduce dose rate without affecting the total power used. The tubes should be aligned in staggered rows as carefully as possible to obtain the maximum "area" efficiency. Beam absorption in the tube walls varies between wide limits because the beam does not enter normal to the tangent at all points.

Considering all losses, the calculated beam efficiency is about 50% for all tubes from $\frac{1}{4}$-inch to 1-inch with fluid pressures up to 100 atmospheres at 70° F. This pressure can be extended by using slightly heavier-walled tubes without incurring proportionally greater losses in efficiency.

While all the chamber designs discussed here are particularly appropriate for incompressible fluids, similar techniques might be used for compressible fluids. With the latter, we estimate that magnetic systems can be used to confine the beam's penetration range by providing a long mean free path in an orbit.

5. Conclusion

These three techniques: (1) beam inversion, (2) intermittent filters, and (3) the treatment of pressurized fluids in continuous flow—indicate that higher efficiencies are possible and that materials may be processed which otherwise would have been excluded from consideration. Undoubtedly, the earliest uses of electron processing will not involve them. Certainly, more engineering development is needed to apply them industrially. But the "surface" of technique development has hardly been scratched.

This analogy is also applicable to the other areas discussed: that of accelerator developments and their installation for processing use. Imaginative engineering applied in all three areas will yield significant results.

NUCLEAR INSTRUMENTS AND METHODS 6 (1960) 33–44; NORTH-HOLLAND PUBLISHING CO.

PERFORMANCE OF A NUCLEAR EMULSION SCANNER†

PAUL V. C. HOUGH

The University of Michigan, Ann Arbor

Received 15 September 1959

A machine has been constructed which meets many of the needs for scanning of nuclear emulsions as emulsions are used in charged particle nuclear spectroscopy. Methods developed for track detection are reviewed briefly. In more detail an account is given of the performance of the machine in scanning plates exposed at the Michigan 42″ cyclotron over a seven months period. Finally, some special techniques which may have other applications are described.

1. Requirements for a Scanner to be used in Charged Particle Nuclear Spectroscopy

In typical experiments in charged-particle nuclear spectroscopy a well collimated, monoenergetic beam of protons, deuterons, or alpha particles falls on a thin target and reaction particles at arbitrary angle relative to the incident beam are analyzed in momentum by a high-resolution magnet. Usually several hundred momentum channels are available at the image plane of the magnet and nuclear emulsions have often been used[1,2]) to record in all these channels simultaneously.

The particular geometry at the image plane of the Michigan analyzer magnet is shown in

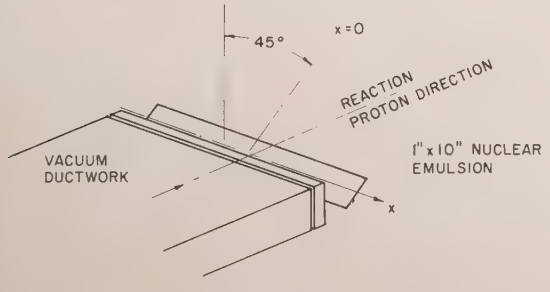

Fig. 1. The geometry at the image plane of the Michigan analyzer magnet.

fig. 1. The useful region of image plane extends from $x = +100$ to $x = -120$ mm (in the coordinate system of the figure) and corresponds to an energy variation equal to 15% of the central energy. The overall system resolution is about 20 keV for (d,p) reactions and is limited primarily by a 15 keV spread in energy of the 7.8 keV deuteron beam on target. With this resolution, a 10 MeV proton group will have a width $\Delta x \approx 4$–5 mm at the emulsion.

With this background, we can give a reasonable set of requirements for an emulsion scanner used to read plates exposed at the magnet image plane:

1.1. TRACK DETECTION EFFICIENCY

A scanner need not have high absolute efficiency and probably any efficiency greater than about one-half would be quite satisfactory. However, the efficiency should be reproducible and constant for all emulsions used in a given experiment. Probably a fluctuation of 5% in efficiency would be tolerable for all nuclear structure experiments because of uncertainties in nuclear reaction theory.

1.2. SPURIOUS COUNTING

In exposures at the cyclotron for high energy proton groups (corresponding to low excitation of the residual nucleus) even long exposures will still yield regions on the emulsion where no

† This work was supported by the Michigan Memorial Phoenix Project and by the U.S. Atomic Energy Commission.

[1]) Buechner, Browne, Enge, Mazari and Buntschuh, Phys. Rev. **95** (1954) 609.

[2]) Bach, Childs, Hockney, Hough and Parkinson, Rev. Sci. Instr. **27** (1956) 516.

tracks at all are found. This observation leads to the difficult conclusion that a scanner should introduce no spurious counts. More realistically, 10–20 tracks are certainly required to establish the presence of a proton group and therefore a spurious count of 3–4 over a 4–5 mm width of emulsion is probably satisfactory.

1.3. SCANNING SPEED

It has proved possible at the Michigan cyclotron to expose five to ten 1″ × 10″ nuclear emulsions per day for a number of days. Since an accelerator will normally be used for other experiments, this is probably an upper limit to the production rate for a single magnet image plane. On the other hand, a multigap magnet[3]) will increase this rate by an order of magnitude. It appears then that a scanner should be able to read 25–100 1″ × 10″ nuclear emulsions per day under the rather extreme demands placed on it by a multi-gap magnet installation.

2. Track Detection Methods

Details of electronic and optical methods developed to detect slow proton tracks are given elsewhere[4]). Here we only want to review the logic of the scheme so as to make clear the reasons for the performance characteristics listed in the next section.

[3]) W. W. Buechner, private communication.

[4]) Hough, Koenig and Williams, Electronics (McGraw-Hill, March 27, 1959).

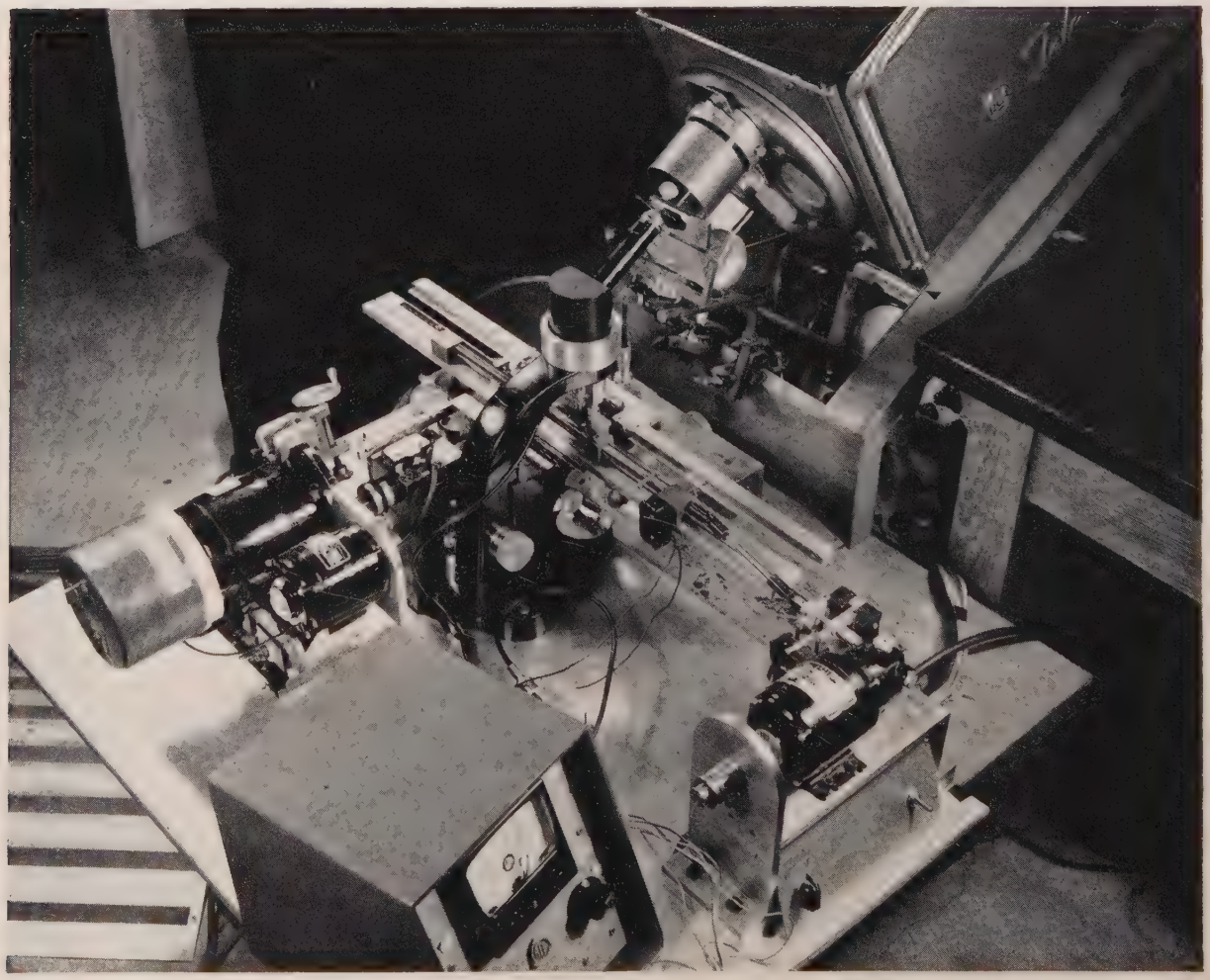

Fig. 2. The scanner microscope, showing the motor driven stage.

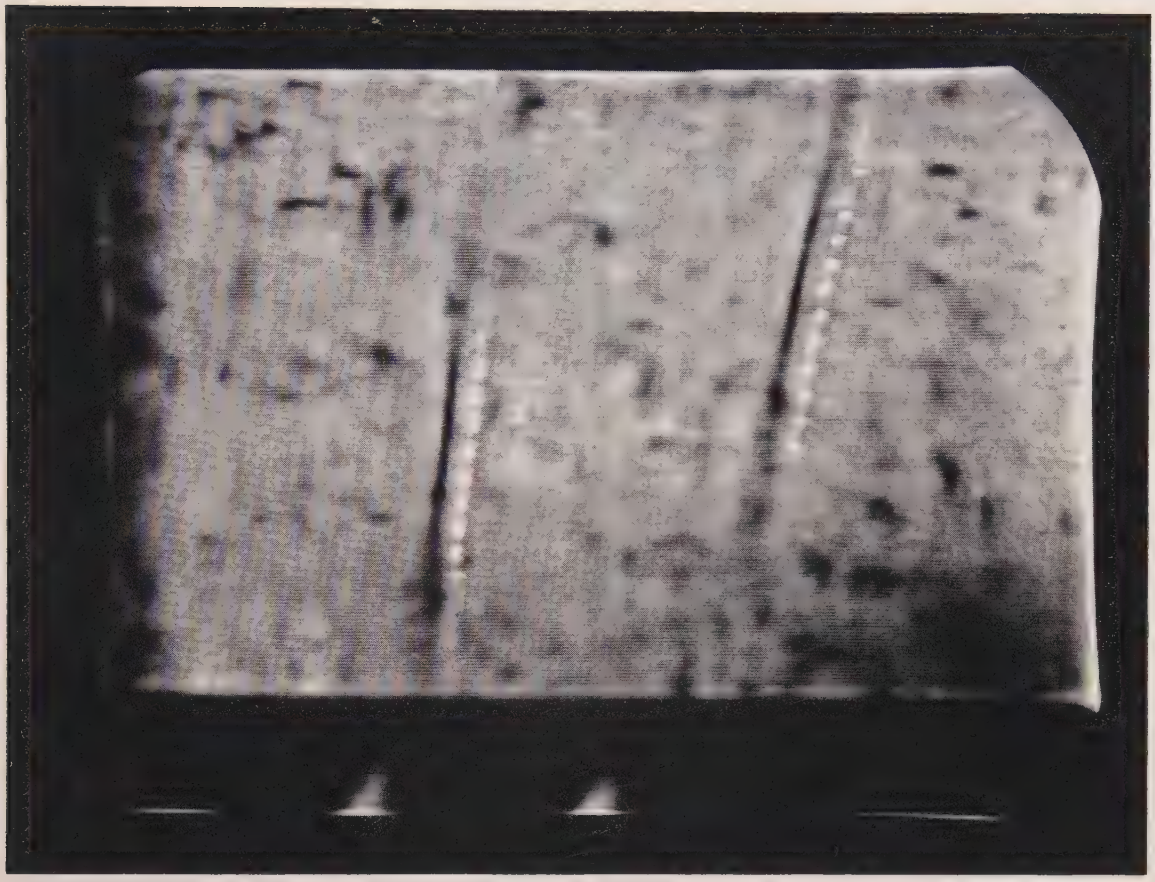

Fig. 3. A typical emulsion scene photographed from a television receiver wired to the Image Orthicon Television Camera. For an explanation of the white marks beside the tracks and at the bottom of the field see section 2, §§ 3 and 4.

2.1. PATTERN OF SEARCH OVER THE EMULSION

A motor driven stage (fig. 2) moves the 1″ × 10″ emulsion under a microscope in a series of traverses of the short dimension, each traverse followed by an advance of the plate. During a traverse the stage moves continuously, but by means of a pulsed light source 140 separate fields of view are presented to a television camera and associated computer for analysis. Each field of view is 0.12 mm × 0.18 mm; corresponding points in successive fields are separated by 0.15 mm; and successive traverses are separated by 0.25 mm. Normally the track count for four traverses is recorded as a single datum and so points are available for each mm along the emulsion. However, because of the gaps between fields and between traverses, each point corresponds to a search area only 0.56 mm wide (extending across the plate). The emulsion is examined at only one depth, midway between top and bottom of emulsion, so scanning is effective only for tracks which penetrate the emulsion completely.

2.2. THE DETECTION OF EMULSION GRAINS, ESPECIALLY THE GRAINS MAKING UP TRACKS

A standard Leitz 22x oil immersion objective and 10x eyepiece are used to project an image of the emulsion scene onto an Image Orthicon television camera tube. Fig. 3 shows a typical emulsion scene photographed from a television receiver wired to the camera. (The white dots to the right of the tracks are explained in paragraph 3 below, and the white splashes at the bottom in paragraph 4.) Two alterations have been made in the microscope optics:

It is found that the contrast is considerably enhanced by blocking off a band of light entering the microscope condenser in a plane containing the tracks and the optic axis; this leaves two "crossfire" beams illuminating the emulsion.

Also it is found helpful to introduce a cylindrical lens of radius of curvature 15 cm adjacent to the eyepiece so that the image of each grain becomes a short line roughly parallel to most tracks. This trick tends to patch gaps in tracks without seriously patching together background grains into false tracks.

Kodak NTB2 or Ilford G-special emulsion are used to provide strong tracks with tolerable background grain density.

The portions of the scene detected by a special screening circuit are shown in fig. 4. A narrowness criterion is incorporated in the screening circuit so that any large-area opacities which may occur are ignored.

2.3. THE RECOGNITION OF A TRACK BY ITS CONTINUITY

Delay and coincidence units are used to establish the existence of a grain just one scan line after a previous grain. A continuous track will of course give the required coincidence. The coincidence resolving time is chosen so that tracks at angles up to $\pm 45°$ to the vertical will still give a coincidence. An actual counting operation is performed along a track by this (delay + coincidence) technique; in fact a continual testing of background grains for the possibility that they are linked to form tracks proceeds at all lateral positions in the field of view. An output pulse which we name "track segment pulse" is produced when the count along any track reaches 16, and for each 8 counts thereafter. Since the number of television scan lines used per field is about 180, the number of track segment pulses for a track crossing the entire field is 23. A more typical number of

Fig. 4. The portions of the scene of fig. 3 which are detected by a special screening circuit.

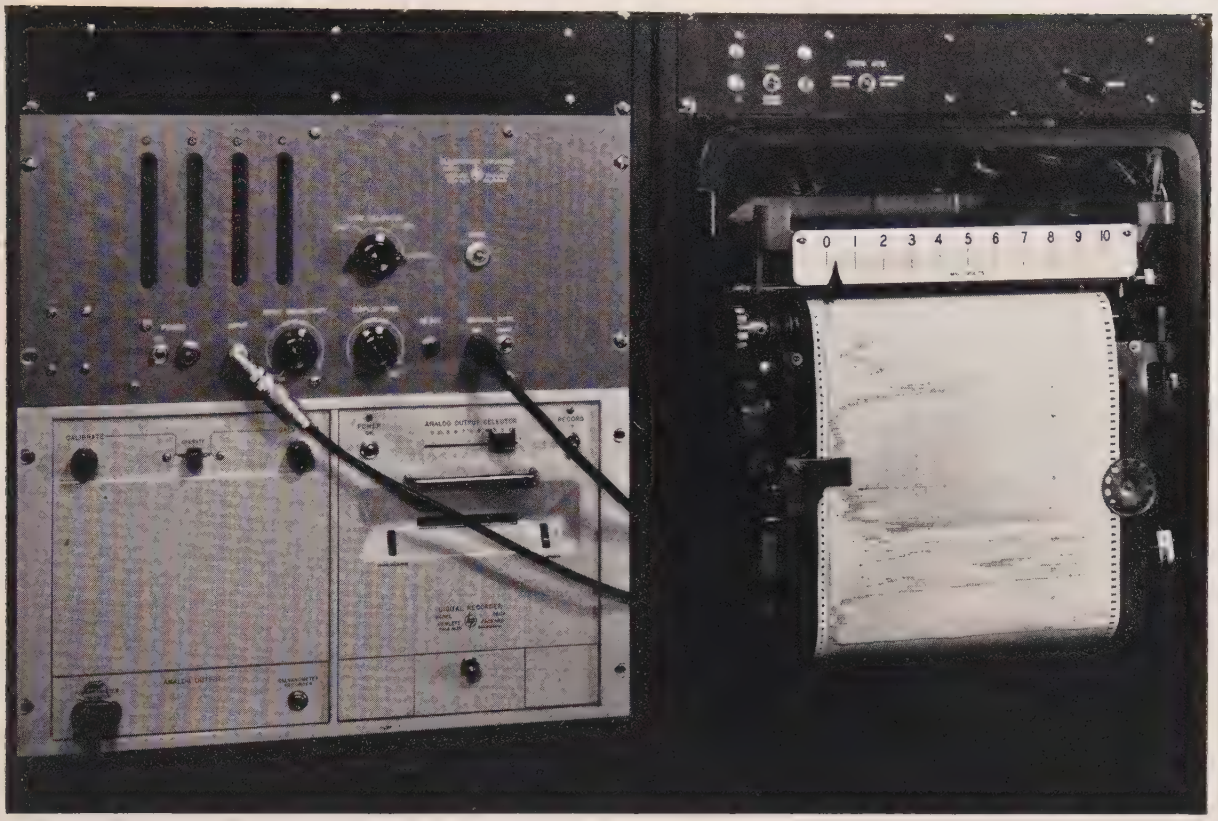

Fig. 5. Track counts accumulated for four traverses are printed on paper tape, and also plotted with appropriate error bars on a chart recorder. The strong groups are plotted with a factor 10 scale change.

track segment pulses for a track is 8–10 as shown in a display of these pulses as as white dots to the right of each track in fig. 3. The doubling of pulses for the left track occurs because the exposure extends over several television scanning periods and the count along the track has begun at two different points in the different periods.

2.4. GENERATION OF A SINGLE OUTPUT PULSE PER TRACK

Owing to different quality of development for different tracks and to more or less favorable location of a track in the field, the number of track segment pulses obtained per track varies widely. In order to obtain one count for each track the following technique is used: an oscilloscope beam is swept along a fixed line in synchronism with the horizontal deflection of the television scanning beam. Whenever a track segment pulse occurs the oscilloscope beam is intensified and a flash of light is produced. For vertical tracks all flashes for one track occur in one spot. The oscilloscope screen is projected back into the television camera at the bottom of the field of view. The camera tube integrates the light from the flashes originating in any one spot, i.e., from one track. Finally, a single television scan line through the spots is devoted to reading out the number of spots and therefore the number of tracks. (The two spots for the two tracks of fig. 3 appear dimly at the bottom of the figure. The brightness distribution is distorted badly by the television receiver; as actually used, the spots have a uniform intensity over a vertical distance equal to that of the black band of the figure. The read-out line is centered in the black band.) It is possible to set a discriminator level on the final spot readout to select only tracks with more

than a specified number of track segment pulses, usually 5 or 6.

2.5. FINAL OUTPUT

The number of spots detected is accumulated in a scaler until four traverses across the plate width are completed. Then this number is printed on paper tape and plotted on a chart recorder as shown in fig. 5. The error bars are obtained via a square-root potentiometer mounted on the shaft of the chart recorder. A recorder scale change from 200 tracks to 2000 tracks full scale can be seen for three intense groups in fig. 5.

3. Scanner Performance

3.1. TRACK DETECTION: ABSOLUTE EFFICIENCY AND REPRODUCIBILITY

On comparing the scanner with a human observer for a series of proton groups and a series of plates, the scanner count may be found anywhere between 80% and 120% of the human count, for equal search areas†. The machine-human ratio changes only slowly with position on the plate so that peak positions and peak contours are reproduced fairly accurately, but the failure of the machine to maintain constant efficiency is a major defect.

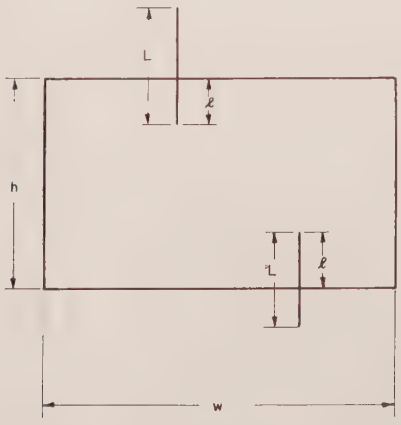

Fig. 6. Two tracks of length L shown in extreme positions for detection. The minimum length within the field required for detection is l.

The difficulty has been traced to the use of isolated fields of view as the search pattern for the scanner. Referring to fig. 6, define $w =$ width of field of view, $h =$ height of field of view, $L =$ length of track in good focus (as judged by the electronics), $l =$ length of track within the field of view required for the track to count. Evidently if the upper end of a track falls within the area $w \times [h + (L - l) - l]$ the track will count, and therefore the effective search area is increased over the geometrical area $w \times h$ by the factor

$$\frac{h + (L - l) - l}{h}.$$

The parameter l is easily held constant, usually at the value $l = \frac{1}{4}$ h, but L is subject to fairly wide variation with quality of emulsion development and especially with slight changes in the optical and television systems. This variation in L and the corresponding variation in search area is responsible for the major part of the observed variation in machine detection efficiency.

Simply considering the scanner as a counter, this problem of searching in isolated fields shows up clearly. Because tracks can have any fraction of their length inside the field of view the pulse height distribution from tracks observed in a collection of isolated fields necessarily extends down to zero. Now since the scanner uses a simple level discriminator to record all track pulses above a certain arbitrary height, if the mean pulse height changes (i.e., the mean track length as judged by the electronics changes), the fraction of pulses above a fixed level will in first order respond linearly. The scanner, regarded as a counter, is a counter without a plateau.

The scanner is still quite useful in searching for new particle groups and for identification of the mass of the target nucleus responsible for new groups by reading spectra at a number of reaction angles. However, human scanning is needed for absolute counts over the peaks.

Recently, an alternate scanner search pattern of continuous strips has been provided at a factor 4 reduction in speed. The results of two

† A smaller fluctuation of $\pm$ 5% is quoted in ref. [4]), but this is incorrect.

such machine scans are compared with a hand scan in fig. 7, showing a much more constant

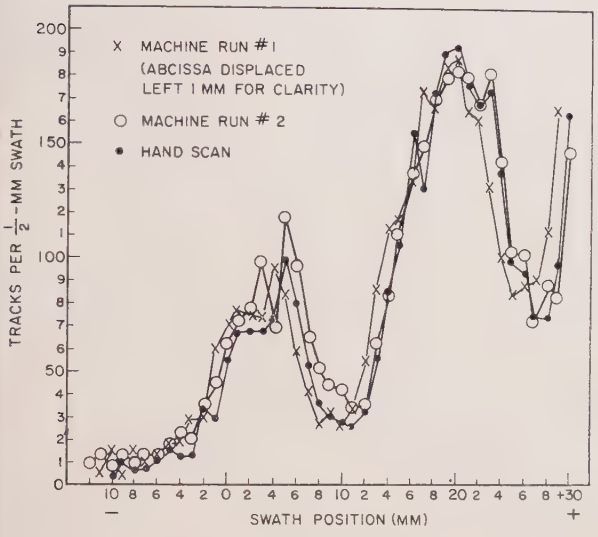

Fig. 7. Preliminary results for continuous strip scanning. Two machine scans are compared with a hand scan of the same region.

detection efficiency. It seems that it may be possible to carry out also by machine the absolute counting required.

3.2. SPURIOUS COUNTS

The background count introduced by the machine averages about one per plotted point, i.e., per geometrical search area equal to a strip 0.56 mm wide extending across the 1-inch dimension of the plate. Most of this machine background arises from neutron recoil tracks which are easily rejected by a human observer.

At first, emulsion surface marks often introduced whole blocks of spurious counts. Fortunately it was found that surface marks are easily removed by rubbing off the top few microns of processed emulsion with paper tissue soaked in methyl alcohol. This cleaning process is now followed routinely and is necessary for low background.

The scanner background is low enough so that it is not a limitation in nuclear spectroscopic applications.

3.3. SHORT-TERM AND TIME-AVERAGED SCANNING RATES

We have noted above that a "point" plotted for each mm of the analyzer magnet image actually corresponds to the geometrical search area of a strip 0.56 mm wide. So about half the plate area is normally scanned.

The scanner plots four points per minute and therefore reads the 220 mm useful range of an image plane in 55 minutes. Normal cleaning, recording and checking operations between plates occupy another 20 minutes, so that in steady, trouble-free scanning plates are read at the rate of one every hour and 15 minutes.

Averaged over an eight hour day it is possible to read five image planes (1″ × 10″ plates) and fairly easy to read four. For the past few months it has proved useful to employ undergraduate assistants to put on a second shift from 5 to 11 P.M. in which case another three or four plates are normally read. In sum, 7–9 image planes can be read per day, or about 1800 plotted points. By comparison a human scanner will produce between 100 and 150 plotted points per day.

Because of operator fatigue, the machine rate could probably not be maintained for months. It has not been necessary to try, because on the one hand large scale cyclotron exposures are ordinarily interspersed with exploratory runs or experiments with counters, and on the other, it has unfortunately been easy for the machine to saturate the three available human scanners with absolute counting jobs.

3.4. PROBLEMS OF OPERATION AND MAINTAINANCE

The whole system uses 635 tubes: 128 in locally designed and built circuits, 154 in the television system, 132 in broad band amplifiers, 103 in various other commercial units, and 118 in power supplies. In view of this complexity, arrangement is made to check the performance of any part of the scanner by switching in a synthetic signal which imitates a straight, vertical, continuous track. As a final integral check, at the beginning and end of each scanning

period a standard proton group is counted and the machine required to produce a count within $\pm$ 10% of the correct value.

During scanning runs, the track segment pulses defined in section 2, paragraph 3, are displayed continuously on a television screen. The resulting pattern changes at a 60 cps rate, but it is still possible to detect tracks by eye and for low track densities to verify the performance of the machine track by track. At higher track densities visual checking becomes impossible, but a gross failure of any part of the machine is usually obvious.

The failure rate of the circuitry built in our laboratory is about the same as the failure rate of the television system, and for about the same number of tubes. Tube failure has been the most frequent but not the most annoying cause of circuit failure. More troublesome have been the development of bad contacts at solder joints and the development of high frequency oscillations in portions of the circuit which had been free of difficulty since construction, often a year or two earlier. The effort and especially the quantity of highly skilled effort which can go into uncovering the cause of failures has encouraged the development of very complete records of normal circuit performance, especially

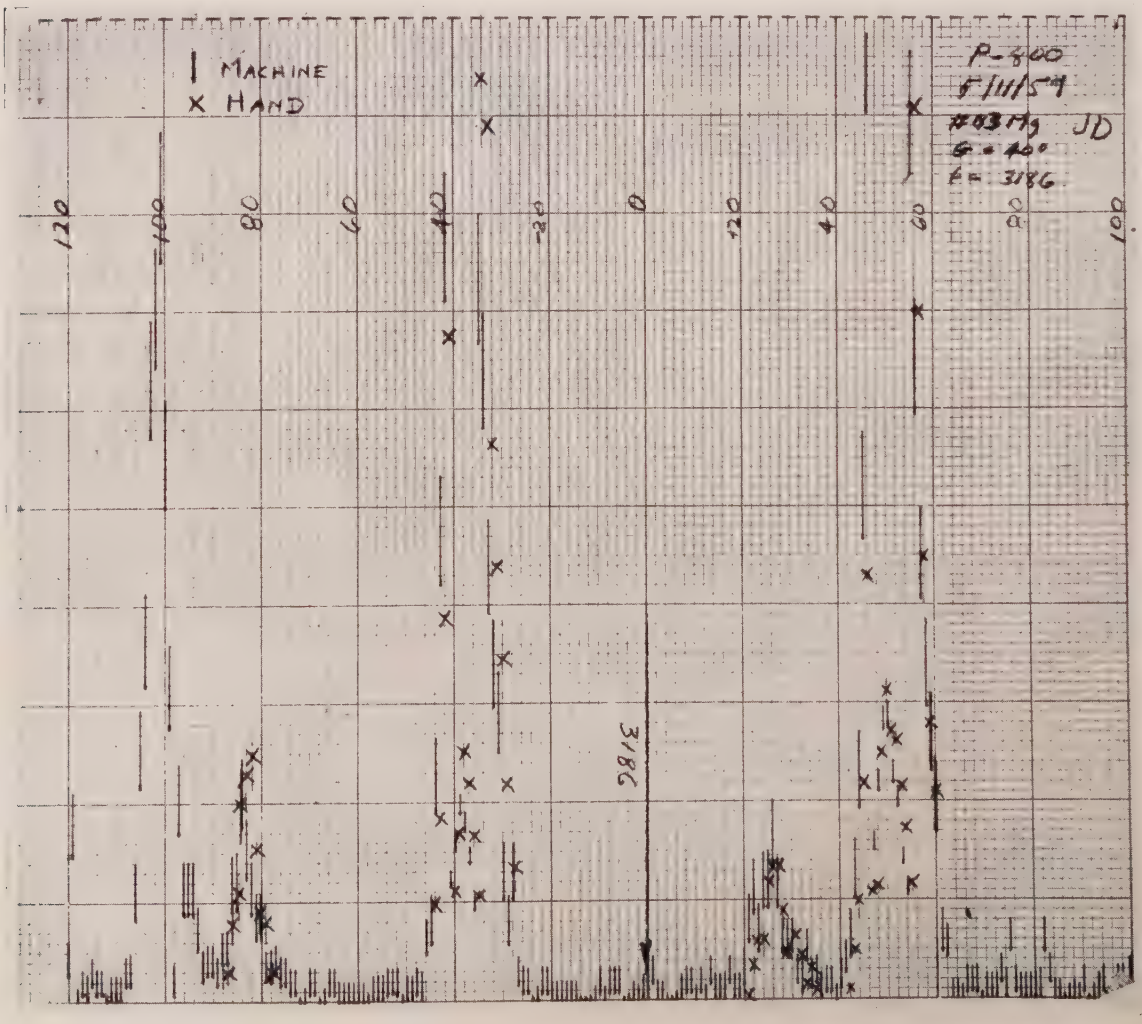

Fig. 8. A typical machine scan. Hand counts over the peak are also shown. The lateral shift of hand and machine data is due to a different convention in reading the left end of the plate.

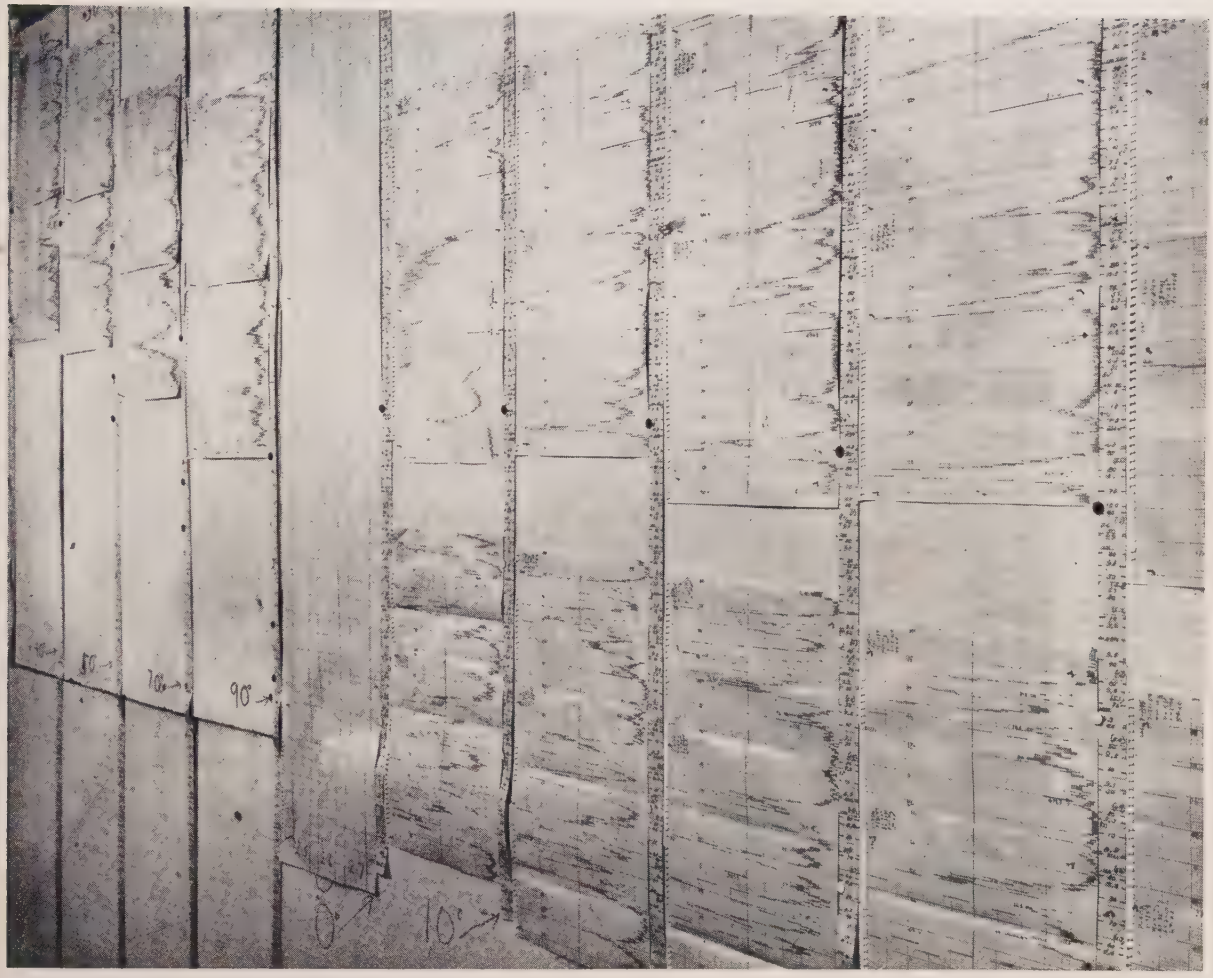

Fig. 9. An analysis board used to keep track of an investigation of the level structure of Mg^{25}. For details see the text.

a comprehensive collection of oscilloscope drawings.

3.5. RESULTS OBTAINED OVER A SEVEN MONTHS PERIOD

Over the first seven months of 1959 the scanner read 206 1″ × 10″ plates exposed at the cyclotron. About 30 plates were not read, 4 because of a development failure and the rest because similar exposures had been read by machine and the existence and rough intensities of the various proton troups had been established. At the beginning of the period scanning requests were met with great difficulty and often several days would elapse while operational difficulties were traced down. A shift from Kodak NTB to Kodak NTB2 (or Ilford G-special) emulsion, the development of a really reliable focus control for the microscope, and a number of small engineering improvements have made scanning much easier so that by the end of the period relatively untrained personnel could read plates on demand within the performance specifications we have quoted.

Fig. 8 shows a chart of a machine scan, with hand counts over several peaks also plotted. The lateral shift of hand and machine data is due to a different convention in reading the left end of the plate.

Finally, as a general indication of the kind of work done by the scanner, we show in fig. 9 a photograph of part of an analysis board used to

keep track of an investigation of the level structure of Mg^{25}. The board is divided into halves, the left half devoted to proton groups of energy between 4 and 8 MeV, the right half to groups between 8 and 14 MeV. In each half, channels are established for mounting spectra of reaction protons observed at angles 10°, 20°, 30°, 40°, 50°, 70° and 90°. (About twice as many angles are run for an angular distribution.) In each channel the same energy scale is established: the scale is non-uniform, with a rate of change of energy with position at any energy approximately equal to that of a scanner chart run at that energy. Therefore overlapping charts fit together to give continuous spectra. The analysis board is mainly a bookkeeping aid, useful for planning exposures and deciding what work is completed. By looking at the forward-angle charts the qualitative stripping angular distribution of a particular group is clear, and by inspection of the large-angle charts, the change in proton energy with angle is evident and therefore even by inspection one can make a close estimate of the mass of the target nucleus responsible for the group. The energies of the usual contaminant groups from carbon, oxygen and hydrogen can be plotted on the board once for all.

4. Some Special Techniques

4.1. AUTOMATIC FOCUS CONTROL FOR A MICROSCOPE

In scanner operation it is necessary to control the position of the microscope objective relative to the top surface of the emulsion to within $\pm$ 10 microns. This particular number follows from the need to keep a focal region about 20 microns deep entirely within a thickness of processed emulsion equal to 40 microns. Without focus control, reasonable care in leveling the microscope stage will reduce variations in objective-emulsion separation to about 50 microns. This residual variation is of two types: (1) the focus changes abruptly by 15–20 microns according to the direction of traverse; (2) the focus changes slowly with lateral position due to a nonzero angle between the plane of the top surface of the emulsion and the plane of the stage motion.

A very simple mechanical control reduces focus variations to about $\pm$ 5 microns. In fig. 10, spring A is used to load the lower part of the objective against the emulsion. The tungsten carbide ball B is rigidly attached to the loaded objective by the heavy steel piece C and contitutes the bearing point against the emulsion.

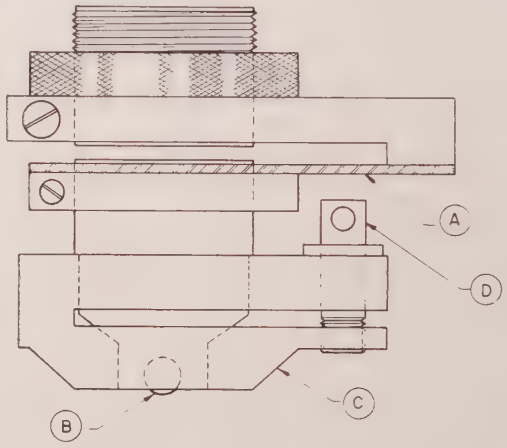

Fig. 10. A simple mechanical focus control which maintains the plane of best focus a fixed distance below the emulsion surface with an accuracy of about $\pm$ 5 microns.

The bearing point is displaced from the optic axis of the objective by about 4 mm, perpendicular to the plane of the paper. The screw D is turned with a small removable wrench to distort piece C by a mil or two, moving the ball B up or down relative to the objective and thereby adjusting the depth at which the focus is controlled. In making the initial adjustment of the control the objective is lifted via the tungsten carbide bearing about 6 mils from its equilibrium position by raising the microscope stage. Then a restraining cam (not shown) is installed to catch the objective after a drop of 2 mils. This allows the objective to slide smoothly onto the emulsion again after leaving it at the end of scanning traverses.

4.2. ELECTRONIC CONSTRAST ENHANCEMENT FOR FASTER HUMAN SCANNING

Given a television system to look at emulsions, the various types of electronic analysis

Fig. 11a and b. A normal scene with two possible forms of electronic contrast enhancement.

used in wholly automatic scanning can be presented also on a television receiver for easier human scanning. Without going into detail, fig. 11 shows a normal scene with two possible forms of electronic enhancement. A defect in some applications would be the discrimination likely to occur against tracks which are parallel to the television scan lines.

Acknowledgements

It is a pleasure to thank G. R. Garrison, Director, and F. M. Remley, Technical Director, of the University of Michigan Television station for generous assistance. The excellent technical development work of J. A. Koenig was essential at every stage of the investigation. D. E. Damouth has been responsible for the development of continuous-strip scanning which shows such promise for reproducible efficiency. The contribution of R. O. Winder, W. Williams, and B. Cosby in the creation of certain component parts of the scanner is gratefully acknowledged.

NUCLEAR INSTRUMENTS AND METHODS 6 (1960) 45–49; NORTH-HOLLAND PUBLISHING CO.

ELEKTRONENOPTISCHE KONSTRUKTION VON INHOMOGENEN BESCHLEUNIGUNGSRÖHREN

E. KOLTAY

Institut für Experimentelle Physik der L. Kossuth Universität zu Debrecen, Ungarn

Eingegangen am 24. August 1959

The numerical application of the poligon method given by Gans[4]) proved to be a simple and reliable procedure for the design of the accelerating tube with inhomogeneous field of the high voltage generators. We made calculations using this method in connection with the accelerating tube of our Van de Graaff generator of 2 MV rated voltage. For the axial potential we used the data given by Kirkpatrick and Beckerley[9]).

1. Einführung

In Verbindung mit der bei den atmosphärischen Hochspannungsgeneratoren allgemein gebräuchlichen Beschleunigungsröhren von inhomogenem Feld sind Mitteilungen in der Literatur kaum zu finden, die einfache elektronenoptische Konstruktionsverfahren von hinreichender Genauigkeit gäben. In der Mehrheit der Fälle werden die Beschleunigungsröhren empirisch, im Wege der Einstellung von mechanischen und elektrischen Daten der auf Grund von plausibelen Überlegungen aufgebauten Röhren eingestellt. Dem Ausgang liegen meistens die Kurven von Spangenberg zugrunde[1]). Sie lieferen aber im allgemeinen nur Näherungswerte zur Konstruktion. Der Grund davon liegt darin, das die ausgeführten Elektroden im Interesse der Herabsetzung von Wirkungen der im Rohre auftretenden Sekundärerscheinungen gewöhnlich mehr komplizierte Form haben, als diejenige in der Arbeit von Spangenberg.

Dieses Konstruktionsverfahren hat auch einen anderen Nachteil. Auch noch im Falle der einfachen Form ergeben sich nähmlich die zusammengehörigen Objekt- und Bildweiten, bzw. die Brennweiten und die Lagen der Hauptebenen. Der Durchmesser des Bündels bleibt aber unbekannt, als Funktion der längs der optischen Achse gemessenen z-Koordinate, dessen Kenntniss von dem Standpunkte der Konstruktion auch sehr wichtig ist.

Eine Arbeit von hervorragender Bedeutung ist der aus dem Gansschen Verfahren ausgehende Artikel von U. Timm[2]). Die Resultate, die mit der Anwendung von dieser Arbeit zu bekommen sind, stimmen nach den Messungen von D. Kamke und H. Seguin[3]) mit den Erfahrungen gut überein. Die erwähnte Funktion $r = r(z)$ ist aber hier auch nicht unmittelbar zu bekommen.

Nach unseren Erfahrungen erweist sich die unmittelbare numerische Anwendung des Ganssschen Poligonverfahrens als eine einfache und genaue Konstruktionsmethode der inhomogenen Beschleunigungsröhren. Die Reihenfolge der numerischen Aufgaben sind auch an die Rechenеigenschaften einer einfachen Handrechenmaschine gut anzupassen, und dementsprechend ist das Rechen ohne Speziellapparaten und grössere Schwierigkeiten durchzuführen. Ihrer Natur nach ergibt diese Methode unmittelbar den gewünschten Strahlengang $r = r(z)$.

2. Die Ganssche Poligonmethode

Zur Lösung der Bahngleichung des sich in rotationssymmetrischem Feld bewegenden paraxiellen Elektrons (bzw. Ions)

$$\frac{\mathrm{d}^2 r}{\mathrm{d}z^2} + \frac{\phi'}{2\phi}\frac{\mathrm{d}r}{\mathrm{d}z} + \frac{\phi''}{4\phi} r = 0 \qquad (1)$$

[1]) K. R. Spangenberg, Vacuum Tubes (Mc Graw Hill, 1948).

[2]) U. Timm, Z. Naturforschg. **10a** (1955) 593.

[3]) D. Kamke und H. Seguin, Z. Naturforschg. **10a** (1955) 1036.

wo $\phi = \phi(z) = \phi(z,r)_{r=0}$ das sog. Achsenpotential,

$$\phi' = \frac{\mathrm{d}\phi}{\mathrm{d}z} \qquad \text{und} \qquad \phi'' = \frac{\mathrm{d}\phi'}{\mathrm{d}z}$$

sind, gab R. Gans die folgende Näherungsmethode[4,5]).

Man ersetzt die in Frage stehende Kurve $\phi = \phi(z)$ durch ein durch die zu den z_i Punkten des Intervalls $z_0 < z < z_n$ gehörigen $\phi(z_i)$ $(i = 0, 1, 2, \cdots, n)$ Werte gezogenen Poligon, und man sucht statt der Lösung der Gleichung (1) die sich aneinander passenden Lösungen der Gleichungen

$$\frac{\mathrm{d}^2 r}{\mathrm{d}z^2} + \frac{\phi_i'}{2\phi_i}\frac{\mathrm{d}r}{\mathrm{d}z} = 0 \tag{2}$$

im Inneren der einzelnen Intervallen, bzw. diejenige der Gleichungen

$$\frac{\mathrm{d}^2 r}{\mathrm{d}z^2} + \frac{\phi_i''}{4\phi_i} r = 0 \tag{3}$$

in den Teilungspunkten. Aus den Gleichungen (2) ergibt sich beim Übergang von dem Punkte z_i zu dem Punkt z_{i+1} für r_{i+1}:

$$r_{i+1} = r_i + \frac{2r'_{i,r}\sqrt{\phi_i}\,[\sqrt{\phi_{i+1}} - \sqrt{\phi_i}]}{\dfrac{\phi_{i+1} - \phi_i}{z_{i+1} - z_i}} \tag{4}$$

bzw. aus den Gleichungen (3) für die Veränderung der Bahnneigung beim Übergang von dem $n+1$-ten Intervall zu dem $n+2$-ten:

$$r'_{i+1,r} - r'_{i+1,l} = -r_{i+1}\frac{\dfrac{\phi_{i+2} - \phi_{i+1}}{z_{i+2} - z_{i+1}} - \dfrac{\phi_{i+1} - \phi_i}{z_{i+1} - z_i}}{4\phi_{i+1}} \tag{5}$$

wo $r'_{i+1,l}$ bzw. $r'_{i+1,r}$ der linke bzw. rechte Differentialquotient in dem Punkte z_{i+1} ist. Wie man aus der Substitution $i + 1 = 1$ sieht, bei gegebenem Achsenpotential $\phi = \phi(z)$ von den r_0 und $r'_{0,r}$ Werten abgehend sind die Werte r_1 und $r'_{1,r}$ durch einen Schritt, die Werte r_n und $r'_{n,r}$ aber durch $n - 1$ aufeinander folgende Schritte zu bekommen. Es entsteht durch die Darstellung der bekommenen Werten die Bahn des Ions mit bestimmten Anfangsbedingungen im Raume, der von dem Gesichtspunkte der Elektronenoptik mit der Achsenpotentialverteilung $\phi = \phi(z)$ charakterisiert ist.

3. Ausführungsform der Elektroden. Achsenpotential

Zur Durchführung der geschilderten Berechnungen ist es notwendig, die Achsenpotentialverteilung zu kennen. Im Falle der Rohr-Immersionslinse sind diese Daten aus potentialtheoretischen Rechnungen bekannt[6,7]), bei mehr komplizierten Elektrodenformen aber sind durch experimentelle Methoden, hauptsächlich mit der Methode des elektrolytischen Troges auszumessen.

Die gebräuchlichen Elektrodenformen[8]) unterscheiden sich mehr oder weniger von den Rohr-Immersionslinsen zwecks der Verminderung der Sekundärelektronenerscheinungen, die durch die Ionenbombardierung der Metallbauteile des Rohres hervorgerufen werden. Diese Aufgabe wird durch die übliche Anordnung in Fig. 1 mit den Blenden B und C im Spalte gut gelöst. Die Öffnung der Blende B ist etwas kleiner, als diejenige von C. Somit ist das Bombardieren von C zu vermeiden und dementsprechend entstehen die Sekundärelektronen hauptsächlich im Inneren der Elektrode S, woher sie wegen der Anwesenheit der Blende A nur mit sehr kleiner Wahrscheinlichkeit in den vorigen Beschleunigungsspalt eintreten können. Die nach den Isolatorwänden laufenden geladenen Teilchen werden durch die Aussenelektrode D aufgefasst. Die Durchmesser des Bündels werden an der Stelle der Blenden durch die elektronenoptischen Eigenschaften der Linsen und die Abmessungen der ersten Blende bestimmen. Die optimalen Verhältnisse sind im Falle zu erreichen, wenn die Öffnungen der Blenden an die entsprechenden Bündeldurchmesser angepasst sind.

Damit wir die Rechnungen mit der Achsenpotentialverteilung der Rohr-Immersionslinse

[4]) R. Gans, Z. tech. Phys. **18** (1937) 41.

[5]) A. A. Rusterholz, Elektronenoptik I (Verlag Birkhäuser, Basel, 1950).

[6]) S. Bertram, Proc. Inst. Radio Engrs., N.Y. **28** (1940) 418.

[7]) R. Gáspár, B. Koltay-Gyarmati und I. Tamássy-Lentei, Acta Phys. Hung. **9** (1959) 369.

[8]) E. W. Titterton, Nucleonics **10**, No. 5 (1952) 28.

durchführen können, haben wir Beschleunigungselektroden nach der Fig. 2 angewandt. Die Rolle der Blenden A, B und C übernehmen hier die in feldfreien Bereichen aufgestellten

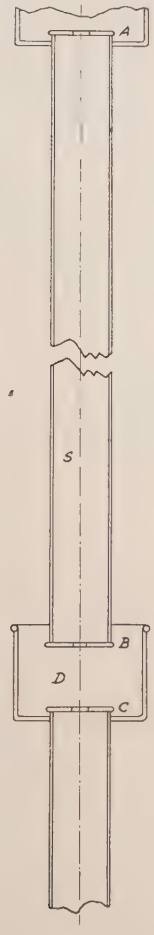

Fig. 1. Gewöhnliche Elektrodenanordnung mit Blenden und Aussenelektrode zur Verminderung der Sekundärelektronenerscheinungen.

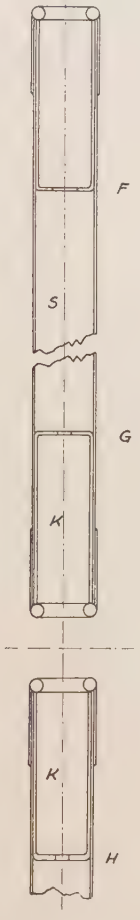

Fig. 2. Die bei uns angewandten, mit Blenden versehenen Rohr-Immersionslinsen. Sie zeigen die Eigenschaften der Anordnung in Fig. 1.

Blenden F, G und H, die Aussenelektrode D wird aber durch den Faraday-Käfig K ersetzt. Mit der Hilfe dieser Elektrodenanordnung ist es uns gelungen die Probleme der sekundären Elektronen auch im Falle der Rohr-Immersionslinse zu lösen, was zugleich eine wesentliche Vereinfachung der Konstruktion und Ausführung bedeutet.

Zur Berechnung des Achsenpotentials sind uns zwei leicht verwendbare Formeln zur Verfügung gestanden. Die theoretische Arbeit von Bertram[6,5]) gibt für das Achsenpotential die folgende Formel:

$$\phi(z) = \frac{\phi_a + \phi_b}{2} + \frac{\phi_b - \phi_a}{2.64S} \ln \frac{\mathrm{ch}\ 1.32\ (z + \frac{1}{2}S)}{\mathrm{ch}\ 1.32\ (z - \frac{1}{2}S)} \qquad (6)$$

wo ϕ_a bzw. ϕ_b das Potential der Elektrode a bzw. b, S die Spaltweite (in Einheiten des R gemessen) sind. Die andere Formel rührt von der analytischen Näherung der mit Anwendung des elektrolytischen Troges durch Kirkpatrick und Beckerley bekommenen Messergebnisse her[9]). Es lautet:

$$\phi(z) = \frac{\phi_a + \phi_b}{2} + \frac{\phi_b - \phi_a}{b} \int_0^z exp\ [-(\pi/b^2)\, z^2]\, dz \qquad (7)$$

wo

$$b = 2R \left[0.73 + 0.53 \left(\frac{S}{2R}\right)^2\right].$$

Die Formel entspricht der Elektrodenanordnung der Fig. 3, wo wie in praktischen Fällen, die Elektroden mit Toroiden versehen sind. Die Funktion $\phi = \phi(z)$ ist leicht zu berechnen mit Hilfe der Tabellen der Gausschen Funktion.

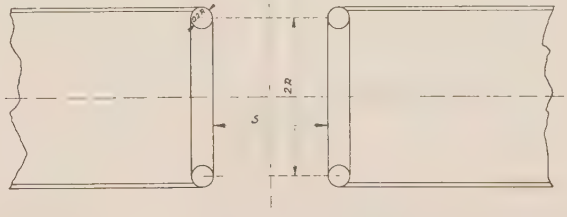

Fig. 3. Der Formel (7) entsprechende Elektrodenanordnung von Kirkpatrick und Beckerley.

Wie es von der Fig. 4 im Falle $S = 2R$ zu sehen ist, stimmen die beiden Funktionen (6) und (7) ziemlich gut überein. Bei unseren Rechnungen haben wir die Funktion (7) angewandt, weil unsere Elektroden genau nach Fig. 3 ausgeführt waren.

4. Rechnungstechnische Anmerkungen

Bei dem aus Beschleunigungsspalten vom bekannten Achsenpotential und von feldfreien Zwischenräumen zusammengesetzten inhomogenen Beschleunigungsrohr haben wir die

[9]) P. Kirkpatrick, J. G. Beckerley, Rev. Sci. Instr. **7** (1936) 25.

Rechnungen auf folgende Weise durchzuführen.

Als erste Näherung nützen wir eine Elektrodenanordnung, die aus den Beschleunigungsspalten von Fig. 2 im Wege von plausibelen Überlegungen bei Berücksichtigung der technischen Daten des Generators zusammengestellt ist. Von den experimentell bestimmten Daten der äussersten Strahlen, die aus der Nachbeschleunigungslinse der Ionenquelle her-

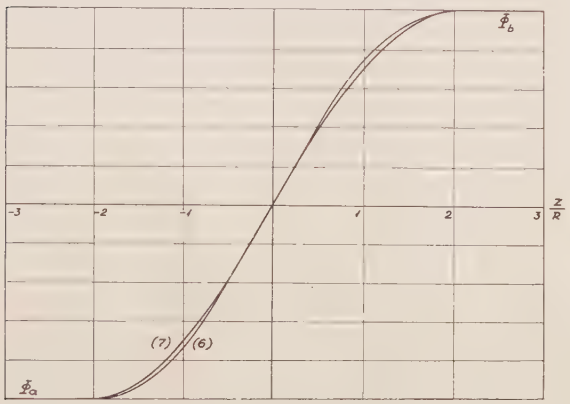

Fig. 4. Die Übereinstimmung der Achsenpotentiale nach Formeln (6) und (7).

austreten abgehend berechnen wir den Strahlengang des ersten Spaltes. Die so bekommene Strahlrichtung wird bis zum Felde des zweiten Spaltes unverändert verlängert. Dieselbe Methode wird auch in den weiteren Spalten angewandt. Nach der Auswertung der erhaltenen Ergebnissen wird es möglich die Lage der Spalten längst der Achse zu verbessern. In der zweiten Näherung führen wir mit dieser Anordnung die oben geschilderten Rechnungen durch. Nach unseren Erfahrungen gelingt es allgemein die Elektrodenanordnung von bestimmten Abbildungseigenschaften in drei oder vier Schritten zu finden.

Die mehrfache Durchrechnung des Rohres wird dadurch sehr erleichtert, das ein grosser Teil der angewandten Daten von den Anfangsbedingungen unabhängig sind, und so sind sie in den höheren Näherungen unverändert anzuwenden.

Aus Gleichungen (2) bis (5) ist es ersichtlich, das sich die Genauigkeit der Methode mit wachsender Feinheit der Einteilung des Intervalls $z_0 < z < z_n$ bessert. Ähnlicherweise ist es zweckmässig die Breite der Intervallteilen mit der wachsenden Neigung der Kurve $\phi(z)$ zu verkleinern und umgekehrt.

5. Ergebnisse. Experimentelle Kontrolle

Mit Anwendung der geschriebenen Methode haben wir das Beschleunigungsrohr des Van de Graaff Generators von 2 MV Nominalspannung

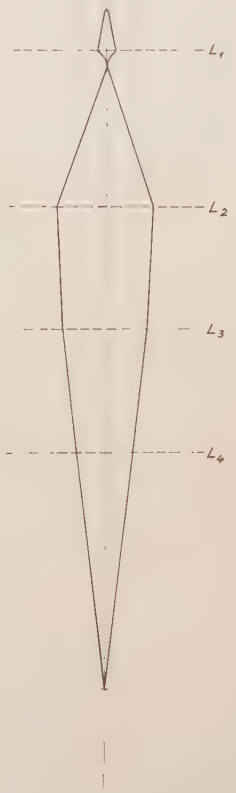

Fig. 5. Der Strahlengang im Beschleunigungsrohr bei Generatorspannung 1 MV. Die Strichellinien bezeichnen die Lage der Mittelebenen der einzelnen Spalten. Mit starker Verzerrung der radialen Koordinate.

unseres Instituts konstruiert. Das Rohr enthält vier Beschleunigungsspalte nach der Elektrodenanordnung der Fig. 2. Die Nachbeschleunigungslinse hatte nur die Aufgabe den Austrittswinkel des Bündels nach der Ionenquelle zu vermindern. Der ausgemessene Divergenzpunkt des so erhaltenen 15 keV-Bündels dient als Objektpunkt für die erste Linse. Der Strahlengang im Rohr

bei der mittleren Generatorspannung 1 MV ist in der Fig. 5 mit starker Verzerrung der radialen Koordinate geschildert. Die Strichellinien bezeichnen die Lage der Mittelebenen der einzelnen Spalten. Die Figur 6 veranschaulicht

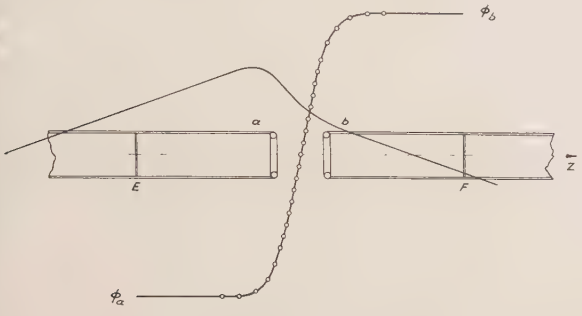

Fig. 6. Der Strahlengang im ersten Spalte, in verzerrter radialen Koordinate. Die Punkten auf der Achsenpotentialkurve bezeichnen die Feinheit der bei den Rechnungen gebrauchten Einteilung.

die Lagerung der Blenden, die Form der für den äussersten Strahl des Bündels bekommenen Bahn in verzerrter radialen Koordinate und die Feinheit der bei den Rechnungen gebrauchten Einteilungen. Die Punkten auf den Achsenpotentialkurve $\phi(z)$ bezeichnen die einzelnen Teilungspunkte z_i des $z_0 < z < z_n$ Intervalls. Die so erhaltene Bildweite der Fig. 6 stimmt genau mit derselben überein, die mit der Extrapolation der entsprechenden Spangenbergschen Kurve bis zum Spannungsverhältniss $V_2/V_1 = 16.6$ zu bekommen ist.

Zu dem Vergleich der Rechnungsergebnisse mit der Eigenschaften des ausgeführten Röhres haben wir den Zusammenhang $i_{\text{Target}} = f(V_{\text{Generator}})$ ausgemessen. Die Anwesenheit eines Maximums bei der Spannung 1 MV beweist die Genauigkeit der angewandten Methode.

Anmerkungen

Ich möchte Prof. Dr. A. Szalay für die Anregung zu dieser Arbeit und sein Interesse danken.

Nach der Verfertigung meiner Arbeit habe ich private Mitteilung darüber bekommen, das ähnliche Konstruktionsverfahren auch E. Jordan, der Mitarbeiter des Instituts für Allgemeine Kerntechnik der Technischen Hochschule, Dresden angewandt hat.

NUCLEAR INSTRUMENTS AND METHODS 6 (1960) 50–56; NORTH-HOLLAND PUBLISHING CO.

THE PROPORTIONAL COUNTER AS A CHARGED PARTICLE SPECTROMETER

S. ABID HUSAIN† and A. A. JAFFE

The Physical Laboratories, The University, Manchester, England

Received 25 August 1959

A proportional counter is described which is suitable as broad range charged particle spectrometer for the investigation of nuclear reaction products. Its performance has been investigated experimentally and an energy resolution of 1.6% has been obtained with protons of 8 MeV.

1. Introduction

There are widespread applications for broad range, large solid angle spectrometers in the study of the energies of the charged products of nuclear reactions. Broad range magnetic spectrographs, while capable of yielding excellent energy resolution require long exposure times and much subsequent analysis. Also, the initial effort involved in their construction is usually large. Scintillation counters are unlikely to yield further improvement in energy resolution in the immediate future and the present limit of about 3% for particles in the energy range of 5–10 MeV, is not always easy to realise.

Proportional counters, used in conjunction with a pulse height analyser, have been extensively employed in the measurement of low energy β-ray and γ-ray spectra[1,2]). Except for one application to α-particle spectrometry[3]), they have never been applied, apparently as a tool in the investigation of the spectra of charged particles from nuclear reactions.

The counter to be described was designed for use as a spectrometer covering an energy range from about 4–10 MeV. Although the primary intention was to investigate its suitability for use in the study of (He^3,p) and (t,p) reactions, the technique should prove useful in other applications, some of which will be discussed below.

2. Energy Resolution

Most of the factors affecting the energy resolution of the proportional counter are well known and have been treated in detail[1,2,4]). The ultimate limit of the resolution will depend on the statistical fluctuations in the ionisation and the gas multiplication processes. There are no experimental data as to the value of this limit at the relatively large energies which are of interest here. With gas multiplications significantly greater than unity the relation $\Delta E/E \approx 2.4/\sqrt{N}$, might be expected to hold (ΔE is the full width at half height of the distribution of pulses from a monoenergetic source of energy E, and N the mean number of ion pairs in the initial ionisation). This relation has been empirically verified for $N < 3000$. For particles of 5 MeV in a counter filled with argon $N \approx 1.8 \times 10^5$, and the above relation predicts a limit of 0.6% for the energy resolution.

The gas multiplication available in the proportional counter is useful for two reasons. The first is that the output pulse height may readily be made large compared with any amplifier or microphonic noise. A gas multiplication of about 10 should be sufficient, with

[1]) D. West, Prog. Nuc. Phys. **3** (Pergamon Press, London, 1953).

[2]) S. C. Curran, Handbuch der Physik **45** (Springer-Verlag, Berlin, 1958) 174.

[3]) K. W. Allen, E. Almqvist, J. T. Dewan and T. P. Pepper, Phys. Rev. **96** (1954) 684.

[4]) D. H. Wilkinson, Ionisation Chambers and Counters (Cambridge University Press, 1950).

† On leave from Atomic Energy Commission, Govt. of Pakistan.

particles of 5 MeV and above, to ensure output pulses one hundred times the noise even with collection times of less than one microsecond. Thus the proportional counter appears more favourable, for this application, than a gridded ionisation chamber of the type which has been used for α-particle spectrometry[5]). The relatively large gridded ion chamber, which would be required to accomodate protons at a desirably low gas pressure, would result in an unfavourable signal to noise ratio, since it would have a large capacity and is likely to be microphonic. The second advantage provided by the gas amplification is that it reduces the dependence of the output pulse height on the spatial distribution of the initial ionisation. This effect is of particular interest here and is treated in more detail in the following section.

3. Pulse Height Spread with the Position of Initial Ionisation

Since it is desirable to use differentiation time constants which are short compared with the total positive-ion collection time, the output pulse height is dependent on the position of the initial ionisation. In previous treatments[2,4]), which apply in the case of extremely large gas multiplication this effect has not been considered quantitatively. The simplest and most generally useful case is that in which the ionisation from a single event is produced at a constant distance from the counter wire, for example by a short track or one which is parallel to the counter axis.

Suppose the ionisation (q^+, q^-) is formed at a radius r_0 in a cylindrical proportional counter, whose anode and cathode have radii a,b respectively, and that the gas multiplication and electron collection takes place before the positive ions have moved a significiant distance. A positive ion sheath $(G - 1)\, q$ will have been formed very near to the central anode wire (G is the gas multiplication) in addition to the positive charge at r_0. The potential of the wire will continue to fall as positive ions move towards the cathode, and can readily be shown to have changed by an amount,

$$H = [\ln r_1^2/a^2 + (G - 1) \ln r_2^2/a^2]\; q/2C \ln b/a \qquad (1)$$

where r_1 and r_2 are the radial distance of the positive ions of the initial ionisation and of the avalanche respectively, and C is the capacity between the anode and cathode.

The electric field strength is proportional to $1/r$ and the equation of motion of a positive ion is $\mathrm{d}r/\mathrm{d}t = \mathrm{K}/r$, where K is a constant depending on the gas pressure, ion mobility, the counter dimensions and applied voltage. With the above stated initial conditions we therefore have,

$$r_1^2 = (b^2 - a^2)\; t/T + r_0^2 \qquad r_1 < b$$

and

$$r_2^2 = (b^2 - a^2)\; t/T + a^2$$

where T is the total transit time of a positive ion from $r = a$ to $r = b$ and t is the elapsed time from the production of the avalanche. The maximum signal obtained by the complete collection of all positive ions is $H_{\max} = Gq/C$. Otherwise by substitution in eq. (1) it is given by,

$$H = \{\ln [(b^2/a^2 - 1)\; t/T + r_0^2/a^2] + \\ + (G - 1) \ln [(b^2/a^2 - 1)\; t/T + 1]\}\; q/2C \ln b/a \qquad (2)$$

provided that none of the positive ions have reached the cathode. It is desirable to allow the pulse to rise for a time $t \ll T$ which is made practicable by its initial rapid rise. The special case $t/T = a/b \ll 1$ may be taken as an example and corresponds closely the time required for the pulse to attain half its maximum value. Since $b/a \gg 1$, substitution in eq. (2) and neglecting very small terms gives,

$$H = [\ln (b/a + r_0^2/a^2) + (G - 1) \ln b/a]\; q/2C \ln b/a \qquad (3)$$

when $t = aT/b$, so that the output pulse will vary between the limits $H \approx (G + 1)\, q/2C$ and $H \approx Gq/2C$ according to the position of the initial ionisation over the counter cross-section $a < r_0 < b$.

Eq. (3) may be used to find the pulse height distribution $N(H)\,\mathrm{d}H$, the relative number of pulses with height between H and $H + \mathrm{d}H$ for monoenergetic particles distributed randomly across the counter cross-section. Thus, assuming the elapsed time, $t = aT/b$, it is given by

$$N(H) \propto (b/a)^n \qquad \text{where} \quad n = [2CH/q + 1 - G];$$

[5]) H. W. Fullbright, Handbuch der Physik **45** (1958) (Springer-Verlag, Berlin, 1958) 1.

The distribution extends over the limits of H mentioned above. The full half width $\Delta H = q \ln 2/2C \ln (b/a)$ and the relative half width $\Delta H/H = \ln 2/(G + 1) \ln (b/a)$. The pulse height distribution may thus be made arbitrarily sharp by increasing the gas multiplication or, less effectively, by decreasing the wire diameter. With $b/a = 500$ a gas multiplication of 10 would be sufficient to reduce $\Delta H/H$ to 1%.

The above results, which apply only to short tracks or tracks parallel to the counter wire are however, extremely useful since they indicate the upper limit of the pulse height spread with position. If the particle tracks do not fill the whole of the counter cross-section, or if they are randomly orientated in direction, the resultant spread, for monoenergetic particles, will be less than the value derived above.

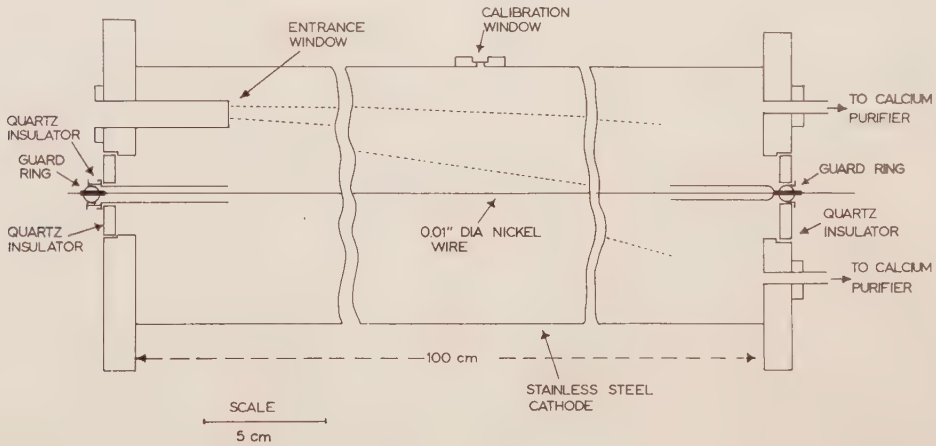

Fig. 1. Diagram of the experimental counter.

4. Construction

Fig. 1 shows the construction of the experimental counter. Ideally the charged particles should lose the energy only in the region of good cylindrical symmetry. Entry along a diameter would require an unreasonably large counter (and one with correspondingly long collection time). Oblique entry through a cathode window would result either in passage at small angles of incidence or the introduction of large variations in track length outside the sensitive volume. Thus a thin window is provided at the end of a re-entrant tube (B) which allows the particles to enter the sensitive volume directly. This tube does, of course, produce some distortion of the field. The potential of the guard tube A (V_A) may be varied to reduce end effects, and the best value was found empirically as described below. The effect of multiple scattering on the particle tracks was estimated for various cases. For example, with 8 MeV incident protons on the counter filled to atmospheric pressure with argon, the root mean square deviation of the track from its geometrically expected end was found to be about 2.7 cm.

A nickel wire 10 mil diameter was used as anode because it could be mounted with soft solder and readily replaced if necessary.

5. Performance

The counter was filled with argon-methane mixtures containing about 15% methane. The gases used were of commercial quality. The pulse height distribution for α particles from ThC and ThC′, injected through the calibration window, is shown in fig. 2. Gas multiplications of about 10 were used; the required counter voltage then being 2500 volts. At this setting a change of 220 volts in the counter voltage changed the output pulse-height by a factor of two. The overall drift in the pulse height due to the counter and the associated equipment

was found to be less than $\frac{1}{2}\%$ in several hours. Purification of the gas over hot calcium effected little improvement in the resolution of the freshly filled counter, and no marked deterioration was observed for about a week after filling.

The effect of varying the potential of the tube which shields the wire from the entrance tube was investigated by injecting α-particles, shows the spectrum obtained with 5.7 MeV incident protons; the pulse height spectrum was calibrated by varying the incident proton energy and observing the position of the elastic peak. The energy of the elastically scattered protons from O^{16} and C^{12} was found to agree with the predicted value (for incident beams of several different energies in the range 4.9 to 5.7 MeV) with an r.m.s. error of 12 keV

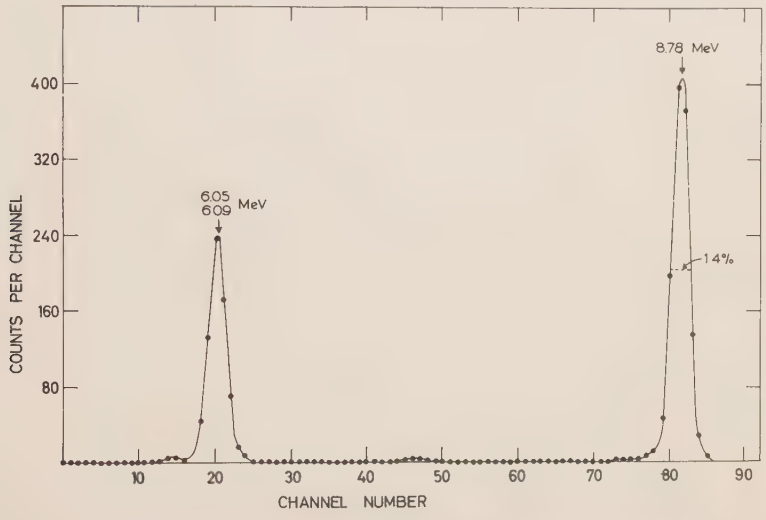

Fig. 2. The α-particle spectrum from ThC and ThC'. The small peak between channels 40 and 50 is assumed to arise from α-particles hitting the counter wire.

from the same source, through the entrance B. The relatively short range of these particles within the counter provides a sensitive test of the conditions close to the entry window. The potential of the shield tube V_A, was found to be fairly critical and the best energy resolution was obtained when V_A was set at the same potential as that of the counter wire and not at some relatively negative potential, as had been expected. At this optimum setting the α-particle energy resolution was approximately half that obtained by injection through the calibration window. This was considered to be satisfactory since, in normal use, a relatively small fraction of the particle energy would be lost in this region.

The counter was next tested with protons from a Van de Graaff accelerator scattered through 90° by a thin aluminium foil. Fig. 3 and the energies of the first and the second excited states of Al^{27} were found to be 0.835 ± 0.01 and 1.02 ± 0.01 MeV respectively, in excellent agreement with the accepted values. A plot of the output pulse height against the calculated energy of the protons on leaving the target yielded an intercept of 3.7 MeV for zero pulse height. This indicates that the total path between the scatterer and the sensitive volume of the counter was 20 cms N.T.P. air equivalent. This value was used to estimate the energy dissipated in ionisation of the counter gas, by incident protons of various energies, indicated in fig. 3. If so desired, the absorption path between the target and the sensitive volume of the counter, which in our case includes two Melinex windows each 1 mil thick, one on the target chamber and one on the counter, could be greatly reduced. Thinner

foils could be used and it would be possible to eliminate completely one window and the air path between the target box and the counter.

Protons of higher energy were produced by means of (d,p) reactions on targets of natural magnesium oxide and of aluminium, and some

6. Discussion

The proportional counter which has been described can readily be used to investigate simultaneously all protons in a spectrum extending from 4–10 MeV, in the presence of a background of γ-rays and fast neutrons; the resolution is about twice as good as that

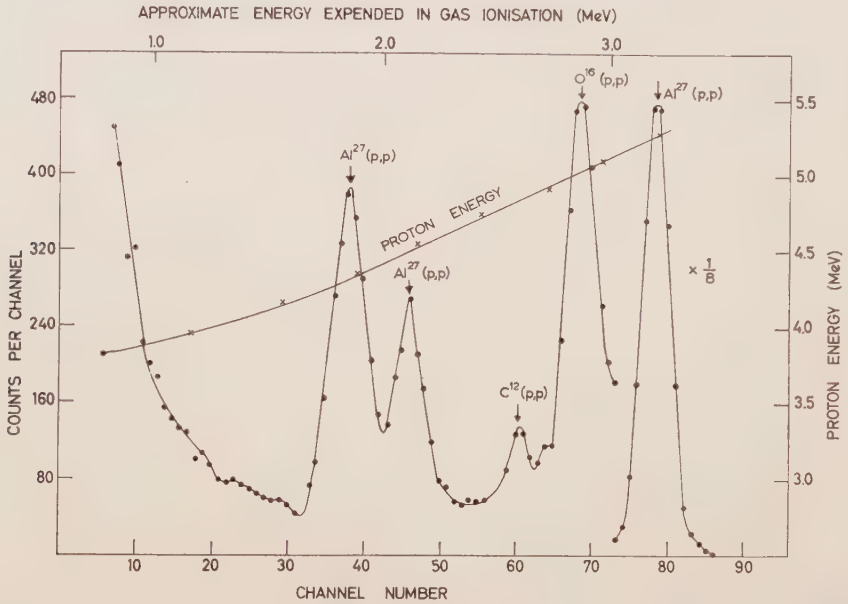

Fig. 3. The 90° proton spectrum from a thin aluminium foil with an incident beam of 5.7 MeV protons.

specimen results are shown in figs. 4 and 5. The proton spectrum from the reaction of Al^{27} (d,p) Si^{28} shown in fig. 5 has been taken with an expanded pulse height analyser scale to emphasise the attainable resolution. For example, the proton group of 8.1 MeV has a full width at half height of 1.6% in energy, before applying corrections for the spread due to target thickness ($\approx$ 40 keV) and for the fact that this group contains protons leaving the Al^{28} nucleus in both the ground and the first excited states, which are seperated by only 30 keV.

No attempt was made to shield the counter in these experiments, and the incident proton and deuteron beams were simply collimated by a series of holes in aluminium discs. This arrangement undoubtedly resulted in large background of γ-rays and fast neutrons.

obtainable using scintillation counters. It is probable that, with improvement of gas filling, counter uniformity and the associated electronic equipment, an energy resolution of 1% or better could be obtained.

The energy range of 6 MeV, which is available with protons, could be used without difficulty to study the upper 6 MeV of a more energetic proton spectrum by interposing suitable absorbers. The energy range covered by the counter itself could be increased by increasing the gas pressure.

With a sufficiently thin window, or at somewhat higher energies than were available in the above experiments, the counter should prove useful for spectroscopy of deuterons, alpha particles etc.

A simple development would be to insulate separately a short length of the counter wire at

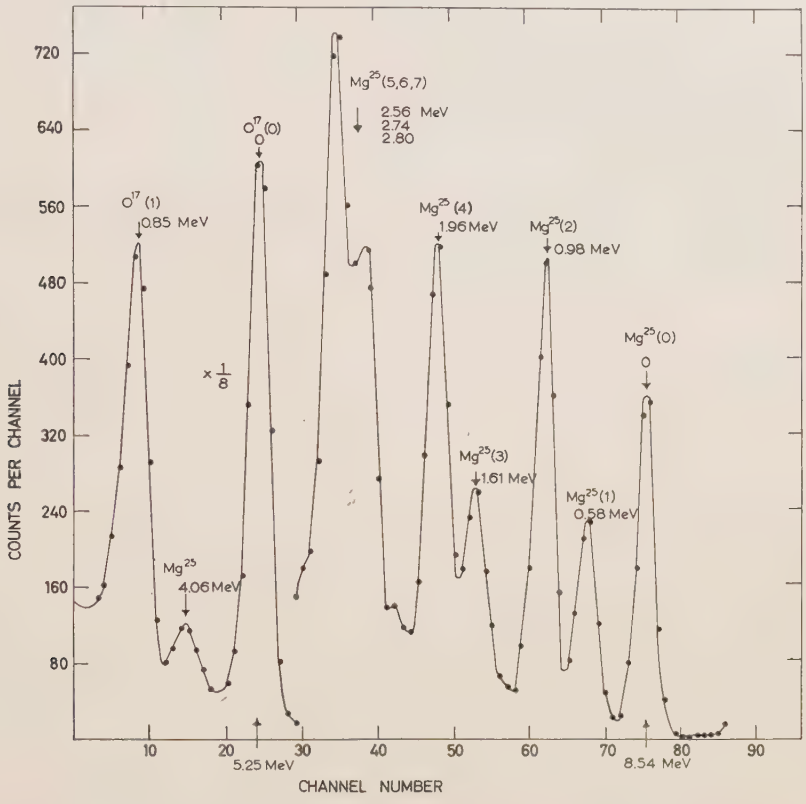

Fig. 4. The 90° proton spectrum from a magnesium oxide target bombarded with 4.1 MeV deuterons.

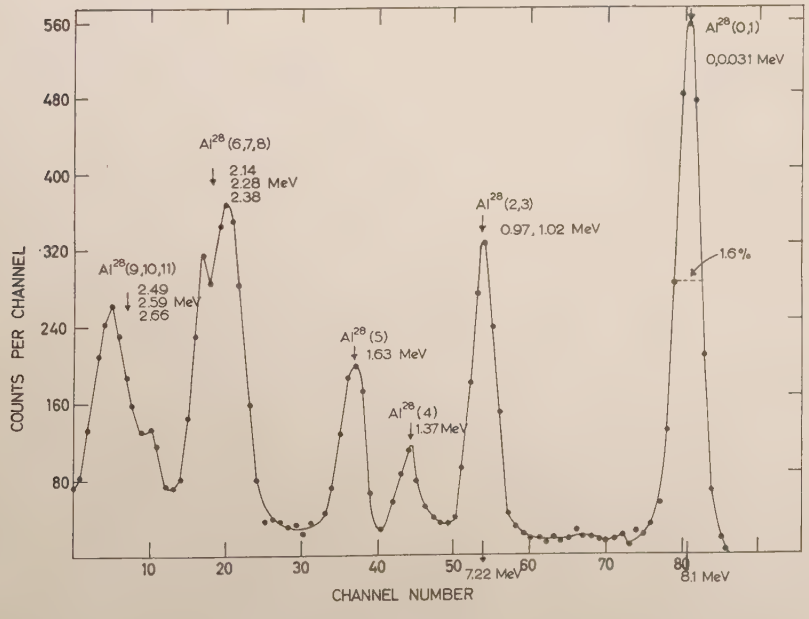

Fig. 5. The 90° proton spectrum from an alluminium target bombarded with 3 MeV deuterons.

the opposite end of the counter to the entrance window. The pulse from this short length of the counter, in anticoincidence with the main pulse, would enable one to eliminate the particles which pass through the counter without stopping. Thus protons could be analysed in the presence of other protons of much higher energy without ambiguity. Also, deuteron spectra could be obtained despite the presence of a high flux of protons of similar or higher energy, for example in a study of (p,d) reactions.

Acknowledgement

One of us (S.A.H.) is indebted to the Nuffield Foundation for a Fellowship.

NUCLEAR INSTRUMENTS AND METHODS 6 (1960) 57–65; NORTH-HOLLAND PUBLISHING CO.

A PULSE TO DIRECT CURRENT VOLTAGE COMPARATOR

C. H. VINCENT and W. G. KING

United Kingdom Atomic Energy Authority, A.W.R.E., *Aldermaston, Berks.*

Received 10 August 1959

A simple instrument is described which enables pulse voltages to be measured very accurately by comparing them with direct current voltages. The pulses may be of the order of 1 microsecond to 10 milliseconds in duration and up to 60 volts or so in amplitude, of either sign. The error in the measurement is of the order of a few parts in 10^4, at most, for the larger voltages.

1. Introduction

It has been possible to measure direct current voltages for many years with an accuracy of the order of $\pm$ 0.01% or better, by means of readily obtainable standard laboratory measuring instruments. A precision potentiometer may be used in conjunction with a voltage divider having a choice of accurate fixed ratios. Pulse voltages, however, are normally measured by means of a vacuum tube voltmeter or by means of an oscilloscope, and the accuracy obtainable is rarely better than $\pm$ 1%. The present device is the result of an attempt to find a simple means of comparing a pulse voltage accurately with a nearly equal direct voltage. The latter may then be measured, enabling the pulse voltage to be determined more accurately than would otherwise be possible. The pulses may be of the order of 1 microsecond to 10 milliseconds or more in duration. This covers a range of pulse lengths commonly used in electronic circuits. The pulses to be measured are applied to a diode, in the forward direction, and the method used depends on the initiation of conduction current through this diode, as a direct voltage reverse bias which is applied to it is decreased. Any ordinary general purpose laboratory oscilloscope, such as might be used for examining the input pulse, may be used as an indicator for the comparator, provided that it includes a suitable amplifier.

2. Principles of Operation

The circuit of the comparator is shown in fig. 1. An accurately measured reverse bias is applied to the cathode of the diode D_1. If this

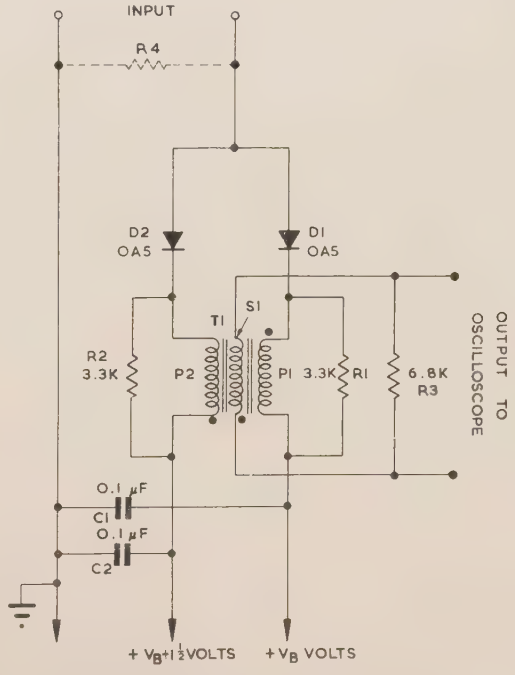

Fig. 1. Pulse comparator lead circuit.

bias voltage is appreciably greater than the positive peak voltage at the input terminal, D_1 does not conduct, and there is no output from the secondary winding S_1 of the transformer T_1,

which is connected to the oscilloscope, as shown. As the bias is reduced, a point is reached where D_1 starts to conduct perceptibly at the peak of each pulse, and a small pulse appears at the output terminal. This pulse may be amplified by the oscilloscope amplifier, to obtain maximum sensitivity. The limit to the gain which may be usefully employed is set by the residual output, from the transformer secondary terminal, which appears when D_1 is not conducting. The current through the self-capacity of D_1 due to the input pulse could be a major source of such output, but the circuit is arranged so that this current is counterbalanced by the corresponding current through the diode D_2, which is supplied with 1.5 volts more bias than D_1, by means of a dry cell, and is therefore also not conducting. The transformer T_1 has two similar primaries P_1 and P_2, connected in opposition, and the whole circuit is arranged symmetrically, to keep the balance as close as possible. The two condensers C_1 and C_2 complete the circuit to earth for the pulse currents, and may also help by shorting out stray induced voltages at the points concerned. Damping resistors R_1, R_2 and R_3 are connected across the primary and secondary windings of the transformer, to prevent ringing with the self-capacities present.

It should be noted that what the comparator measures is the positive peak potential at the input terminal. (It can equally well be made to measure negative peak potentials, by reversing the bias voltages and reversing the diodes.) The comparator measures this positive peak potential at the input terminal very precisely, as we shall show, but, as with any precision instrument, some care is necessary in interpreting the results, to obtain the greatest possible accuracy, and the following facts need to be taken into account.

2.1. VOLTAGE EXCURSIONS OF REVERSE SIGN IN THE WAVEFORM

If the input waveform goes negative with respect to earth as well as positive, a separate measurement or allowance must be made for this, if the peak to peak value or total voltage excursion is required. (A typical example of this is the case where the source of pulses is a resistive load, which is fed with current through a large blocking condenser. The correction for rectangular pulses in this case, in terms of the mark to space ratio of the pulses, is well known).

2.2 LOADING OF THE SOURCE BY THE COMPARATOR

Although the input impedance of the comparator is quite high, when the diodes are not conducting (which is the relevant condition), it may be necessary to correct for its loading of the source, if it is required to find the pulse amplitude in its absence with the highest possible precision, owing to the high accuracy of the comparator. The comparator is approximately equivalent to a load resistance $\frac{1}{2}r_r$ of about 10 megohms or higher, with the type 0A5 diodes shown (where r_r is the effective dynamic resistance of each diode), in parallel with a capacity of about 6 picrofarads, provided that the latter is not added to appreciably by connections (see next section). It is desirable to keep the capacity loading as small as possible, since it affects the shape of the pulse, and it is difficult to correct for, if it is appreciable at all. If the output impedance of the source is a pure resistance r_s, the amplitude of the pulse waveform is reduced (neglecting the capacity effect) by the factor.

$$\frac{r_r}{r_r + 2r_s} \doteq 1 - \frac{2r_s}{r_r}.$$

2.3. LOSS OF BIAS DUE TO REVERSE CURRENT LEAKAGE

The direct current voltage that is accurately measured when the comparator is in use is the potential V_B at the cathode of D_1. However, the diodes pass a small reverse current, when a reverse voltage is applied to them. This current is not a precisely linear function of the reverse voltage, but it may be approximately specified, in the static case, by stating a reverse static resistance R_r, which is of the order of 80 megohms or more for each diode, using specially selected 0A5's. Such a current raises the mean or direct current potential at the input terminal to

an extent depending on the resistance of the pulse source to a direct current passed back through it. Let this resistance be denoted by R_s. The voltage developed across R_s can then be shown, after allowance for the 1.5 volts extra bias on the second diode, to be

$$\frac{2\,(V_B + 0.75)\,R_s}{R_r + 2R_s}.$$

The actual bias voltage applied to D_1 is then

$$\frac{R_r}{R_r + 2R_s} V_B - \frac{2R_s}{R_r + 2R_s} 0.75 \doteq \left(1 - \frac{2R_s}{R_r} V_B\right).$$

(The second term on the left-hand side is normally a relatively small one.)

Neither the dynamic nor the static characteristics of the diode will normally be strictly linear. Nevertheless, usefull corrections may be made with the aid of the approximations made by stating resistance values for them, since we should be dealing here with small errors only. (A more accurate correction for the leakage current could, of course, be made by reference to the reverse static characteristic of the diode, if necessary.) Note that if $R_s = r_s$ and $R_r = r_r$, the coefficient of V_B in 2.3 above is the same as the factor given in 2.2 above. This implies that the corrections would cancel. R_s will equal r_s if the source is a resistive load fed from a high impedance current source. R_r may or may not approximate to r_r, depending on the type of diode used. The results of measurements on the 0A5 in this respect show that the dynamic input impedance to the comparator is somewhat less than the parallel reverse static resistance of the two diodes.

If there is not a low resistance direct current path at the point at which the voltage is being measured, for example, if it is a terminal which is connected to a source of pulses through a blocking condenser, then a resistor to complete the direct current path must be provided in parallel with the comparator, and the loading due to this must be allowed for. It is possible that in some cases a suitable choke could be used instead of this resistor. A pair of terminals are provided inside the comparator, at the input terminal, to which such a resistor or choke may be soldered, if required. Fig. 1 shows a resistor R_4 in this position.

3. Construction

As stated above, it is desirable that any extra capacity loading due to the cable connecting to the comparator should be small, to avoid distortion of the pulse, especially for short pulses. For this reason, the comparator proper is made in the form of a small head unit, in a cast alloy box, which can be placed near the point where the pulse voltage is to be measured. Two such heads are provided, one for positive pulses and one for negative pulses, with the diodes connected accordingly. When they are not in use, the two heads are mounted on a chassis (see fig. 2), which also contains a stabilized

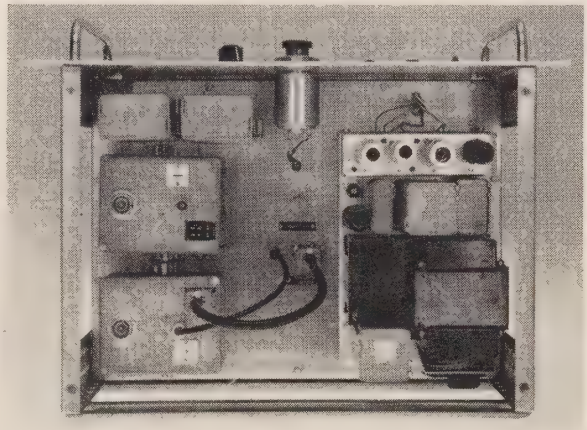

Fig. 2. Pulse comparator (Top View).

power supply and the 1.5 volt dry cell needed to raise the second bias voltage. A small commercially available stabilized power supply (Solartron type AS516, rated at 250 volts, 60 milliamps) is suitable for the purpose, and is built on to the main chassis.

This main chassis also contains a ten turn "Helipot" (see fig. 3) by means of which the bias on D_1 can be accurately set, after proper adjustment of the power supply voltage. The range of bias available is from 0 to 100 volts. If the greatest possible accuracy is desired, the Helipot output may be connected to a voltage divider, and the voltage measured by means of a precision potentiometer. The Helipot then

continues to serve as a means of adjusting the voltage, but its calibration is no longer accurate, to the diodes, this switch also modifies the connections to the head unit, as it changes

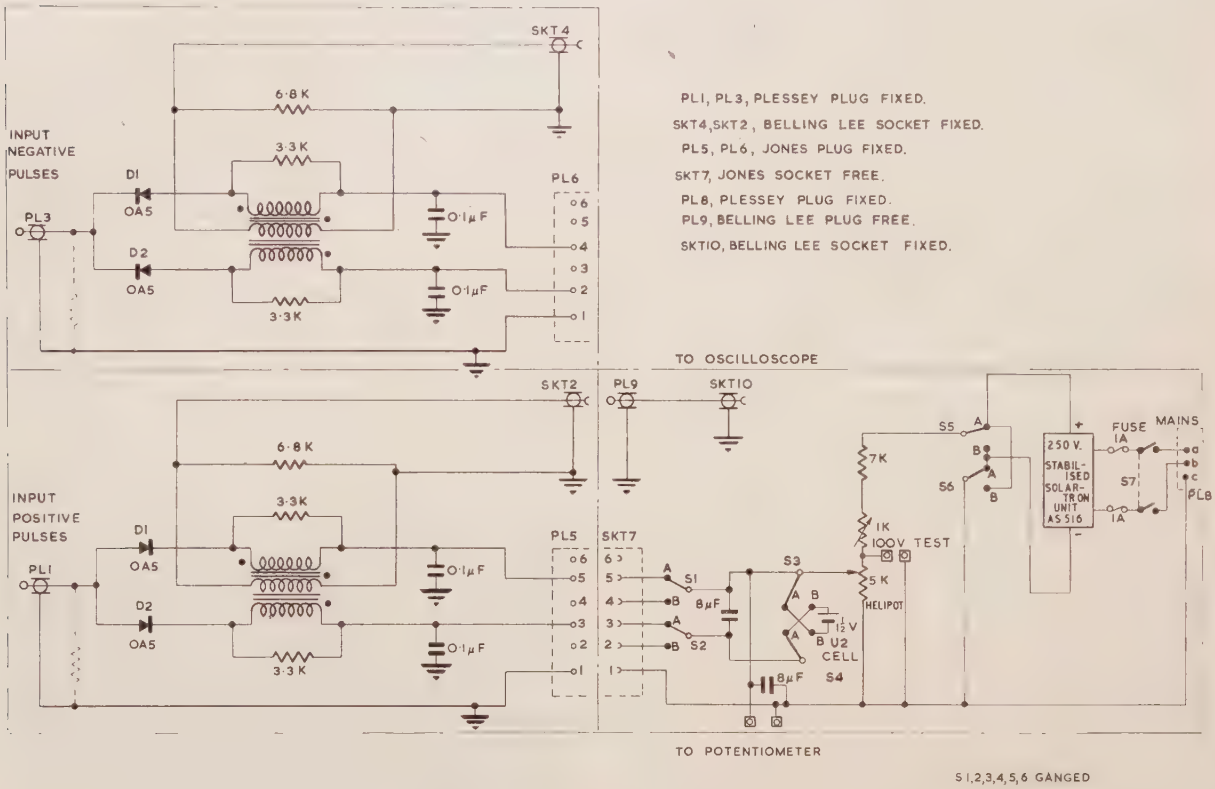

Fig. 3. Pulse comparator circuit.

owing to the loading by the voltage divider. The 8 microfarad condensers shown in fig. 3 are provided to short out stray voltage pickup. It is desirable to avoid loops in connections, as far as possible, to prevent magnetically induced pick-up, and for this reason provision is made to run the cable to the oscilloscope back to the control chassis and then on to the oscilloscope, rather than direct to the oscilloscope.

When the source impedance is low and the loading effect of the connecting cable is not serious, either head unit may be used in place in the main chassis. Short cables are provided for connecting either head to the main chassis, when it is mounted on the latter, and longer cables for external use. The bias voltages in the main chassis may be reversed by means of a ganged switch. As serious damage could be caused if a forward bias was applied by accident position, so that a bias of the wrong sign cannot be applied to either head.

The symmetrical layout of the interior of the head units is shown in fig. 4. The components

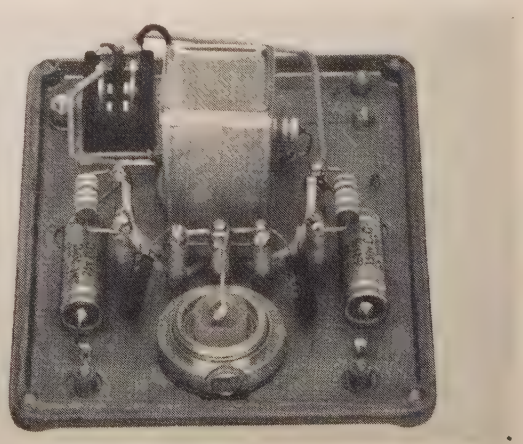

Fig. 4. Head unit (internal view).

are all mounted on the lid of the shielding box, as shown. The construction of the positive and negative heads is identical, except for the polarity of the diodes and for the change in the pins used in the bias supply plug and socket. The coaxial input socket is visible in a central

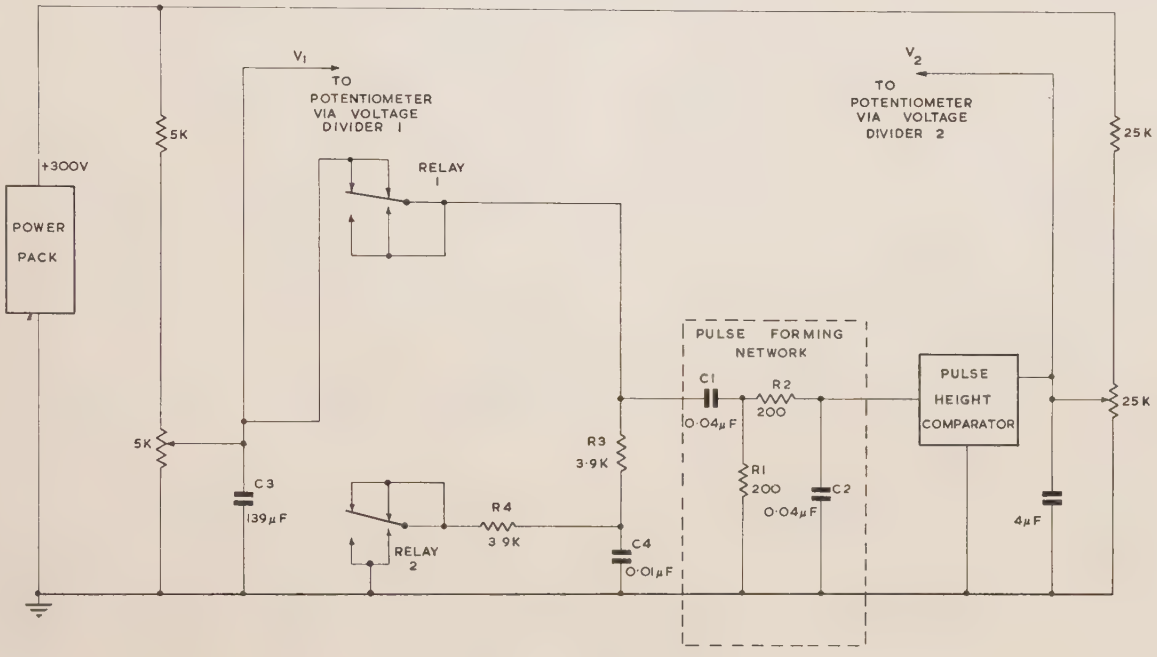

Fig. 5. Testing circuit (first method).

position, with the diodes on either side of it. The rectangular metal box in the centre is the shield of the transformer, and the two primary damping resistors can be seen on either side of it. The secondary damping resistor is at the rear of the transformer shield, by the output socket. The 6-pin bias supply connector is at this end of the lid, also.

4. Precautions in Use

The method of use of the instrument is clear from the above description. The safety arrangement incorporated in the switching automatically prevents bias of the wrong sign being applied to a head. It should be noted that when a head is being used (with bias of the correct sign), it is undesirable that large pulses of the wrong sign should be applied at the input, as the total reverse voltage applied to the diodes is then the sum of the pulse and bias voltages, and this may exceed the rated maximum reverse voltage of the diodes (100 volts). It has already been mentioned that measurements with the comparator are made by reducing the bias, which should therefore be set initially at a greater value than the expected value of the pulse voltage. This also avoids any possibility that current flowing during the pulse may exceed the maximum current rating of the diodes, which is, however, 500 milliamps peak. The final adjustment, for greatest accuracy, is made by increasing the bias again until the conduction pulse just disappears. The bias voltage is then measured.

5. Experimental Tests of the Comparator

The accuracy of the comparator was tested by two methods, one using pulses of about 20 microseconds duration and the other using square waves of about 10 milliseconds duration, both waveforms being derived from a direct current source by a switching action. The two circuits used are shown in figs. 5 and 6 respectively. In each case, the critical bias voltage at

which the operator found the output signal to appear was plotted against the known input voltage to the comparator. In both cases, the comparator reading agreed very closely with the input voltage, except for a small zero error (of the order of 10 millivolts) which was found to be interfere with the use of the comparator. The integrating time-constant (2 microseconds) was very short compared with the duration of the square wave (10 milliseconds) and with the duration of the timebase sweep used, so that the final maximum value would be reached to an

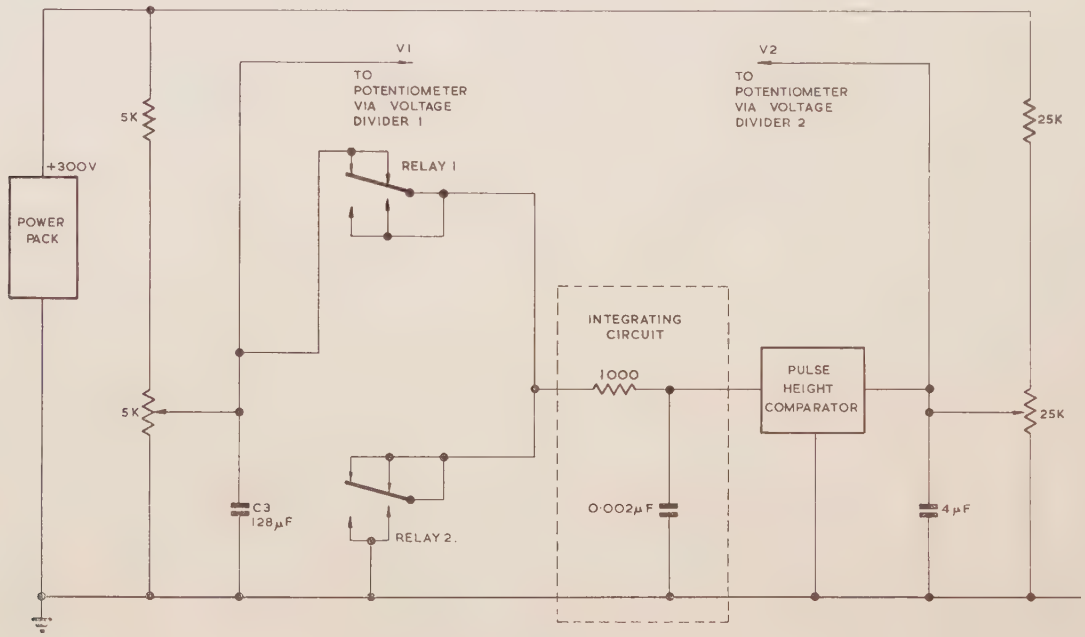

Fig. 6. Testing circuit (second method).

a function of the temperature of the diode.

In the first method (fig. 5) the ratio of the pulse voltage to the direct current input is a function of the ratio of the two capacities C_1 and C_2 and the ratio of the two resistances R_1 and R_2, only. It was therefore possible to eliminate the necessity for measuring these capacities and resistances by making them as nearly equal as possible, in each case, and then taking the mean values of measurements made with these components interchanged. The theoretical calculation of the pulse height could then be carried out on the basis of exact equality. Small corrections were made for the fact that the capacity of C_3 was finite, rather than infinite, and for the capacity loading due to the comparator and its connections. In the second method (fig. 6) the integrating circuit shown was used to prevent an excessively sharp initial rise which would accuracy within 1 part in 10^5 or better. This method had the advantage that the voltage dividers which were being used (in conjunction with a precision potentiometer) to compare the direct current input and bias voltages were set to the same ratio. They could therefore be interchanged to eliminate errors in their calibration.

5.1. RESULTS

In each case, the standard deviation of the measured points from the best fit straight line through them (by Least Squares) was only of the order of 6 millivolts. There are four combinations in which the four components R_1, R_2, C_1, C_2 may be used in the first method, and if these are grouped in appropriate pairs and the means taken (that is, the mean of R_1, R_2, C_1, C_2 and R_2, R_1, C_2, C_1, and the mean of R_1, R_2,

C_2, C_1 and R_2, R_1, C_1, C_2) we obtain two independant values for the slope of the bias against input line. These two slopes were 1.00045 and 1.00051, respectively, in very satisfactory agreement with each other. The mean value is therefore 1.00048. The departure from unity is unexplained, but is believed to be due to an effect in the pulse generating circuit, probably due to stray inductance. By the second method, the slope obtained was 0.99953. It is encouraging to note that the two discrepancies are of opposite sign (in fact, the mean value is extremely close to unity) as this suggests that the remaining unexplained error is not in the comparator. It seems unlikely that the error in the latter can exceed a few parts in 10^4, at most.

6. Calibration of the Working Diode for Zero Error

It follows from the above discussion that the zero error for the particular working diode in use in the only parameter of the voltage comparator that needs to be determined experimentally before the comparator is ready for use. It is not necessary to have an accurately calibrated pulse generator to measure this zero error. Any suitable pulse generator will do, provided that it can be used in conjunction with a fixed attenuator which reduces its output in an accurately constant ratio. If the critical bias voltage is plotted against the nominal pulse voltage, both with and without the attenuator present, and the best-fitting line (Least Squares) is determined in each case, the zero error B of the comparator may be calculated from the values of the intercepts on the bias voltage axis. Let these be I_A and I_U for the attenuated and unattenuated cases respectively. It can then be shown that

$$B = \frac{I_A - \theta I_U}{1 - \theta}.$$

The value of the attenuation factor θ does not need to be very accurately known, provided that it is sufficiently small. It would appear to be practicable to use a factor of the order of 0.01, with a maximum attenuated output of the order of 0.5 volts. The actual value of θ for the attenuator in use does not need to be known accurately beforehand, as it may be determined with sufficient accuracy from the ratio of the slopes of the two best-fit lines. Once the zero error has been determined, of course, the comparator may be used to calibrate the pulse generator accurately.

6.1. VARIATIONS WITH TEMPERATURE AND BETWEEN DIODES

The variation of zero error with temperature was investigated by maintaining a comparator head at a variety of temperatures from 23.5° C to 45.0° C, and measuring the parameter D, as described above, in each case. The results are shown in fig. 7. The zero error B decreased from a positive value through zero to a negative value, as the temperature was increased, with a mean temperature coefficient of — 4.2 millivolts per degree centigrade. The variation of the zero error from one diode to another was measured for 7 diodes under similar conditions of temperature and use. The mean value and standard deviation of the values obtained were respectively 12 $\pm$ 7 millivolts (at 26° C).

7. Rise-Times and Pulse Durations

The comparator was tested with a variety of pulses ranging from about 1 microsecond to 10 milliseconds in duration. It was found that with rise-times less than about 0.5 microsecond the residual output due to the feed through the capacity of the diodes was excessive, in spite of the balancing out action of the circuit, and interfered with the observation of the threshold of conduction, reducing the accuracy. The duration of the pulses which are to be measured does not seem to be particularly important, so long as the approach to the maximum value occurs at a reasonable speed. The limitation in this respect lies in the low frequency pass limit of the output transformer. If the approach to the maximum value is sharp, an output signal will appear when the conduction level is reached, and it does not matter if this signal falls off after a time interval set by the transformer characteristics. If the approach to the maximum is

very slow, however, there will be a loss of sensitivity, as the slowly increasing conduction current in the primary winding of the transformer will induce only a reduced voltage in the secondary. Nevertheless, the limitations of the comparator in this respect are not severe, as is shown by the fact that a good reading is obtained even with an ordinary 50 cycles per second alternating current waveform. The accuracy of the comparator in this case has not been fully investigated, but it agreed with the best meter available to well within the limits of accuracy of the latter.

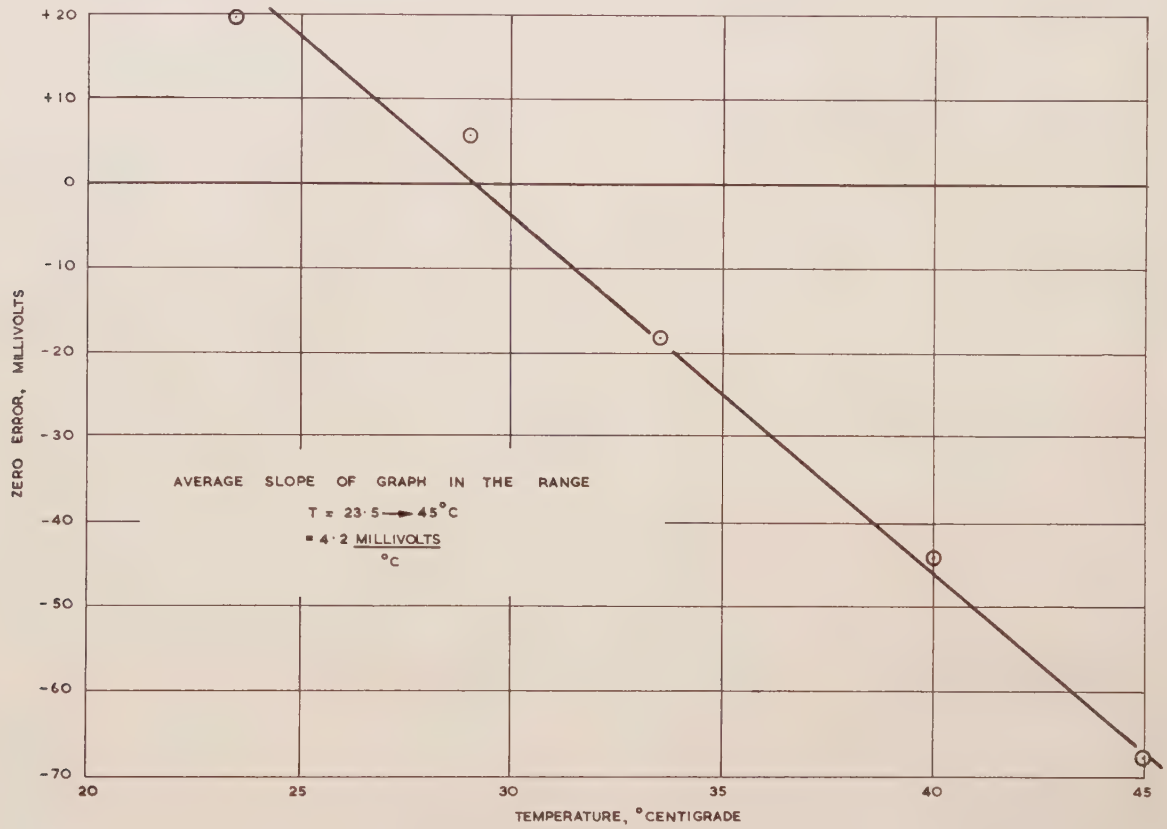

Fig. 7. Variation of zero error with temperature.

8. Practical Details

A typical oscilloscope used for the measurement of A and B in the tests of the comparator described above was a Solartron type CD513. It had a bandwith of 2 megacycles per second and was set to a sensitivity of 10 millivolts per centimetre. No systematic variation of results with oscilloscope gain or other conditions was observed, although there were naturally optimum conditions giving maximum accuracy. Consistent results were obtained as between one observer and another, with little or no training or practice required to operate the comparator.

The 0A5 diodes used were specially selected to have a high back resistance, being connected in series with a galvanometer and a 60 volt battery for the measurement of this. Only diodes giving a reverse current of less than 0.75 microamp. at this voltage were accepted. The two diodes used in each comparator were also matched as closely as possible as a pair with equal back resistances.

8.1. CONSTRUCTION OF THE OUTPUT TRANSFORMER

The details of the transformers used are shown in fig. 8. Both primary and secondary windings were wound with 36 SWG S.C.C. wire. Each

was made on a dummy former, on which was wound a double layer of thin paper to facilitate easy removal of the finished coil. The coils were wavewound to a ratio of 1:1, and throughout the winding polystyrene cement was used to bond the layers. When the cement had set, the coils were removed and assembled on the final former, care being taken to ensure that the primary windings were in opposition. The coils were then cemented into place and the transformer assembled as shown. The assembly was mounted in a tinned steel screening can, and the final dimensions were 2.5 centimetres square by 4 centimetres high. Fig. 9 is a photograph of the transformer assembly with the screening can removed.

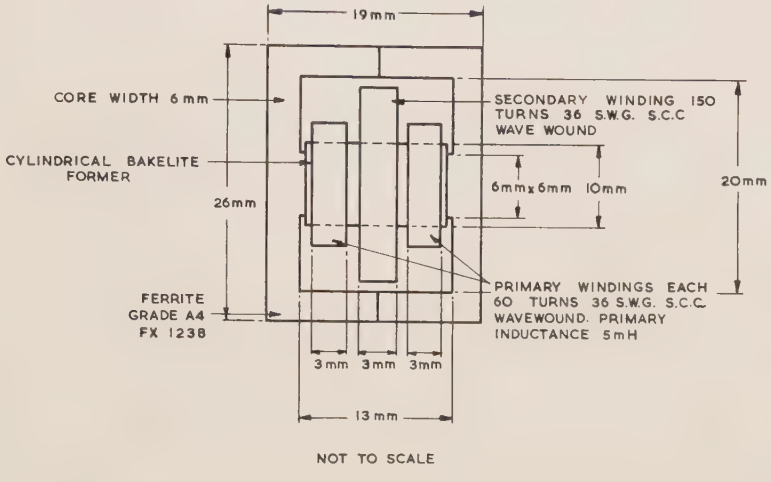
19mm
CORE WIDTH 6mm
CYLINDRICAL BAKELITE FORMER
26mm
FERRITE GRADE A4 FX 1238
SECONDARY WINDING 150 TURNS 36 S.W.G. S.C.C WAVE WOUND
6mm x 6mm 10mm
20mm
PRIMARY WINDINGS EACH 60 TURNS 36 S.W.G. S.C.C. WAVEWOUND. PRIMARY INDUCTANCE 5mH
3mm 3mm 3mm
13mm
NOT TO SCALE
THE CORE IS MOUNTED AND SCREENED TO SPECIFICATION U.D.E. TYPE 50. COMPRISING COMPONENTS 3-7 13952 TO 13959, 14026, 12763 AND 11984 (A.E.R.E. HARWELL.)

Fig. 8. Construction of the output transformer.

Fig. 9. Output transformer (photograph).

9. Conclusions

The pulse comperator is a valuable instrument for the accurate calibration of pulse generators and pulse amplitude measuring equipment generally, as it can be used to give a direct reference of pulse amplitudes to standard direct current measuring equipment of high absolute accuracy and reliability. Moreover, its own error in making this reference is small. At the present state of development of the instrument, the error in measuring a pulse voltage V_p may be estimated conservatively as less than $\pm$ (0.0005 V_p + 0.010) volts. It should therefore be possible to increase the absolute accuracy of pulse amplitude calibrations appreciably by the use of the comparator.

Acknowledgement

It was originally intended that the capacity and back resistance of the working diode should be conterbalanced by means of a suitable capacitor and parallel resistor in the second primary circuit. The authors are indebted to Mr. G. C. H. Heywood for the valuable suggestion that a second diode might be used for this purpose.

NUCLEAR INSTRUMENTS AND METHODS 6 (1960) 66–71; NORTH-HOLLAND PUBLISHING CO.

INTERNAL TARGET FOR A BETATRON

H. MORINAGA and T. KUROYANAGI

Department of Physics, Tohoku University, Sendai, Japan

Received 17 August 1959

Internal bombarding technique to produce high specific activity on small samples being used for 25-MeV betatron at Tohoku University is described. The samples are placed inside the doughnut at the end of a blind cylinder inserted from outside; thus samples are bombarded under one atmosphere, just behind the bremsstrahlung target where the X-ray density is extremely high. Design and the operational characteristics as well as some examples of its application are presented. More than 1 millicurie of Cu^{62} was produced and the specific activity becomes 500 times compared with external bombardment.

1. Introduction

For producing radioactivities with a betatron or a synchrotron, samples to be irradiated are usually placed in the X-ray beam outside of the doughnut. The distance from the bremsstrahlung target to the samples can not be shortened to less than 20 or 30 cm even for small machines. Because of the large beam cross section it is not possible to get high specific activities in the samples. This is sometimes a serious drawback of a betatron or a synchrotron for radioactivity production.

In order to get much higher specific activity, an internal probe technique has been developed by Becker, who placed the bremsstrahlung target and the sample together in the doughnut[1]) In one case, 37 microcuries of Cu^{62} was reported to have been produced on a copper foil. This method, however, is not quite convenient for studies of short-lived activities, since the vacuum of the doughnut must be broken every time the target is put in and taken out.

We have been using an internal bombardment technique for the 25-MeV betatron at Tohoku University which gives comparable activities as ref.[1]) and does not require the vacuum to be broken every time before and after the bombardment. The whole assembly is quite simple and rugged and easy to handle with. It is being used quite successfully for the irradiation of expensive small samples or enriched isotopes as well as for the study of very short half-lived activities in which the samples must be brought to the counting position within a fraction of a minute after the termination of the bombardments. It seems to be worth while reporting the experiences with our internal target since installation of such an internal target may turn out to be useful in some cases especially when the production of activities with a betatron or a synchrotron is undertaken.

2. Design and Performance

The internal target assembly consists of a brass cylinder and a sample holder, as shown in fig. 1.

On the internal end of the brass cylinder, a platinum cap of 0.2 mm thick is hard soldered, which stops the betatron vacuum. The cylinder is supported on a frange which terminates a side arm of the glass betatron doughnut with an "○" ring. The position of the platinum cap can be adjusted by four screws on a guide cylinder which also tightens the "○" ring. Plugging in and out of the cylinder is also easily done by slightly loosening the screws on the frange without breaking the vacuum.

The platinum cap is flat on the top and the side of the cap is made long enough (3 mm) so that the electron beam may not hit the brass part of the cylinder.

[1]) R. A. Becker, Rev. Sci. Instr. **10** (1959) 773.

The sample to be activated is placed right inside of this platinum cap by a sample holder which can be inserted from outside. The heads on the inside of the outer brass cylinder was used to keep the direction of the target correct during the irradiation. The samples, which are

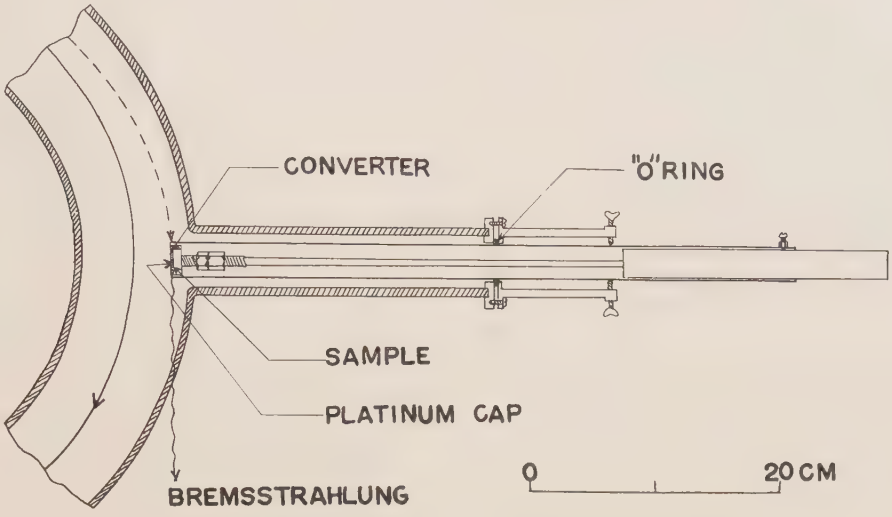

Fig. 1. The internal target assembly with the sample holder.

of the sample holder are made of aluminium, on which grooves are cut to keep the sample in at the right position (fig. 2). Several different types of the head were prepared to meet different bombarding requirments. In most of the cases, an additional platinum or gold converter was attached to the head to the side where beam hits. When the sample is of heavy material this converter was dispensed.

These heads are attached to the top of the stem of the sample holder. The outer end of the

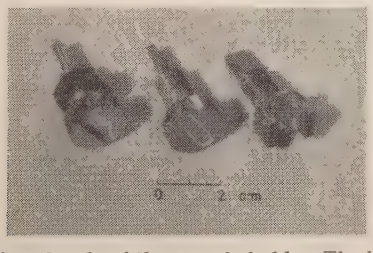

Fig. 2. Various heads of the sample holder. The left one has a large groove and the middle one has a very shallow groove. The right one is designed to hold two KBr pieces vertically to the beam.

stem was a brass cylinder which just fits into the outside cylinder. A rubber tape was used to push the sample holder assembly tight on the inner surface of the platinum cap. Small pivot

usually of powder form, were either filled into the groove on the aluminium head or wrapped in aluminium foil before being put into the groove. After the bombardment the aluminium cover was broken and the sample was taken out.

The target was placed at about three centimeters outside of the betatron stable orbit. This distance has been known to yield the maximum efficiency in case of the external bombardment.

In order to adjust the vertical position of the target, small pieces of potassium bromide crystals were irradiated on the sample holder. The KBr pieces were placed in a special head (fig. 2), which held them vertically to the beam. After a few minutes irradiation blue coloring showed the place where the beam hit, indicating the relative height of the target to the beam. A few times bombardment are enough to bring the target to the correct position. Fig. 3 shows an example of the irradiated potassium bromide crystals. From this coloring, rough idea of the beam size may be obtained, but in order to know the distribution of the activity in the sample various stack pieces of copper and tantalum was irradiated at the target position.

An example of the distribution of the Cu^{62} activity in a large sample of copper without the

platinum converter is shown in fig. 4. Seven round copper disks of 0.25 mm thick and 19 mm in diameter were irradiated and the activities

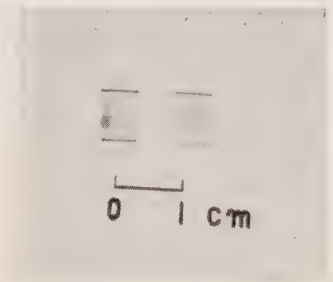

Fig. 3. The irradiated KBr pieces.

on various parts of the disks were measured with a G-M counter after cutting the disks into pieces. Here, it is seen that the half width of the activation in vertical direction is about 3

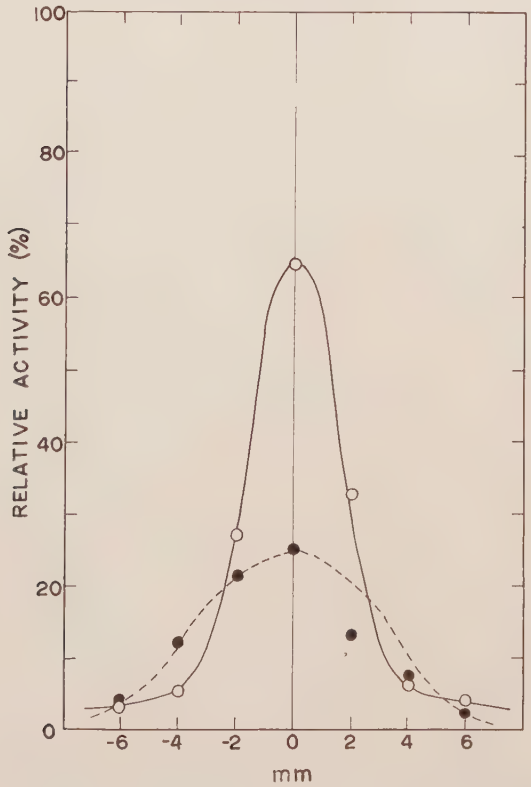

Fig. 4. Distribution of the Cu^{62} activity on one of the seven stacked disks bombarded inside the platinum cap without the converter. This particular figure shows the distribution of the activity on the deepest disk (No. 7) which was at 1.9 mm distant from the platinum cap. Open circles show the activity on 5.4 mm from the entrance of the beam and closed circles show the distribution of activities at 15.5 mm from beam entrance.

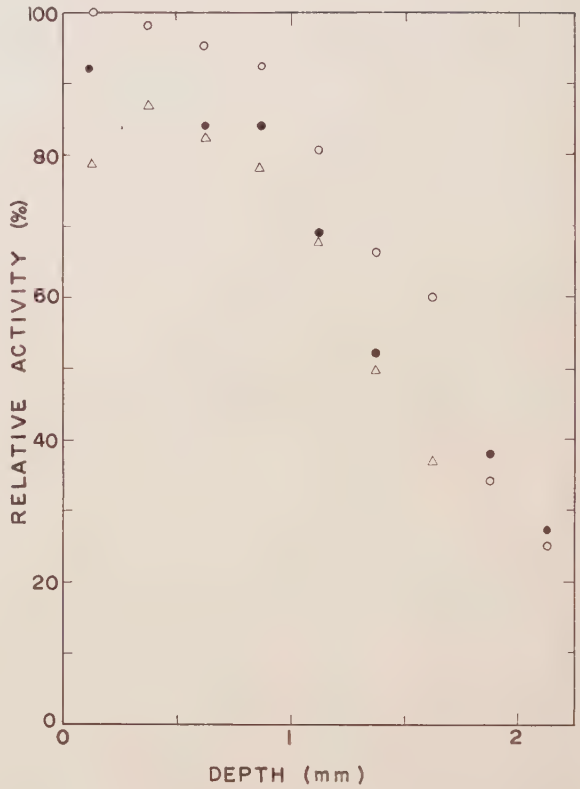

Fig. 5. The Cu^{62} activities produced on stack pieces of 7 mm × 19 mm × 0.25 mm copper sheets. The activity decreases as going deeper. Closed circles show distribution for no converter, open circles for 0.6 mm platinum converter, and triangles for 1 mm platinum converter thicknesses.

mm for the copper plate right behind the platinum cap (No. 1). The width does not change much from the point closer to the beam entrance to the point farther. The spread of activation increases as going forth from the entrance to the plate placed deeper in the target (No. 4 and No. 7) as expected. The former fact probably indicates that the activation on the No. 1 disk is mostly due to the X-rays produced within platinum cap. Fig. 4 shows the distribution of activity on the disk No. 7.

Since, many of the actual irradiations were performed in a thin grooves of 5 mm or 7 mm in width and 0.5 to 2 mm in depth cut on a head of the sample holder, more detailed distribution of activities were measured in stacked copper strips of 7 mm width and 19 mm long and 0.25 mm in thickness. Fig. 5 shows the distribution of activities on various points in such

copper strips as a function of depth taking the thickness of converter as parameter. No drastic change is seen in the distribution. The total activity was measured for three different platinum converter thicknesses, 0, 0.6 mm and 1 mm, respectively. The ratio was 8:10:9. In order to obtain this ratio, thin Cu plates were placed between the platinum cap and the converter, as a monitor of the beam intensity.

Under the best condition, 1.2 millicurie total saturation activity was produced. The specific activity at the best point was found to be 500 times higher than the case of external bombardment.

Fig. 6 shows the dependence of activity distribution on expander current. Three different values of expander primary current, 100 mA, 150 mA and 200 mA, were tried. There was practically no change in the distribution. This shows that the beam hits the platinum cap to fairly farther inside ($\approx$ 1 mm) not because of

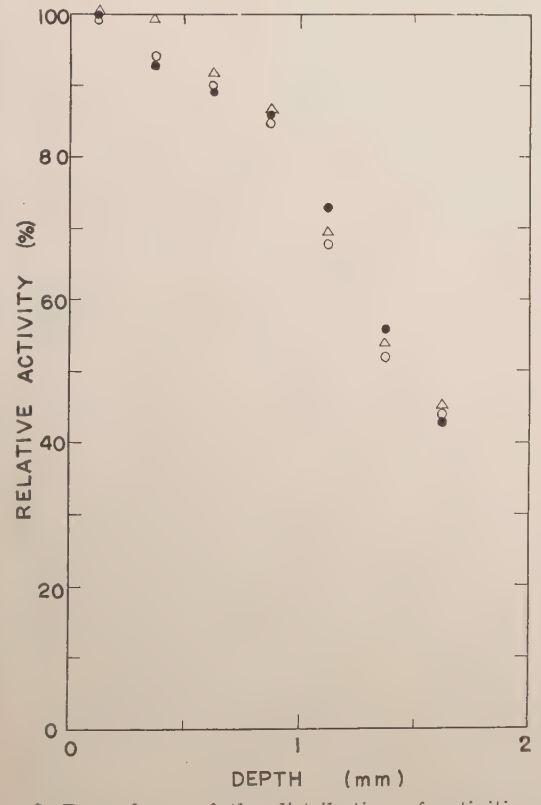

Fig. 6. Dependence of the distribution of activities on expander currents; closed circles for 100 mA, open circles for 150 mA, and triangles for 200 mA expander current.

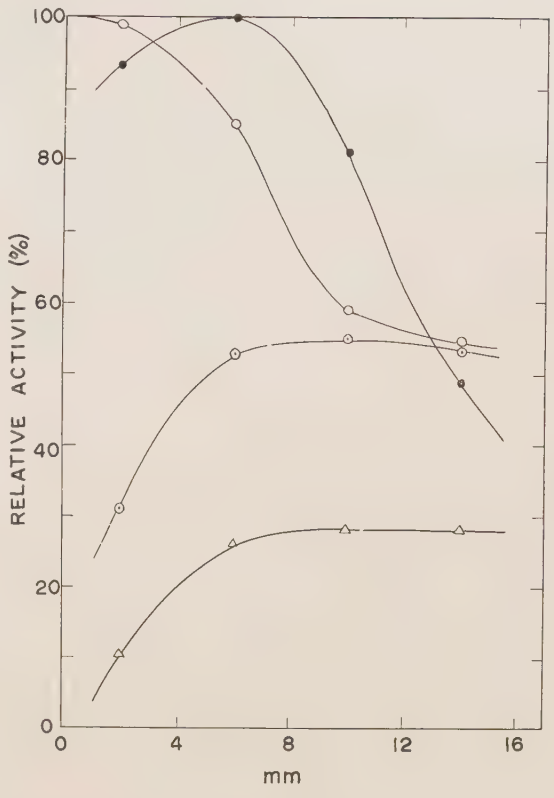

Fig. 7. Distribution of Cu^{62} activities as functions of distances from the beam entrance. Closed circles are for the No. 1, the top plate, open circles for No. 4, open circles with points, No. 7, and triangles for No. 9 copper plates of 0.25 mm thickness. The 0.6 mm platinum converter was used.

the disturbance of the magnetic field due to the expander current but because of the betatron oscillation. Since the clearance of the gun and the target from the stable orbit is order of a few centimeters and the amplitude of the betatron oscillation decreases as $1/\sqrt{H^2}$, the amplitude at 25 MeV should be about $\sqrt{50\,000 \text{ volt}}/\sqrt{25\,000\,000 \text{ volt}}$ of a few centimeter, which is order of a millimeter. This electron beam size practically determines the working characteristics of the internal target. Therefore, one can expect neither too thin electron beam nor too thick beam.

Fig. 7 shows the more detailed distribution of the Cu^{62} activity. From these measurement one sees that such grooves used were quite enough for utilizing the beam, but if one need

[2]) D. W. Kerst and R. Serber, Phys. Rev. 60 (1941) 53.

higher specific activity or if the sample is too small, the volume of those grooves must be smaller or the sample must be placed right behind the converter in smaller pack.

When the sample is of heavy material the distribution of the activity in the sample may be different. To determine the distribution in heavy material 16 tantalum strips of 0.1 mm in thickness and of the same sizes as copper strips used before were irradiated in stack. No converter employed. The distribution of the activity was found to be not markedly different (fig. 8).

The sample holder system described above is heated because of the eddy current but can be used for materials with high melting points (> 300° C). For materials with lower melting point a special sample holder with water cooling is being used. Since magnetic field does not cut

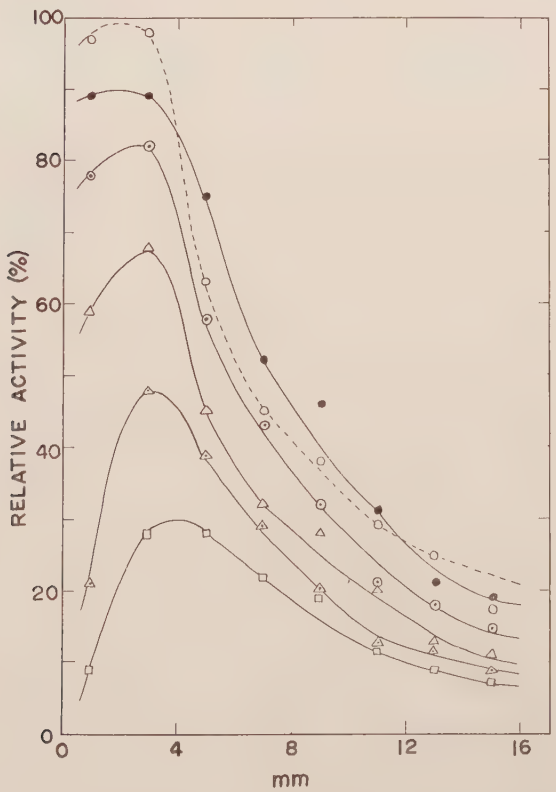

Fig. 8(a). Distribution of Ta^{180} activity in tantalum samples as a function of distances from the beam entrance. Closed circles for No. 1, open for No. 4, open with points No. 7, triangles No. 10, triangle with point No. 13, and squares are for No. 16.

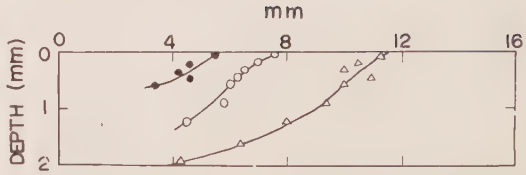

Fig. 8(b). Equal activity lines in tantalum samples. Closed circles for 70%, open circles for 50% and triangles for 30% of the highest specific activity point.

through the platinum cap much, even very volatile materials can be put on this water cooled sample holder and irradiated behind the platinum cap without any trouble.

Also, it should be mentioned that there is no need to change the target when an external bombardment becomes necessary during a series of internal bombardments. It was found that the empty platinum cap serves as an excellent bremsstrahlung target for external bombardment. This empty target seems to be quite enough for producing intense and good-sized beam outside the doughnut.

3. Examples of Application

There are some nuclides which were previously still unknown but could be made practically only by the (γ,p) reactions. Usually the (γ,p) cross sections are not large enough to produce the residual activity in good quantity by ordinary bombarding geometry of a betatron. Moreover target isotopes are often not abundant. Using our internal target we have so far identified several of them[3,4]). They are Co^{63}, Ga^{75}, As^{81}, In^{121}, In^{123}. Among this Co^{63} is obtained from the (γ,p) reaction on Ni^{64} which has only 1% abundance among nickel isotopes. Half life is approximately 50 sec. It would be difficult to study the radiations from such (γ,p) products by the external bombardment. Here several 99.99% nickel strips of 5 mm wide and 0.1 mm in thickness were bombarded in stack. Since such (γ,p) products have usually high energy β-rays, the measurement of the end-point can be made with organic scintillator without any chemical separation if the sample is thin enough.

[3]) H. Morinaga, T. Kuroyanagi, H. Mitsui and K. Shoda, to be published.

[4]) H. Yuta and H. Morinaga, to be published.

As^{81} has half-life of 30 sec. Quick chemical separation proved that this activity belongs to arsenic and not to selenium. The chemical process was performed soon after the bombardment and it took only 2 minutes before start counting after the termination of the bombardment. This was possible since the sample was only 0.2 g of SeO_2.

For identifying In^{121g}, In^{121m}, In^{123g}, In^{12mg} 50 mg each of the Sn^{122} and Sn^{124}enriched, SnO_2 was used. They were wrapped in aluminum foil and placed right behind the paltinum cap close to the converter. All these activities have half lives of order of minutes and seconds; the shortest of them was 10 sec In^{123g}. For measuring the gamma-rays which characterize the isotopes the sample was taken out by string and it took only 3 sec to bring the sample after the bombardment to the counting position at about 10 meter apart.

Studies of activity produced by photo-reactions on rare earth elements are one of the project carried out in our laboratory using this internal target. Here, pure samples of rare earth elements are extremely expensive. The use of internal target is very much suited in such case. The amount of samples used are from 50 to 200 mg in most of the cases.

Finally, it may be mentioned that such ease and efficiency of the internal target in producing radioactivity with a betatron may open a new use of medical or industrial betatron. Especially in medical field, radioactive isotopes are finding their use more and more and sometimes shorter half-lived isotopes of other kind than usually supplied from reactors are desired because of its safety or because of their characteristics of radiations. Some of them could be produced easily with a 20 to 25 MeV betatron. With the internal target described here it is quite possible to produce several hundred microcuries of such isotopes without any other additional skill than operating a betatron and handling usual radioactive materials. 10 minutes N^{13}, 20 minutes C^{11} and 32 minutes Cl^{34} may be of such examples.

Acknowledgement

This work was assisted in large extent by the members of our nuclear spectroscopy group, especially by Mr. H. Yuta who contributed much in the design and test of the system in earlier stage. Authors are also indebted to Prof. M. Kimura for giving them opportunities to use his betatron laboratory.

NUCLEAR INSTRUMENTS AND METHODS 6 (1960) 72–82; NORTH-HOLLAND PUBLISHING CO.

A FAST NEUTRON TIME-OF-FLIGHT SPECTROMETER

JAGADISH B. GARG

The Physical Laboratories, University of Manchester

Received 10 August 1959

A time-of-flight spectrometer for the measurement of neutron energies in the range 0.5 to 15 MeV has been constructed. The full time resolution width of the prompt γ–γ coincidence curve from a source of Co^{60} is 6.5×10^{-10} sec. This time resolution corresponds to an energy resolution of about 1% for neutrons of energy of 1 MeV, for a flight path of 1.5 metres, and it thus enables the study of closely-spaced levels in nuclei. The limitations on the time resolution obtained are discussed and ways of further improvement are suggested.

1. Introduction

In connection with a programme for the study of some neutron-producing reactions, the requirement has arisen for an electronic means of accurately determining the energies of neutrons emitted in these processes. The usefulness of the time-of-flight method in the measurement of neutron energies is now well established, and a considerable amount of work using these techniques has been reported in recent years[1–6]). However, there is a need of further improvement of the time resolution of these spectrometers, in order to be able to resolve closely-spaced neutron groups.

The time-of-flight of a neutron of energy (E_n) measured in MeV is given by the relation

$$t = \frac{72.3D}{\sqrt{E_n}} \text{ nsec} .$$

where D is the flight path in metres. Hence for a flight path of one metre—the distance generally used is limited by the source intensity—the interval of time for neutrons of energies in the range (0.5–15 MeV) is of the order of a few nanoseconds to 100 ns.

The resolution in energy of neutrons is related to the time resolution by the formula:

$$\frac{dE}{E} = \frac{2\,dt}{t} .$$

In fig. 1 the energy resolution vs neutron energy is shown for various values of the time resolution of the spectrometer and the flight path. This shows that in order to get a resolution of the order of 1% for 1 MeV neutrons for a flight path of one metre, one should have a time resolution less than 0.5 nsec.

The present article describes the construction and performance of such a time-of-flight spectrometer using plastic scintillators 2″ diameter × 2″ thick and RCA photomultipliers type 6810 A. The time resolution obtained is 6.5×10^{-10} sec. for a prompt coincidence curve recorded with a source of Co^{60} which emits two γ-rays in cascade.

2. Principle of Time-of-Flight Spectrometry

2.1.

The basic problems involved in using time-of flight techniques can be divided into two parts:

(a) the production of a signal giving the time zero at the start of the flight of neutron, whose energy is to be measured.

(b) the production of another signal corresponding to the end of its flight.

[1]) L. Cranberg and J. S. Levin, Phys. Rev. **100** (1955) 434.

[2]) G. C. Neilson and D. B. James, Rev. Sci. Inst. **26** (1955) 1018.

[3]) J. B. Garg and B. Torki, C. R. Acad. Sc. **246** (1958) 750.

[4]) G. K. O'Neil, Phys. Rev. **95** (1954) 1235.

[5]) A. J. Elwyn, H. H. Landon, S. Oleska and G. N. Glasoe, Phys. Rev. **112** (1958) 1200.

[6]) Bogdanov, Vlasov, Kalinin, Rybakovand Sidorov, Proc. International Conference on Neutron Interactions with the Nucleus, U. S. Atomic Energy Commission report TID-7547 (1957) (unpublished).

Two different methods are in general used for the production of the time zero.

1. The first uses a pulsed beam of particles to initiate the neutron emission. This can be achieved by modulating the beam of charged particles striking the target. The method used for modulating such a beam depends both on the energies involved and the type of particle acceleration which is used.

In general the requirements to be fulfilled are (a) that the duration of this pulse should be much shorter than the time of flight of the highest energy neutrons involved. (b) The repetition period of the pulse should be longer than the time of flight of the neutron group of the lowest energy to be observed.

These two conditions impose some limitations on this technique as will be seen from the following examples.

Let us consider neutron energies within the range (0.5–15 MeV). For a flight path of one metre and an energy of 15 MeV the flight time is about 18 ns, so to obtain an energy resolution of the order of 5% the time resolution must be less than 0.5 ns, and hence the pulse duration must be shorter than this value. The time of flight of a neutron of energy of 500 keV over one metre is 100 nsec, so that the repetition rate should be less than 10^7 pulses per second. However, it is desirable to make the repetition rate smaller than this value, to avoid the possibility of recording the flight time of a neutron group in the subsequent cycle. Thus we see that the fulfilment of these two conditions causes a reduction in the intensity of the beam by a factor of about 10^3. However it has been suggested by Devons† that by producing a circular or elliptical scan instead of a linear

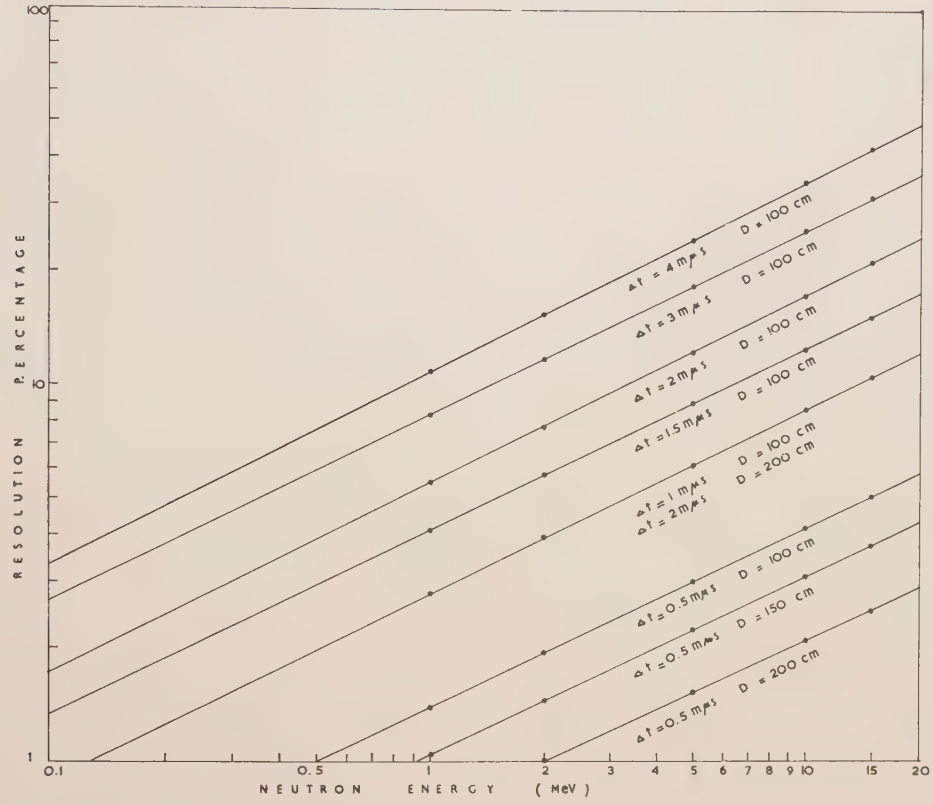

Fig. 1. Energy resolution for neutrons of different energies for various values of the time resolution Δt of the spectrometer and the neutron flight path, D. These values do not include contribution to energy resolution due to the thickness of the scintillator employed.

† Proc. of the Rehovoth Conference on Nuclear Structure (1957) (North Holland Publishing Co., Amsterdam, 1958).

scan, of the beam on a suitably made target one can reduce this loss in intensity by a factor of 10 or so.

2. The second method is the detection of the associated particle or the γ-rays emitted from the neutron-producing reaction. The detection pulse gives the effective time zero. The main requirement for this method is that to obtain the maximum rate of coincidence, the detector should be kept as close as possible to the neutron source. There will be a delay corresponding to the time of flight of the associated radiation from the target to the detector, so that this delay must be estimated and allowed for in the measurement of the neutron flight time.

This technique cannot of course be used when no particle or γ-ray is emitted in association with the neutron, e.g. in processes in which the neutron emission leaves the residual nucleus in the ground state.

One of the great advantages of the associated particle method is, that it offers the possibility of selecting a particular group of neutrons in coincidence with its associated particle or γ-ray, by using energy selection in the side channels, and thus studying in detail, the angular distribution of this particular group. In addition, this method does not suffer from the limitations of the first method. The time resolution which can be achieved is only limited by the scintillators and photomultipliers employed. In recent years there have been considerable improvements in photomultipliers, which introduce the possibilities of achieving minimum time resolution.

2.2.

We shall now discuss the various factors limiting the minimum time resolution obtainable from photomultipliers and scintillators. In a scintillator-photomultiplier assembly the rise time of a pulse (i.e. the time taken by the pulse to rise to 90% of its maximum amplitude) produced at the anode by an ionizing particle incident on the scintillator is determined by two factors:

(1) the decay time of the fluorescence of the scintillator, and

(2) the transit time of the electrons through the photomultiplier.

However, the rise time of the anode pulse is not always constant, but is subject to fluctuations due to the scintillator and photomultiplier characteristics.

The various causes of these time fluctuations can be enumerated as follows. (1) Fluctuations in the time of photon emission from the scintillator. This arises from two factors: (a) the exponential decay of the fluorescence, (b) the transit time of the ionizing particle through the scintillator volume before the interaction takes place. This latter time delay for charged particles with typical energies is in the range 10^{-11}–10^{-10} sec. For γ-rays the time delay fluctuation can be taken as equivalent to the thickness of the scintillator divided by the velocity of light, which is of the order 10^{-10} sec for a thickness of one inch of the scintillator. For neutrons this time delay can be quite appreciable since it is given by the mean free path divided by the velocity of neutrons, and it is different for neutrons of different energies.

(2) Fluctuations due to the photon collection time on the photocathode.This again arises from the finite size of the scintillator, and of the light guide, if one is used for optical coupling.

(3) Fluctuations in the transit time of electrons in the photomultiplier which arise due to two factors (a) the transit time of photoelectrons from the photocathode to the first dynode, and (b) the transit time spread from secondary electrons between dynodes.

Post and Schiff[7]) have shown that the mean time delay for the appearance of the first electron on the photocathode for a total number (R) of photoelectrons produced is given by

$$t = \frac{\tau}{R}\left(1 + \frac{1}{R}\right); \qquad R \gg 1 \tag{1}$$

where τ is the decay time of the fluorescence. This formula, in the case of n photoelectrons, is modified to

$$t = \frac{\tau}{R}\sqrt{n} \qquad \text{if} \qquad R \gg n\,. \tag{2}$$

[7]) R. F. Post and L. Schiff, Phys. Rev. 80 (1950) 1113.

Hence to obtain minimum fluctuations from this effect, one should use a scintillator having the least value of τ/R. The plastic and liquid organic scintillators are the most suitable. These have also the added advantage of possessing a high efficiency for the detection of neutrons. It is also desirable to obtain a pulse output of sufficient amplitude from the photomultiplier for a minimum number of photoelectrons produced at the photocathode. The development of high-gain photomultipliers having a photocathode sensitivity of 60 μA/lumen makes it possible to obtain a pulse of several volts amplitude from a single photoelectron, provided care is taken to keep the anode stray capacity to a minimum.

The anode pulse due to a single photoelectron is given by

$$V = Ge/C$$

where G is the gain of the photomultiplier and C is the stray capacity. If the values of G and C are taken as 10^8 and 5×10^{-12} farad respectively, this gives $V = 3.2$ volts for a single photo-elecrron.

3. Magnitude of the Time Fluctuation Produced Due to Scintillator and Photo-Multiplier Characteristics

The time dispersion in the arrival of the first photo-electron due to the scintillator characteristic is given by (1). In the case of the plastic scintillator NE 102† with $\tau_0 = 3.5 \times 10^{-9}$ sec and $R = 100$ (for γ-rays of 200 keV or neutrons of 500 keV); $t = 3.5 \times 10^{-11}$ sec.

This fluctuation in time due to the scintillator characteristics is almost negligible in the case of plastic and liquid scintillators, compared to the time fluctuations arising from other causes.

The measurement of the dispersion in transit time of electrons in different photomultipliers has been made by several authors[8–10]) and the causes have been investigated. It is found that the greatest contribution to this effect comes from the photoelectrons emerging from the photocathode and it depends on its area, shape and uniformity. To minimise this spread it has been found necessary to use curved photocathodes and special cathode-to-first-dynode geometry. It is also found that this fluctuation varies inversely as the square root of the voltage between the photocathode and first dynode, so it is desirable to apply the highest permissible voltage between the first dynode and the photocathode. One can also minimise the time spread by using only a small central area of the photocathode. The values of the transit time fluctuations are generally quoted by the manufacturers of the phototubes, and from the data available RCA 6810 A, 7046 and the recent 7264 tube seem to have the least time spread.

From considerations of high gain and short transit time spread the RCA 6810 A tube has been employed, since this has a gain of 12×10^6 and a transit time dispersion of 3 ns for a photocathode of $1\frac{9}{16}''$ diameter.

From the above discussion it appears that one will obtain the minimum time fluctuation by considering the arrival of the first photoelectron from the photocathode, which requires the application of very high overall voltages on the photomultiplier. However, under these conditions the dark current of the tube becomes troublesome, and it is advisable to operate on the arrival of a few photo-electrons, which will reduce the background noise level considerably, without much loss in time resolution.

4. Time-to-Pulse-Height Converter

The basic requirements of a time-to-pulse-height converter are:

(1) the pulse-shaping which can be achieved by using delay lines of suitable characteristics or non-linear devices.

(2) the linear addition of pulses which can be achieved by a crystal diode or by a 6BN6 tube.

Several such circuits using either crystal diodes or 6BN6 tubes have been developed[11–15])

† Manufactured by Nuclear Enterprises Limited.

[8]) G. H. Minton, J. Res. Nat. Bur. Stand. **57** (1956) 119.

[9]) M. H. Greenblatt, IRE June (1958).

[10]) E. W. Ernst and H. von Foerester, J. Appl. Phys. **26** (1955) 781.

[11]) J. Fischer and J. Marshall, Rev. Sci. Inst. **23** (1952) 417.

and it is very difficult to assess their relative merits. An electronic time resolution of the order

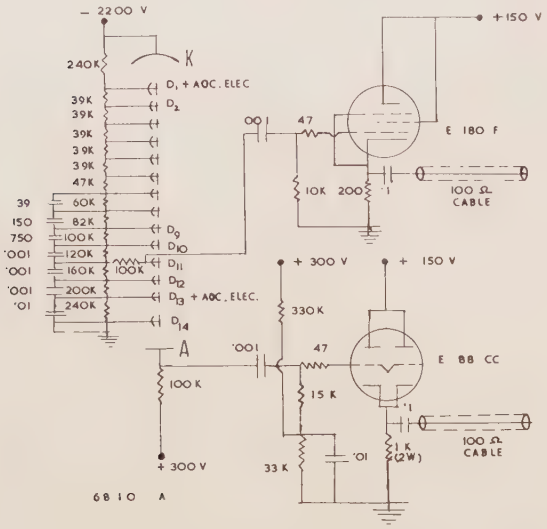

Fig. 2. Circuit diagram of the photomultiplier assembly.

of few times 10^{-11} sec can be achieved by both types of circuits. The main limitations in the final time resolution arise from the scintillators and photomultipliers. However, from the point of view of stability it is found that crystal diodes are very sensitive to changes in temperature and usually require the use of thermostats, whereas no such effect is observed with 6BN6 tubes. It has also been found that the impedance of the semiconductor diodes is a function of time, and their characteristics are not truly linear.

Another disadvantage in using crystal diodes is that the two input pulses are required to be of precisely equal amplitudes since any inequality in the pulses will produce a time delay fluctuation. No such stringent requirement is involved with a circuit using a 6BN6 tube, as the plate current reaches a saturation value.

For these reasons the 6BN6 tube has been employed in the present circuit.

5. The Circuit Details

The circuit diagrams of the photomultiplier assembly and the time-to-pulse-height converter are shown in figs. 2 and 3 respectively. The operation of the time-to-pulse-height converter, which has been designed to work in the delay range of 0 to 100 ns is as follows.

The negative fast rising pulses from the anode of the photomultiplier RCA 6810A, after passing through a cathode follower, enter the limiter circuit which consists of a sharp cut-off

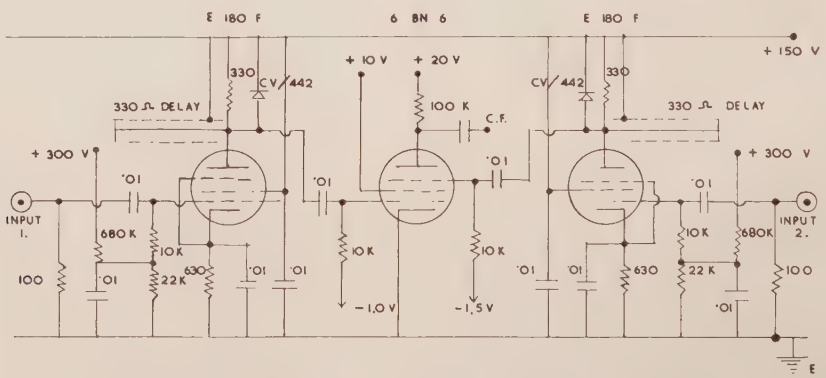

Fig. 3. Circuit diagram of the time-to-pulse-height converter

pentode E180F. This tube is initially in the conducting stage with a plate current of about 15 mA. The tube is driven completely to cut-off by the application of a pulse of about 1.5 volts at its grid, thus producing a positive pulse of about 2.5 V on its anode load, which is a 330 Ω delay line, of duration T. This pulse is rectangular in shape of duration $2T$, having very short rise and decay times. The value of T in the

[12]) W. Weber, C.W. Johnston and L. Cranberg, Rev. Sci. Inst. **27** (1956) 166.

[13]) R. E. Bell, R. L. Graham and H. E. Petch, Can. J. Phys. **30** (1952) 35.

[14]) E. Remy and K. Winter, J. Phys. et Rad. **18** (1957) 112 A.

[15]) G. Jones and J. B. Warren, J. Sci. Inst. **33** (1956) 429.

present case is 50 ns. In order to avoid any reflection of the pulse at the anode and any undershoot which is produced, a matching resistance of 330 Ω and a crystal diode is used. These positive pulses from the limiter circuits are fed to the two grids of the 6BN6 tube, biased at negative voltages of 1 V and 1.5 V respectively. It has been shown by Green and Bell[16]) that, if the 6BN6 tube is operated at low voltages, the positive excursion of the grids required to produce plate current saturation is of the order of 1 V. Hence the tube has been operated at voltages $V_p = 20$ V and $V_{g2} = 10$ V.

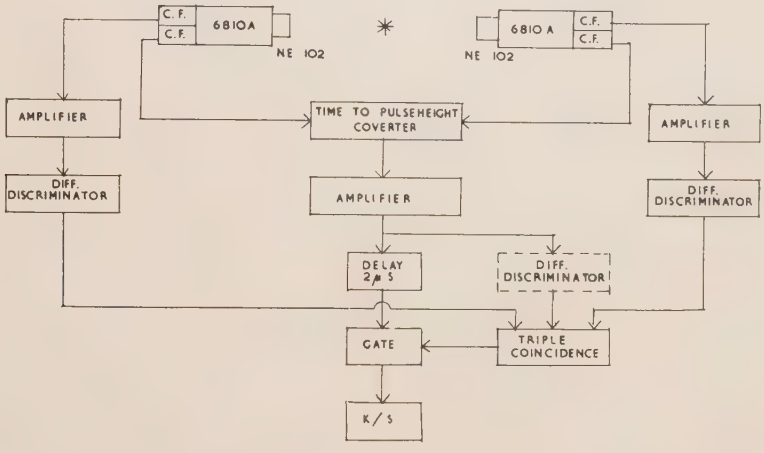

Fig. 4. Block diagram of the time-of-flight spectrometer.

By biasing the grids at a potential of 1 V and 1.5 V, one produces the condition of plate current saturation by applying 2.5 V positive pulses at its grids.

The characteristic of the 6BN6 tube is that no plate current flows unless the two grids are driven positive simultaneously. The duration of time for which this plate current flows is thus proportional to the time of overlap of the two pulses. This current charges the stray capacity of the anode with a time constant, formed by a 100 kΩ resistance on the anode and its stray capacity. The value of this time constant is of the order of 1 μs, which is ten times larger than the maximum duration of the overlap. Consequently a negative pulse of amplitude proportional to the time of overlap of the two pulses is produced at its anode. This pulse is further amplified by a standard linear amplifier and fed to the 100-channel amplitude analyser of which each channel may be made to correspond to a time delay of 1 ns or less by varying the gain of the amplifier. There is also a small positive pulse produced at the anode of 6BN6 tube due to direct feed through the inter-electrode capacity between g_3 and the anode, but by using a long time constant at the anode, the real coincidence pulse produced is many times greater in amplitude than the direct feed-through pulse, and hence practically no interference is produced. The long time constant used also ensures greater stability of the output voltages.

The complete block diagram of the time-of-flight spectrometer as used for the measurement of neutron energies is shown in fig. 4. This makes use of the fast-slow coincidence system with the single channel analysers in the side channels for energy selection. The slow coincidence is also employed in order to avoid the chance coincidences in the time-to-pulse-height converter produced by those pulses which are not of the proper amplitude to operate the limiter circuit correctly. The discriminator after one of the outputs of the amplifier of the time-to-pulse-height converter can be used to ensure the possibility of varying the effective time resolu-

[16]) R. E. Green and R. E. Bell, Nuclear Instruments 3 (1958) 127.

tion of the slow coincidence circuit to any value from a few ns. to 100 ns. This arrangement reduces the chance coincidences considerably, and hence any particular group of neutrons can be studied with greater source intensity, provided the time delay of this neutron group is less than the resolution time of the slow coincidence chosen.

The time converter suffers from the disadvantage that the pulse height is proportional to the time of overlap of two pulses irrespective of the time sequence of their arrival. The consequence of this effect is to produce twice the rate of chance events in each channel. There are many ways of eliminating this effect. In the present spectrometer the pulses from the side channel of the γ-ray detector are delayed by an amount equal to the time resolution of the slow coincidence unit, which ensures that if the pulse from the neutron counter precedes that from the γ-ray counter, it will not be counted. A simple means of estimating the chance coincidence rate is to introduce a delay equal to the time resolution of the slow coincidence circuit into the neutron counter which ensures that no real coincidence (i.e. with the pulse from the initial detector preceding the neutron counter) will be counted, and hence the spectrum recorded will be entirely due to chance coincidences. The essential requirement for these methods to be applied, is that the resolution time of the slow coincidence unit should be well defined within an interval of a few nsec at the chosen value and should remain constant. Such a coincidence unit has been realised in this laboratory and will be reported subsequently.

6. Performance

6.1.

The performance of the time-to-pulse-height converter has been tested as follows.

Two pulses from a fast pulse generator are fed to the two inputs of the limiter circuit, one input being delayed by 70 ns relative to the other by means of appropriate lengths of delay cable, and the gain of the amplifier is increased till one gets a slope of about 10^{-10} sec per channel of the pulse analyser. As shown in fig. 5C, all the coincidences fall in a single channel, showing that the time resolution is much less than 10^{-10} sec.

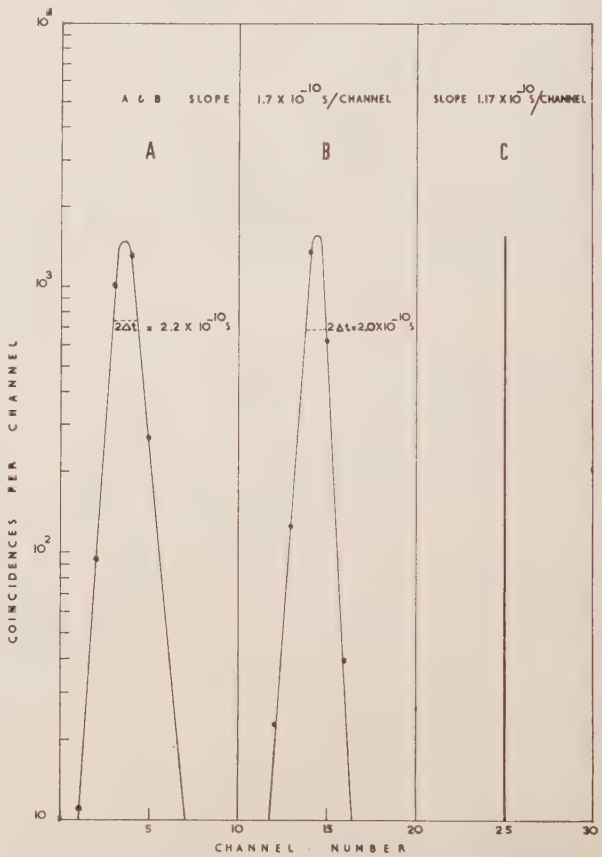

Fig. 5. The time resolution curve obtained by feeding two pulses from a single counter. Curve A is for counter A, and curve B is for the counter B. Curve C is obtained when pulses from a fast pulser are used.

6.2.

The performance of the spectrometer has been first tested by feeding pulses from the same counter to the two inputs of the time sorter (one pulse being delayed with respect to the other by an appropriate delay) and thus observing the coincidence curve on the pulse analyser. The channel width of the pulse analyser was adjusted for minimum time interval, taking care that the amplifier was not saturated. The calibration of time delay vs channel number was obtained in each case by observing the shift in the position of the peak

corresponding to an accurately measured length of delay cable of known delay introduced in one of the channels. The accuracy of this measurement was also checked by using two counters to record the coincidence curve from a Co^{60} source, and thus observing the shift in the peak when one of the counters was displaced away from the source by a known distance d, producing a corresponding time delay equal to d/c. The curves A and B of figure (5) show the time resolution obtained when pulses from the counter A and B respectively are fed to the time sorter. The side channels in the slow coincidence unit were adjusted to accept pulses greater than those produced by γ-rays of 200 keV. Both of these curves show a full width of time dispersion of about 2×10^{-10} sec.

6.3.

Fig. 6 is a typical time resolution curve obtained when the two counters are used to record the prompt coincidences of the two γ-rays emitted in cascade from a source of Co^{60}. This curve shows that the full width of time dispersion is 6.5×10^{-10} sec. As both the counters accept both the γ-rays from the cascade the slope of the curve should be symmetrical about the centre; however a nonsymmetery in the present curve arises due to some difference in the detection efficiencies of the two counters for the two γ-rays. From a comparision of this curve with that obtained by feeding pulses from the fast pulse generator, it is evident that this broadening in the time resolution arises due to the characteristics of the scintillator and photomultiplier.

The performance of the spectrometer has been tested by varying the rate of counting in the two photomultipliers up to a value of 10^4 pulses per second: no variation in the time resolution has been noticed nor any shift in the position of the peak cocurs. A variation in time resolution of the order of 2×10^{-10} sec is noticed when the bias of the side channel discriminators of the two counters, is varied from maximum to minimum. The coincidence curve of fig. 6 was obtained with a counting efficiency of about 70% of the Co^{60} γ-rays, as the discriminator biases in the two side channels were adjusted to accept all pulses greater than those produced by electrons of about 200 keV.

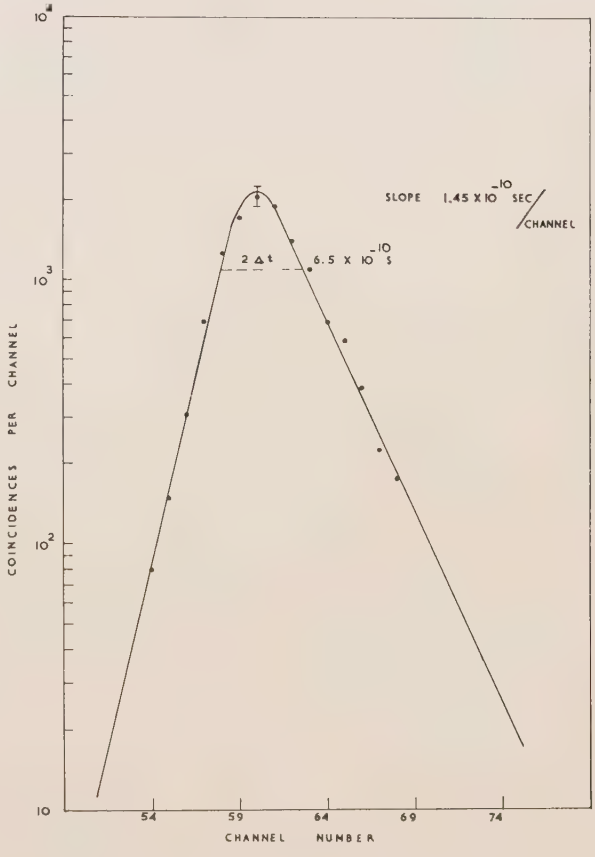

Fig. 6. Time resolution curve obtained for prompt γ–γ coincidences from a source of Co^{60}.

6.4. LINEARITY AND THE CALIBRATION OF THE SPECTROMETER

The linearity test and calibration of the spectrometer has been made by inserting lengths of 100 Ω cable of known delays in one channel and observing the corresponding position of the coincidence peak. This curve is shown in fig. 7. The non-linearity in the region of small delays arises due to the inherent delay of 5 ns in the transit time of electrons in the 6BN6 tube from the grid g_1 to g_3. After compensating this delay by introducing a 5 ns delay cable in the input of g_3, it has been found that the spectrometer is linear from zero delay up to 90 ns. The perfor-

mance of the spectrometer for delays greater than 90 ns has not been investigated.

6.5. STABILITY

The stability of the spectrometer for a period of 24 hours has been tested by feeding pulses from the fast pulse generator to the time-to-pulse-height converter. It has been found that the position of the peak shifts by one channel of the kick-sorter corresponding to a time shift of 1.17×10^{-10} sec. However, it was also observed that this instability arises from the instability of the kick-sorter itself and the stability of the time-to-pulse-height converter is thought to be much better than this.

6.6. PERFORMANCE OF THE SPECTROMETER FOR MEASUREMENT OF NEUTRON ENERGIES

Fig. 8B shows a typical neutron spectrum obtained by bombarding a 200 μg/cm^2 thick target of Al by dueterons of energy 4.5 MeV. The neutron detector was at an angle of about 45° to the γ-ray detector and was at a distance of one metre from the target. The spectrum shows a prominent peak due to $(\gamma$–$\gamma)$ and (n,γ) coincidences and various neutron groups due to (γ,n) coincidences. The energy calibration has been done with reference to the γ peak. A detailed analysis of the results obtained from the study of this reaction will be reported later.

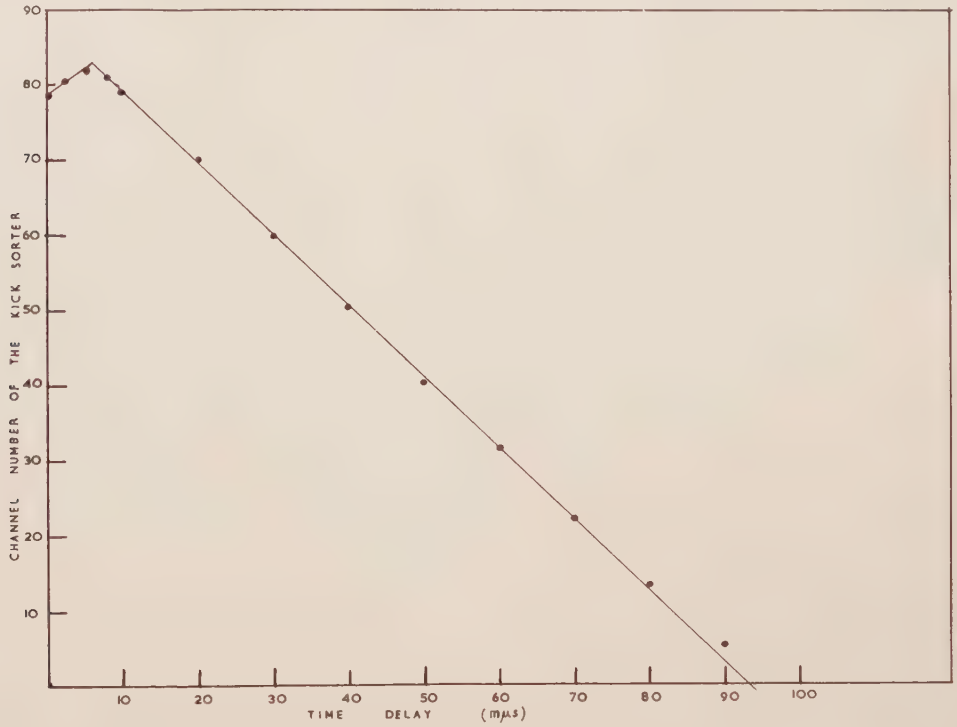

Fig. 7. Time delay ve pulse height calibration curve.

7. Discussion of the Results on the Time Resolution Obtained

It is to be noted that in the present arrangement the two plastic scintillators employed are 5 cm diameter × 5 cm thick, which means that an appreciable amount of time fluctuation arises from the large dimensions of the scintillator. If smaller dimensions of the scintillator are used, an improvement of time resolution is to be expected. For neutron energy measurements, the time fluctuation produced due to the transit time of neutrons through the volume of the scintillator becomes comparable to the time resolution of the spectrometer itself, and hence it is preferable to use a thin scintillator together

with a shorter flight path, to obtain the same counting rate.

A rough estimate of the minimum time resolution ($2\Delta T$) which could be theoretically the performance of the present spectrometer corresponds almost to the theoretical limit imposed by the scintillator and photomultiplier characteristics.

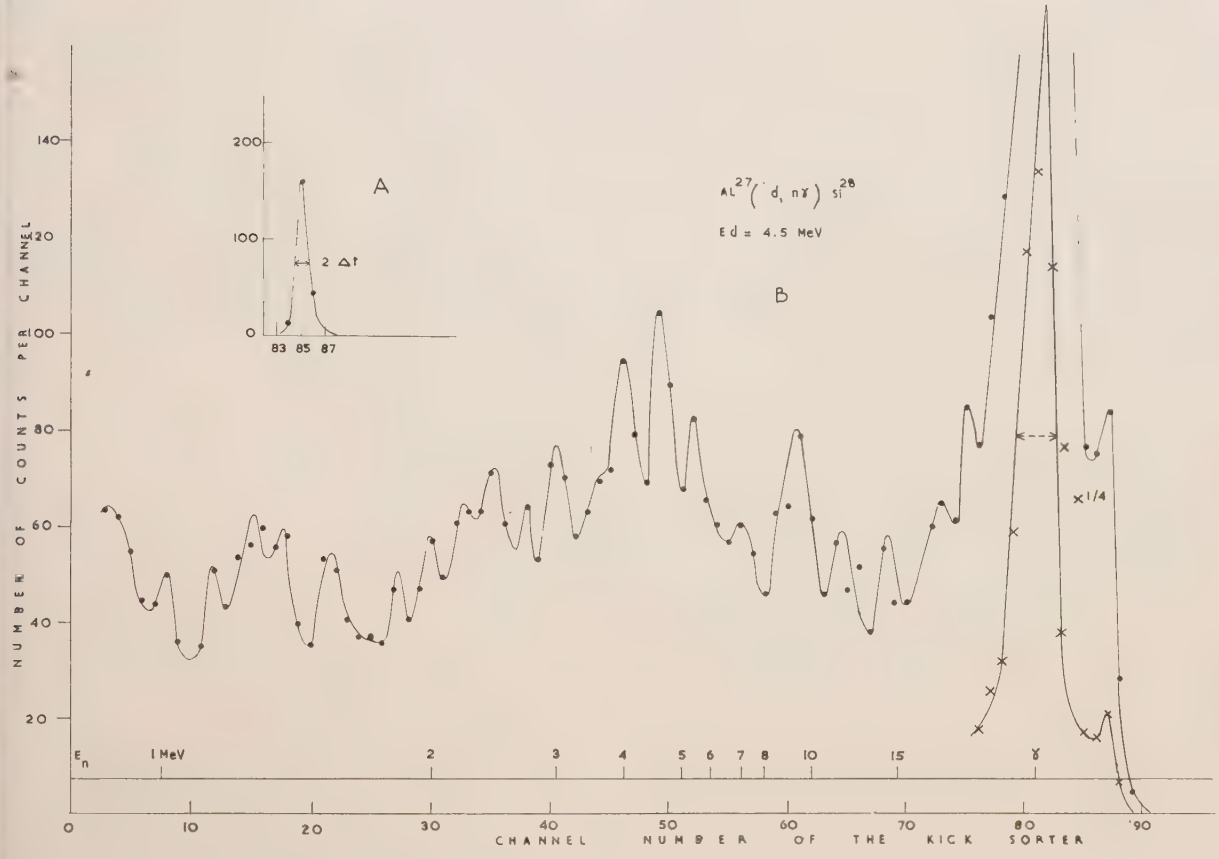

Fig. 8. Neutron time-of-flight spectrum from the reaction $Al^{27}(d,n\gamma)Si^{28}$. The channel width is about 10^{-9} sec. Curve A shows the prompt γ–γ coincidence curve obtained from a Co^{60} source on the same time scale. The exact values of energies of the different neutron groups are not shown on account of the poor statistics of the number of counts.

obtained from this spectrometer, has been made by taking into consideration the contribution to the time fluctuation from various causes as discussed in sections 2.2 and 3. The values for the scintillation decay time of the scintillator NE 102 and the transit time spread of the photomultiplier RCA 6810A have been taken as 3.5×10^{-9} sec and 3×10^{-9} sec respectively†. By supposing that at least ten photoelectrons are needed to produce an output pulse of about 2.5 V amplitude required for the limiter circuit, this value ($2\Delta T$) comes out to be 6.6×10^{-10} sec. Thus we see that

8. Future Possible Improvements

Most of the limitation in the time resolution arises from the fluctuations in the transit time of electrons in the photomultiplier and the characteristics of the scintillator, and there is a great need of improvement in these. The recent tube RCA 7264 using a curved photocathode and face plate appears to offer a time spread of 1 ns† as compared to 3 ns in the RCA 6810 A. RCA 7046 also has a transit time spread of 0.5 ns† if only a small central portion of the

† Values quoted by the manufacturers.

photocathode is utilized†. As large diameter scintillators are required to give a reasonable rate of counting, it is possible to limit the photocathode area illuminated by using suitable light guides of conical shape. It may therefore be possible to gain by a factor of about 2 in time resolution by using these photomultipliers. Similarly as the scintillation decay time of liquid scintillators is shorter and the scintillation efficiency greater than the plastic phosphors, it is possible to improve the time resolution by a factor of two using liquid scintillators. Such an arrangement is envisaged for further improvement of the time resolution of this spectrometer.

† Recent information obtained about the French tube 56AVP, indicates a value of 0.3 ns for the transit time spread.

Acknowledgement

I am greatly indebted to Professor S. Devons, F.R.S., for having provided the opportunity of working in his laboratory and for his enlightening comments on this work. I am pleased to express my gratitude to Dr. J. M. Calvert for having suggested this problem and for his interest in its realization. I wish to express my sincere thanks to Dr. J. B. Birks, Mr. H. M. Ceulemans and Mr. N. H. Gale for many valuable discussions. I also gratefully acknowledge the tenure of a Turner and Newall Post-Doctoral Research Fellowship at the University of Manchester.

NUCLEAR INSTRUMENTS AND METHODS 6 (1960) 83–93; NORTH-HOLLAND PUBLISHING CO.

DEUX PILES ATOMIQUES CONSIDEREES COMME INSTRUMENTS DE PHYSIQUE

P. DELATTRE

Service des Grandes Piles, C.E.N. *Saclay*

Reçu le 3 août 1959

From a certain standpoint, the EL 2 and EL 3 laboratory reactors can be considered as nuclear physics instruments, in the same way as particle accelerators, for example.

The essential difference between accelerators and laboratory reactors lies in the fact that the latter are not solely used for fundamental research but also for research in applied physics, technology, chemistry etc.

The operation of laboratory reactors and their use for research purposes leads to a number of general problems listed in the first three paragraphs of this article. The last four paragraphs, devoted to four precise examples selected among these general problems describe the methods used to solve such problems and the necessary preliminary studies.

1. Généralités

Les piles EL 2 et surtout EL 3 sont des piles laboratoires dont le but est de permettre l'exécution d'expériences qui nécessitent un flux de neutrons. Ces expériences, très variées, sont effectuées par les divers services du C.E.A., dans le cadre des Programmes Généraux. On peut les classer en plusieurs catégories, suivant la nature des recherches auxquelles elles se rattachent:

- Expériences de physique fondamentale
- Expériences de physico-chimie ou de chimie
- Expériences de métallurgie
- Essais technologiques
- Essais de boucles prototypes
- Expériences de biologie.

Cette simple énumération à laquelle on peut ajouter la facrication des radioéléments artificiels, montre clairement que les piles EL 2 et EL 3 doivent être classées dans la catégorie des réacteurs de recherche polyvalents.

La mise en pile des expériences pose un certain nombre de problèmes tant en ce qui concerne la sécurité de fonctionnement des dispositifs expérimentaux qu'en ce qui concerne leur influence sur la pile, en marche normale d'abord, en cas d'avarie ensuite. Ces études préliminaires, qui doivent être entreprises dès que l'avant-projet d'une expérience a été établi par le Service intéressé, incombent au Groupe "Physique et-Expérimentation" attaché au Service des Grandes Piles. Bien que chaque expérience constitue un cas particulier, il est possible de classer les problèmes qui se posent à son sujet dans des catégories assez générales pour être applicables à toute la variété des expériences possibles. C'est à cet aspect très général que nous nous bornerons dans cette première partie.

2. Expérimentation

Chaque dispositif expérimental doit satisfaire à des normes telles qu'en cas d'avarie la sécurité du personnel et des installations soit le moins possible mise en cause. Il faut éviter à tout prix que le réacteur lui-même soit endommagé en cas de mauvais fonctionnement d'un circuit expérimental. Les difficultés à résoudre sont évidemment très différentes suivant qu'il s'agit d'un circuit à haute pression ou à haute température, d'un fluide à forte activité chimique ou devenant très radioactif sous l'effet des neutrons. Dans tous les cas, le plus grand soin doit être d'abord apporté dans la réalisation des circuits de manière à réaliser une étanchéité aussi parfaite que possible; ceci est surtout une affaire de technologues, ou de constructeurs. Il faut ensuite réaliser le contrôle et l'asservissement des circuits de telle sorte que le moindre dérèglement entraîne automatiquement l'exécution d'opérations destinées à "limiter les

dégâts'': arrêt de pompes, de circuits de chauffage, déclenchement de préalerte, arrêt de la pile, etc. Tous les contrôles sont réalisés à partir de mesures physiques effectuées sur les circuits expérimentaux: mesures de températures, de pression, de débit, d'activité, etc. Le choix de ces paramètres physiques, et le poids qu'on leur donne dans le déclenchement des opérations de protection, est un problème souvent délicat et pour lequel aucune doctrine précise n'existe encore.

L'influence sur la pile des dispositifs expérimentaux en fonctionnement normal doit également être examinée avec le plus grand soin. Cette influence peut être multiple et elle dépend en général, non seulement du type d'expérience considéré mais aussi des caractéristiques de la pile. Parmi les éléments qui interviennent dans cette interaction entre la pile et l'éxpérience en fonctionnement normal nous citerons ici, parce qu'ils sont parmi les plus importants, les deux effets suivants:

– Effet sur la réactivité de la pile

– Echanges de chaleur entre dispositifs expérimentaux et pile.

2.1. EFFET SUR LA REACTIVITE

Dans toute pile de recherche, la réactivité disponible pour les dispositifs expérimentaux est évidemment limitée; une consommation de réactivité au-delà de cette limite ne pourrait se faire qu'aux dépens, soit de la puissance maximum de fonctionnement, soit de la durée d'utilisation des éléments combustibles qui ne pourraient plus atteindre leur durée de vie technologique maximum. Evaluer l'antiréactivité provoquée par un dispositif expérimental ou tout simplement par un échantillon à irradier est donc une chose importante qui doit être faite au début de l'élaboration d'un projet d'expérience. Il faut ensuite tenir compte de l'ensemble des projets et établir éventuellement un compromis de manière à n'accorder à chacun d'eux qu'une antiréactivité maximum compatible à la fois avec les possibilités de la pile et avec l'ensemble des expériences que l'on veut y réaliser. En fait, ce problème qui apparaît très compliqué pour une pile comportant un grand nombre de canaux expérimentaux se simplifie pour la raison suivante: pour un réacteur donné, l'antiréactivité provoquée par un échantillon est en première approximation proportionnelle à la section efficace totale de capture de l'échantillon et à un facteur faisant intervenir le carré du flux de neutrons dans lequel on le place; c'est dire que cette antiréactivité décroît très vite quand on passe des zones de haut flux aux zones de bas flux. On s'aperçoit que seul le chargement des canaux expérimentaux situés dans le réseau des éléments combustibles intervient dans cet effet d'antiréactivité; le chargement des canaux situés dans le réflecteur de la pile (et ils sont les plus nombreux) n'a pratiquement pas d'effet sur la réactivité, à moins bien entendu que l'on y introduise en grande quantité des matériaux très absorbants, mais ce n'est pas là un cas courant.

L'évaluation de l'antiréactivité provoquée par les dispositifs situés dans le réseau est plus ou moins aisée. S'il s'agit de matériaux relativement peu absorbants, et en faible quantité, l'application des méthodes classiques du calcul des perturbations permet d'obtenir une bonne approximation. Si, au contraire, les matériaux capturants sont introduits en grande quantité, les méthodes de perturbations peuvent ne plus être applicables; il faut alors recourir à des procédés plus élaborés. Ce dernier cas correspond, par exemple, à l'installation d'une boucle d'essai de combustible dans un canal de grand volume situé au centre du réseau. Il est alors nécessaire de calculer le nouveau Laplacien géométrique de la pile en considérant trois milieux concentriques: canal central, réseau, réflecteur, et en adoptant comme condition à la limite du canal central une longueur d'extrapolation de flux neutronique qui tienne compte des matériaux absorbants qui y sont introduits.

2.2. INTERACTIONS THERMIQUES

La seconde interaction importante entre les dispositifs expérimentaux et la pile est relative aux échanges de chaleur, échanges qui peuvent

avoir lieu dans un sens ou dans l'autre. Les circuits à haute température, situés dans des canaux plongeant dans le modérateur de la pile risquent, s'ils sont mal isolés thermiquement, de transmettre au modérateur une puissance calorifique importante. Si le modérateur est de l'eau, il peut alors se produire une ébullition locale, phénomène peu souhaitable à cause des risques accrus de corrosion qu'il entraîne et des fluctuations de réactivité qu'il provoque. On admet généralement, avec un peu d'arbitraire, que l'échange de chaleur à ne pas dépasser est de l'ordre de 1 watt/cm^2 pour les dispositifs expérimentaux situés dans l'eau lourde.

L'échange de chaleur dans le sens pile-dispositifs expérimentaux est surtout à éviter pour des raisons évidentes lorsqu'il s'agit de circuits à basse température. En résumé, dans tous les cas où le circuit expérimental est à une température différente de celle du modérateur de la pile, on doit s'efforcer de réaliser une isolation thermique excellente. Il faut mentionner cependant le cas particulier où l'on se sert du circuit de refroidissement primaire de la pile pour refroidir le dispositif expérimental. Sur des piles telles que EL 2 et EL 3 ceci ne peut se faire qu'exceptionnellement et pour des irradiations sans liaisons puisque les containers d'irradiation doivent alors respecter rigoureusement la géométrie extérieure des éléments combustibles.

En dehors des problèmes qui viennent d'être cités et qui sont propres à chaque type d'expérience, un certain nombre d'études ou de mesures plus générales sont nécessaires pour permettre la mise en oeuvre rationnelle et fructueuse des piles laboratoires. Ces études et ces mesures ont trait soit à la pile elle-même, soit aux possibilités qu'elle offre pour l'expérimentation.

L'exploitation des expériences effectuées dans les canaux d'une pile nécessite, lorsque l'état des recherches est suffisamment avancé, une connaissance précise des conditions d'irradiation. La dosimétrie des rayonnements, qu'il s'agisse des neutrons thermiques, des neutrons résonnants, des neutrons rapides, des rayonnements γ, est donc d'une grande importance et elle doit pouvoir être réalisée sur place à la demande des expérimentateurs. La mesure des flux de neutrons thermiques est maintenant assez bien connue; il s'agit donc uniquement de mettre en oeuvre des procédés de mesures devenus classiques. Par contre, la mesure des doses de neutrons thermiques intégrées pendant toute la durée d'une irradiation est déjà plus délicate et nécessite encore certaines études ou mises au point. En ce qui concerne la mesure du flux de neutrons rapides, les techniques actuellement utilisées (détecteurs à seuil) sont loin d'être entièrement satisfaisantes et de nombreux laboratoires étudient cette question. Lorsque les expérimentateurs désirent connaître les conditions dans lesquelles ils travaillent en neutrons rapides, il n'y a pas actuellement d'autre ressource que d'effectuer une mesure par détecteur à seuil [par exemple réaction S^{32} (n,p) P^{32} et dosage du phosphore formé] en indiquant toutefois quelle confiance on peut accorder à ces mesures. La dosimétrie des rayonnements gamma peut être effectuée par des procédés maintenant classiques, tels que la chambre à ionisation ou la transformation sulfate ferreux-sulfate ferrique. Ces deux méthodes ne sont pas toujours applicables, soit pour des raisons d'encombrement, soit parce que les flux à mesurer sont trop intenses, soit encore parce que la méthode de dépouillement n'est pas suffisamment aisée (cas du sulfate ferreux). A l'heure actuelle, des méthodes de mise en oeuvre très simple, fondées sur les variations colorimétriques de verres spéciaux ou d'échantillons de chlorure de polyvinyle sont en cours d'étude. Elles permettront certainement de réaliser des mesures précises et rapides.

La connaissance des spectres énergétiques, tant pour les neutrons rapides que pour les rayonnements gamma est également d'un grand intérêt lorsqu'il s'agit d'effectuer des mesures fines. Cette détermination peut être effectuée à l'aide de scintillateurs, d'émulsions photographiques, de compteurs à protons de recul, mais elle est en général très délicate et n'est pas encore entrée dans le domaine de la pratique courante.

3. Physique de Pile

Nous n'avons pas encore évoqué les mesures qui sont effectuées sur le réseau du réacteur lui-même. Il va de soi qu'une connaissance approfondie des caractéristiques physiques du réseau de la pile est indispensable si l'on désire utiliser au maximum ses possibilités; et cette connaissance ne peut être obtenue que par de nombreuses mesures effectuées dans les conditions réelles de fonctionnement.

Un certain nombre de mesures peuvent d'abord être effectuées à basse puissance, sur le réseau chargé de manière à ce qu'il soit très voisin des conditions de criticalité, avec le minimum d'éléments absorbants localisés; la répartition des flux neutroniques dans la pile est alors pratiquement celle qui est déduite de l'application de l'équation de la diffusion dans la géométrie simple, non perturbée, constituée par le chargement des éléments de combustible. On se rapproche ainsi le plus possible des conditions simplifiées que l'auteur du projet s'est imposé dans la première phase des calculs. Les mesures qui sont effectuées sur un tel réseau: mesure de Laplacien, structure fine du flux dans les cellules élémentaires, etc. permettent donc de vérifier, de préciser ou d'ajuster les grandeurs physiques utilisées dans le projet. Ces mesures, effectuées avec le plus grand soin sur chaque pile nouvelle et, pour une même pile, à chaque chargement d'un type nouveau (modification des cellules), présentent un intérêt à la fois pour les projets futurs de réseaux semblables et pour les calculs qu'ont à effectuer les ingénieurs chargés de la mise en oeuvre de la pile afin de prévoir son comportement dans des conditions de fonctionnement diverses et son évolution au cours du temps.

Les mesures effectuées sur le réseau juste critique, malgré toute leur importance puisqu'elles permettent de préciser un grand nombre de grandeurs physiques fondamentales, ne sont cependant pas suffisantes. Les piles sont toujours construites de manière à posséder une réactivité qui permette de compenser les effets de température, d'empoisonnement à court et à long termes, de consommation de combustible, et éventuellement les effets d'absorption des échantillons que l'on désire irradier. Cette réactivité, qui est entièrement disponible sur la pile froide, neuve, et entièrement chargée en combustible, doit d'abord être compensée par l'effet d'absorbeurs situés dans le réseau; ces absorbeurs, réalisés généralement sous forme de barres de cadmium ou de carbure de bore sont ensuite progressivement extraits du réseau au fur et à mesure que se font sentir les effets antiréactifs énumérés ci-dessus. Ces éléments qui peuvent être considérés comme "noirs", c'est-à-dire qui absorbent pratiquement tous les neutrons qui les frappent, provoquent de profondes perturbations du flux neutronique dont la répartition dans le réseau s'éloigne alors considérablement de ce qu'elle était sur le réseau juste critique. Il est donc necessaire d'effectuer sur le réseau réel des mesures de flux nombreuses afin de connaître les conditions pratiques de fonctionnement. Il faut ajouter que cet effet perturbateur des éléments de compensation est évidemment d'autant plus important que la réactivité à compenser sur le réseau froid et neuf est plus grande; ce cas est précisément celui des piles laboratoires, généralement réalisées en uranium enrichi et dans lesquelles par conséquent la consommation de l'U^{235}, très peu compensée par la formation de plutonium, nécessite une grande réserve de réactivité; en outre, la réactivité prévue pour les dispositifs expérimentaux peut ne pas être utilisée en permanence, ce qui accroît encore la compensation à réaliser. Lorsque la réactivité disponible sur la pile froide est très importante, il est toujours possible, bien entendu, de ne charger que partiellement le réseau d'éléments combustibles, et de compléter ce chargement au fur et à mesure de la consommation de l'U^{235}. Un tel procédé, satisfaisant en principe, surtout si le chargement est fait de manière très progressive, présente toutefois de graves inconvénients en ce qui concerne la constance du flux dans les canaux expérimentaux situés à la périphérie du réseau, zone dans laquelle le flux est très sensible à la proximité des éléments combustibles.

En dehors des mesures de flux qui permettent d'obtenir une bonne connaissance des conditions de fonctionnement de la pile travaillant à puissance stable, des mesures nombreuses et variées doivent encore être effectuées afin de prédéterminer le comportement de la pile en régime évolutif, qu'il s'agisse d'évolution rapide (régimes transitoires, généralement accidentels) ou d'évolution lente (montée en puissance, consommation de l'uranium, etc.). Parmi ces mesures, l'étalonnage en réactivité des éléments absorbants utilisés pour le pilotage de la pile, pour la compensation des effets à long terme, et pour la sécurité (arrêt volontaire et brutal du réacteur) est de première importance. Nous reviendrons plus loin sur ce point particulier.

Les effets de température du combustible et du modérateur, effets qui se traduisent par une consommation de réactivité lorsque croît la puissance de la pile, doivent également être mesurés avec soin puisqu'ils constituent un élément auto-régulateur primordial pour la stabilité du fonctionnement.

Enfin, les effets d'empoisonnement de la pile par les produits de fission (principalement xénon et samarium) et de consommation de l'uranium 235 font l'objet de mesures précises; en particulier, la connaissance de "l'overshoot xénon" qui apparaît après un arrêt brutal du réacteur (chute des barres de sécurité par exemple) est d'une grande utilité puisqu'elle permet de définir les possibilités de redémarrage de la pile après un tel arrêt; les effets liés à la consommation de l'uranium 235 doivent également être bien connus puisqu'ils conditionnent la durée de vie d'un jeu d'éléments combustibles.

Il n'est pas possible de décrire ici l'ensemble des mesures qui sont couramment effectuées sur les piles; les méthodes employées sont très diverses et font l'objet de toute une littérature spécialisée. Nous décrirons cependant succinctement, à titre d'exemples, quelques unes des mesures ou études réalisées sur les piles EL 2 et EL 3, soit parce qu'elles présentent un intérêt très général, soit parce que les procédés utilisés sont peu communs.

4. Mesure des coefficients de flux des éléments combustibles

Chaque cartouche de combustible est placée dans un flux de neutrons dont la valeur dépend de sa position dans la pile. Les coefficients de flux, qui n'expriment que des valeurs relatives, sont donc en fait des facteurs de position; ils sont définis d'abord pour les cellules, puis à l'intérieur des cellules, pour chaque cartouche; leur détermination est indispensable si l'on désire connaître les conditions de fonctionnement de chaque élément combustible. Sous une forme mathématique on peut les écrire de la manière suivante:

Pour la cellule i, située à une distance r_i du centre de la pile, le coefficient de flux sera:

$$\alpha_i = A \int_{z_b}^{z_h} \Phi\,(r_i,z)\,\mathrm{d}z$$

$\Phi\,(r,z)$ est la répartition macroscopique du flux neutronique dans l'uranium des cellules,

z_b et z_h sont les cotes de la partie inférieure et de la partie supérieure de l'uranium,

A est un facteur de proportionnalité.

En pratique on normalise les valeurs des α_i en adoptant arbitrairement la valeur 1 pour la cellule la plus chargée, ce qui revient à définir le facteur A par la relation:

$$A = \frac{1}{\int_{z_b}^{z_h} \Phi\,(r_0,z)\,\mathrm{d}z}$$

r_0 étant la distance de la cellule la plus chargée au centre de la pile.

Finalement:

$$\alpha_i = \frac{\int_{z_b}^{z_h} \Phi\,(r_i,z)\,\mathrm{d}z}{\int_{z_b}^{z_h} \Phi\,(r_0,z)\,\mathrm{d}z}. \qquad (1)$$

Pour la cartouche j de la cellule i le coefficient de flux sera:

$$\beta_j = B_i \int_{z_1}^{z_2} \Phi\,(r_i,z)\,\mathrm{d}z$$

z_1 et z_2 sont les cotes de la partie inférieure et de la partie supérieure de la cartouche,

B_i est un facteur de proportionnalité.

En pratique on normalise les valeurs des β_j en adoptant arbitrairement la valeur 1 pour la somme des β_j relatifs à l'ensemble des cartouches d'une même cellule:

$$\Sigma \beta_j = 1$$

c'est-à-dire:

$$\Sigma \beta_j = B_i \int_{z_b}^{z_h} \Phi (r_i,z)\, dz = 1$$

d'où:

$$\beta_j = \frac{\int_{z_1}^{z_2} \Phi (r_i,z)\, dz}{\int_{z_b}^{z_h} \Phi (r_i,z)\, dz}. \qquad (2)$$

Les formules (1) et (2) sont facilement calculables si la forme analytique de la fonction $\Phi (r,z)$ est connue. Ce cas est celui d'une pile de forme géométrique simple non perturbée par des éléments absorbants localisés. Par exemple, pour une géométrie cylindrique on aurait:

$$\Phi (r,z) = \Phi_0 J_0\left(\frac{2.405\, r}{R_e}\right) \sin\left(\frac{\pi z}{H_e}\right)$$

J_0 est la fonction de Bessel de 1ère espèce, d'ordre zéro,

2.405 est la première racine de J_0

R_e et H_e sont respectivement le rayon et la hauteur extrapolés du réseau.

Les expressions (1) et (2) deviennent alors:

$$\alpha_i = \frac{J_0\left(\frac{2.405\, r_i}{R_e}\right)}{J_0\left(\frac{2.405\, r_0}{R_e}\right)}$$

$$\beta_j = \frac{\int_{z_1}^{z_2} \sin\frac{\pi z}{H_e}\, dz}{\int_{z_b}^{z_h} \sin\frac{\pi z}{H_e}\, dz}$$

expressions facilement calculables.

En réalité, comme nous l'avons vu précédemment, le flux neutronique dans le réseau est très perturbé par la présence d'éléments absorbants localisés (barres de compensation et de réglage) et les expressions théoriques des α_i et des β_j ne peuvent, en général, être adoptées. Toutefois, on peut admettre—l'expérience le montre—que la répartition axiale du flux n'est pratiquement pas modifiée par les barres de compensation, sauf au voisinage immédiat de ces barres lorsqu'elles ne sont ni complètement enfoncées ni complètement relevées. Ceci s'explique par le fait que les barres de compensation ont une hauteur très voisine de celle des cellules uranium; lorsqu'elles sont en position basse elles perturbent donc uniformément les cellules uranium voisines sur toute leur hauteur et la répartition axiale du flux sur ces cellules reste un sinus. Dans le cas des barres de compensation partiellement enfoncées, comme dans celui des barres de réglage dont la longueur est très inférieure à celle des cellules uranium, la perturbation de flux provoquée sur les cellules voisines est loin d'être uniforme et la répartition axiale du flux sur ces cellules n'est plus un sinus. En pratique, on adoptera quand même les valeurs calculées des coefficients β_j (ils sont évidemment les mêmes pour toutes les cellules non perturbées) et on apportera à ces valeurs une correction pour les cartouches situées au voisinage d'une barre de réglage ou d'une barre de compensation partiellement enfoncée. Par cette méthode, on trouve ainsi, pour les piles EL 2 et EL 3 dont chaque cellule est composée de 4 cartouches numérotées de 1 à 4, de bas en haut:

Pile EL 2:

$$\beta_1 = 0.232$$
$$\beta_2 = 0.347$$
$$\beta_3 = 0.299$$
$$\beta_4 = 0.122\,.$$

Pile EL 3:

$$\beta_1 = \beta_4 = 0.215$$
$$\beta_2 = \beta_3 = 0.285\,.$$

En ce qui concerne les coefficients α_i, la répartition radiale du flux dans la pile ne permet absolument pas d'adopter les valeurs théoriques. Il est donc nécessaire d'opérer une détermination expérimentale. La première méthode qui vient à l'esprit consiste à mesurer le flux sur chaque cellule à l'aide de détecteurs par activation; cette méthode est malheureusement d'une mise en oeuvre très difficile (mise en

place des détecteurs, irradiation, retrait des détecteurs) et nous avons du y renoncer. Nous avons finalement adopté la méthode qui consiste à mesurer l'activité γ de chaque cellule après un fonctionnement suffisamment long de la pile[1]). En effet, l'accumulation des produits de fission dans chaque élément combustible, donc sa radioactivité, est proportionnelle au flux neutronique dans lequel cet élément était plongé; ceci sous réserve que la majeure partie des produits de fission aient atteint l'équilibre radioactif, c'est-à-dire que l'irradiation ait été suffisamment longue (de l'ordre de un mois pour EL 3). Les cellules sont alors extraites une à une de la pile et sont positionnées dans une géométrie bien déterminée devant une chambre d'ionisation diaphragmée. On tient compte, bien entendu, de la décroissance radioactive qui se produit entre les époques de mesure relatives aux différentes cellules. Il est alors possible de tracer la répartition radiale de flux sous forme de courbes isoflux dans un plan horizontal.

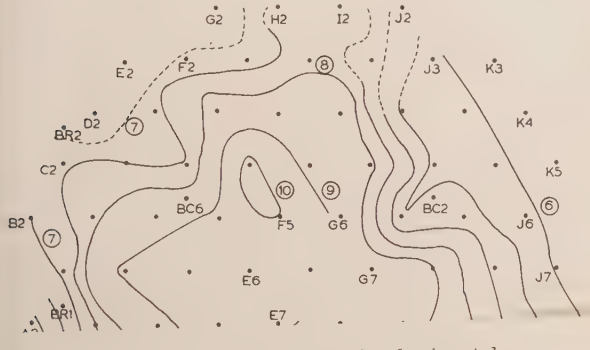

Courbes isoflux dans un plan horizontal

– Les nombres entourés d'un cercle sont les repères des courbes isoflux

– Les points sont placés aux emplacements des cellules de combustible

– Les lettres suivies d'un nombre sont des repères pour certaines de ces cellules

C'est ce qui a été fait sur la courbe ci-jointe. On voit que les courbes isoflux, qui seraient des circonférences pour le réseau ne contenant pas d'éléments absorbants localisés, sont ici très déformées.

[1]) A. Charbonnel et C. Hyver, Note EL 3, No. 5, (non publiée).

5. Echauffement des matériaux en pile

Tous les matériaux mis en présence des rayonnements qui existent au sein des piles subissent un échauffement qui, dans le cas des piles à haut flux, peut devenir considérable. Les matériaux fissiles constituent évidemment un cas particulier puisque chez eux l'énergie calorifique dégagée par les fissions éclipse par son intensité les autres sources de chaleur. Nous ne considérerons donc ici que les corps non fissiles.

La connaissance de l'énergie calorifique dégagée par les rayonnements dans les matériaux mis en pile présente de l'intérêt pour un grand nombre de problèmes concernant l'expérimentation. Parmi ceux-ci, les plus importants peuvent se résumer comme suit:

(a) Certains circuits, à haute pression par exemple, ou contenant des fluides très corrosifs, nécessitent d'être réalisés de manière très robuste, c'est-à-dire finalement avec des matériaux de structure en quantité relativement importante. Le projet du circuit de régulation de température, qu'il s'agisse d'extraire des calories du montage en pile ou de lui en apporter, doit donc tenir compte de cet échauffement parasite des structures par l'action des rayonnements.

(b) Il peut arriver que l'on désire utiliser l'échauffement dû aux rayonnements pour effectuer l'irradiation d'échantillons à haute température. Dans ce cas, les échantillons sont ›rifugés, plus ou moins complètement, et la ›pérature d'équilibre ne peut être évaluée si l'on connaît l'énergie calorifique dissipée s l'échantillon et les propriétés isolantes du rifuge. Pour ce dernier point, d'ailleurs, il tenir compte du fait que les propriétés du rifuge sont modifiées par la présence des ces de chaleur qui y prennent naissance également sous l'effet des rayonnements.

(c) En ce qui concerne les circuits à basse température (gaz liquéfiés), le problème est évident; l'échauffement des structures peut accroître considérablement la puissance nécessaire pour les liquéfacteurs.

(d) De nombreuses expériences nécessitent

la mesure de la température d'éléments situés sous radiations. La méthode la plus couramment employée, parce que très commode, est celle du thermocouple. Malheureusement, la soudure de ces thermocouples s'échauffe par l'action des rayonnements, et ceci peut entraîner des erreurs très importantes. La meilleure solution consiste évidemment à réaliser un contact intime entre la soudure du thermocouple et le milieu de mesure, mais ceci n'est pas toujours aisé. Lorsqu'une telle disposition ne peut être adoptée, il est quand même possible d'évaluer l'erreur commise si l'on connaît la géométrie exacte de montage du thermocouple et la chaleur parasite dégagée dans la soudure et dans les fils de raccordement.

Ces quelques exemples montrent tout l'intérêt d'une étude des échauffements sous radiations. Les causes de cet échauffement sont les suivantes :

Reactions (n,α). Le parcours des α étant très faible, leur énergie peut être considérée comme entièrement dissipée sous forme de chaleur dans l'échantillon. Parmi les corps couramment utilisés ceux qui subissent cette réaction sont relativement rares ; on retiendra surtout le bore et le lithium.

Gamma de capture. Au moment de la capture d'un neutron, il y a émission d'un ou plusieurs photons gamma de transition. L'énergie de ces gamma varie suivant les corps ; il faut tenir compte à la fois de cette énergie et de la géométrie de l'échantillon pour déterminer la quantité de chaleur qui y est abandonnée.

Radioactivité γ ou β. Le noyau formé après capture d'un neutron et émission des photons de transition est généralement radioactif. S'il s'agit d'une radioactivité γ, le problème doit être traité comme pour les γ de capture (énergie du gamma et géométrie de l'échantillon). S'il s'agit d'une radioactivité β, on pourra admettre en général que l'énergie des β est entièrement dissipée sous forme de chaleur dans l'échantillon.

Action des gamma de la pile. Ces γ proviennent des barres d'uranium voisines et des captures neutroniques dans les matériaux de structure de la pile. On peut déterminer leur énergie moyenne et leur intensité, et traiter le problème comme précédemment, en tenant compte de la géométrie de l'échantillon.

Ralentissement des neutrons rapides. Si le corps irradié présente une section efficace de choc élastique appréciable, il ralentit les neutrons rapides et voit ainsi une partie de l'énergie cinétique de ces neutrons dissipée en son sein sous forme de chaleur.

Les considérations qui précèdent montrent comment il est possible d'évaluer par le calcul l'échauffement des matériaux. A titre d'exemple, on trouvera dans le tableau ci-dessous, les résultats de ce calcul pour quelques matériaux particulièrement importants ; on a supposé que les échantillons étaient des cylindres de diamètre 20 mm et de longueur supérieure à 4 ou 5 fois le diamètre, et qu'ils étaient irradiés à l'intérieur de la cartouche de combustible la plus chargée de EL 3, la pile fonctionnant à puissance

Substance	Echauffe-par (n,α) (W/g)	Echauffement par γ de capture (W/g)	Echauff. par absorption des γ de la pile (W/g)	Echauffement par radioactivité β (W/g)	Echauffement par radioactivité γ (W/g)	Echauffement par ralentissement neutrons rapides (W/g)	Echauffement total (W/g)
Al	0	0.066	0.466	0.184	0.016	0	0.732
Mg	0	0.017	0.466	0.003	$\#$ 0	0	0.486
Zr	0	0.031	0.448	$\#$ 0	$\#$ 0	0	0.480
Inox 18/8	0	0.935	0.448	0.014	0.011	0	1.41
Ni	0	1.455	0.448	0.005	$\#$ 0	0	1.91
Cr	0	1.017	0.448	$\#$ 0	0.019	0	1.484
Be	0	0.003	0.540	0.004	$\#$ 0	0.057	0.604
BeO	—	—	—	—	—	—	0.52
Mn	0	4.33	0.448	3.4	0.88	0	$\#$ 9

maximum. Dans ces conditions, les flux au niveau de l'échantillon sont les suivants:

– neutrons thermiques:

$$\Phi = 7.5 \times 10^{13} \text{ n/cm}^2 \text{ sec}$$

– neutrons rapides: $\Phi = 3 \times 10^{13}$ n/cm² sec

– Gamma: 2×10^{8} r/h

(Energie moyenne des photons: 1.6 MeV).

Les principales causes d'imprécision dans ce genre de calcul sont les suivantes:

– L'énergie moyenne des γ de la pile est assez difficile à déterminer et elle varie en fonction de la position dans la pile.

– Les sections efficaces de certaines réactions ne sont connues qu'avec peu de précision.

– La perte d'énergie des photons γ dans un échantillon de forme géométrique donnée ne peut être déterminée qu'avec peu de précision.

Il est donc souhaitable de vérifier la validité des calculs par un certain nombre de déterminations expérimentales. Les méthodes de mesures se ramènent toutes à l'un des deux principes généraux suivants:

– Relevé de températures d'équilibre en différents points d'un échantillon de forme géométrique simple.

– Mesure par une méthode calorimétrique de l'énergie emmagasinée dans l'échantillon.

Ces méthodes sont d'une mise en oeuvre délicate pour des raisons que nous avons déjà vues: problème de la mesure des températures sous radiations et problème de l'isolement thermique du calorimètre. Une étude est actuellement en cours afin de définir et de réaliser un matériel expérimental permettant des mesures précises.

6. Mesures Termiques en Pile

La bonne tenue des éléments combustibles dépend, pour une grande part, de la température. qu'ils atteignent pendant le fonctionnement de la pile. Pour une cellule d'uranium cylindrique pleine, le point le plus chaud se trouve évidemment sur l'axe de révolution et le profil des températures suivant un rayon a l'allure générale représentée sur le schéma ci-dessous. Les écarts de températures sur ce profil peuvent être séparés de la manière suivante:

Δt_1 dépend des dimensions du combustible, de sa conductibilité thermique, et des sources de chaleur (c'est-à-dire du nombre de fissions par unité de temps) qui y règnent.

Δt_2 dépend de la qualité du contact entre uranium et gaine, et de la puissance calorifique évacuée à travers ce contact.

Δt_3 dépend de la conductibilité thermique de la gaine et de la puissance calorifique évacuée.

Δt_4 dépend du coefficient d'échange entre la gaine et le fluide refroidisseur, et de la puissance calorifique évacuée.

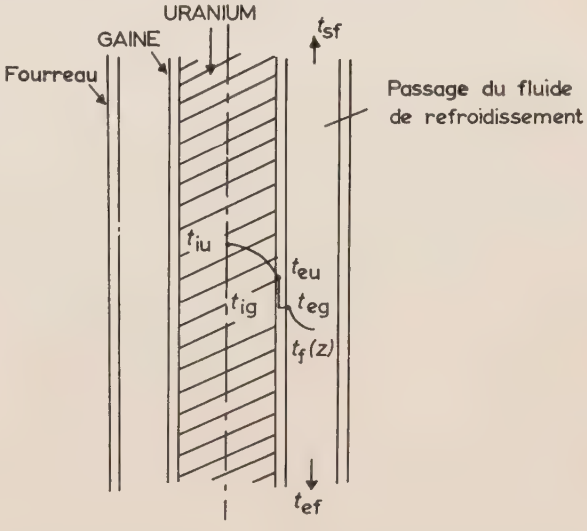

Dans l'uranium: $\Delta t_1 = t_{iu} - t_{eu}$. Contact uranium-gaine: $\Delta t_2 = t_{eu} - t_{ig}$. Gaine: $\Delta t_3 = t_{ig} - t_{eg}$. Gaine-fluide de refroidissement: $\Delta t_4 = t_{eg} - t_f(z)$.

Parmi tous ces paramètres, certains sont mal connus; c'est le cas, en particulier, de la conductibilité thermique de l'uranium et de la résistance thermique équivalente au contact uranium-gaine. Le calcul purement théorique du point chaud uranium, t_{iu} est donc assez hasardeux, et une vérification expérimentale s'impose afin de s'assurer que les normes de températures imposées par les technologues sont bien respectées pendant le fonctionnement de la pile. La mesure peut être faite dans une "cellule indépendante" où les conditions liées au fluide de refroidissement sont variables dans de larges limites. On utilise pour celà une cellule de

combustible spéciale équipée d'un thermocouple au coeur de l'uranium; on relève également les températures d'entrée (t_{ef}) et de sortie (t_{ef}) du fluide de refroidissement dans la cellule, ainsi que son débit.

Le calcul permet d'établir une relation de la forme:

$$t_{iu} - t_{ef} = Q_0 [A (R_u + R_{ug} + R_g + R_{gf}) + B/\omega]$$

Q_0 est la puissance calorifique évacuée par unité de surface extérieure de gaine au point de flux maximum.

A et B sont des constantes connues à partir des caractéristiques de la pile et de la cellule.

ω est le débit du fluide de refroidissement dans la cellule.

R_u, R_{ug}, R_g, R_{gf} sont les résistances thermiques équivalentes respectivement à l'uranium, au contact uranium-gaine, à la gaine, au coefficient d'échange entre gaine et fluide de refroidissement.

On peut également, dans la relation précédente, éliminer le terme Q_0 en faisant apparaître la température de sortie du fluide de refroidissement. La nouvelle relation prend alors la forme suivante:

$$t_{iu} - t_{ef} = (t_{sf} - t_{ef}) [E\omega (R_u + R_{ug} + R_g + R_{gf}) + F]$$

E et F sont encore des constantes connues.

Par une série de mesures à niveau de puissance constant (Q_0 constant) et à débits de fluide variables, il est donc possible de déterminer la forme de la variation de R_{gf} en fonction de ω.

Par une autre série de mesures à ω constant et à différents niveaux de puissance, il est possible de déterminer la somme $R_u + R_{ug} + R_g$.

En définitive, on obtient donc une relation numérique de la forme:

$$t_{iu} = t_{ef} + (t_{sf} - t_{ef}) [a\omega + b] .$$

Le terme entre crochets étant une constante pour toutes les cellules de la pile si l'on travaille à débit constant pour toutes ces cellules (cas de EL 3); il est au contraire différent pour chaque cellule si l'on travaille à débit variable, de manière par exemple à garder constante la différence ($t_{sf} - t_{ef}$) (cas de EL 2).

7. Etalonnage en réactivité des Barres de Compensation de la Pile EL 3

Cet étalonnage est très important puisque seul il peut permettre de mesurer avec quelque précision les phénomènes à court ou à long terme modifiant la réactivité de la pile. Or un tel étalonnage est particulièrement difficile dans le cas d'une pile comme EL 3 où les barres de compensation sont en grand nombre (6) et sont situées assez près les unes des autres. Les effets d'ombre entre barres, qui sont la conséquence de cette géométrie resserrée, sont tels que l'étalonnage d'une barre n'a de signification qu'en fonction de la position des autres barres. Les méthodes classiques qui consistent à étalonner une barre, soit à partir de divergences effectuées sur la pile froide, soit par la technique des modulations, n'ont donc ici qu'un intérêt très restreint et ne permettent d'obtenir un étalon de réactivité que dans une partie très étroite de la course de la barre. En effet, pour opérer l'étalonnage dans une autre partie de la barre, il est nécessaire de modifier la position des autres barres de façon à se retrouver au voisinage de l'état critique; on modifie ainsi les effets d'ombre et finalement les mesures effectuées ne sont guère utilisables en pratique. Pour éviter ce phénomène, il faudrait pouvoir étalonner chaque barre sans modifier la position de ses voisines; ce principe serait applicable si l'on pouvait réaliser un empoisonnement homogène de la pile, soit par adjonction d'un liquide absorbant dans l'ensemble du modérateur, soit par positionnement de matériaux absorbants uniformément répartis le long des cellules de combustible. La première méthode, pour des raisons évidentes, n'est pas possible sur une pile à eau lourde; la seconde méthode nécessite une structure spécialement adaptée des cellules de combustible et oblige à de nombreuses et délicates manipulations; ni l'une ni l'autre de ces méthodes ne sont en tout cas applicables à EL 3. Une dernière ressource subsiste cependant. Elle consiste à adopter une configuration des barres de compensation au départ sur la pile froide et neuve et à étalonner par modulation, fréquemment en cours de la vie d'un jeu de cellules, la

barre de compensation sur laquelle on agit pour compenser l'évolution de la réactivité. On obtient ainsi, pour un programme donné de remontée des barres de compensation, un étalonnage valable pour chaque époque de la vie d'un jeu de cellules. Une seule difficulté demeure, pour la mise en oeuvre d'un tel procédé : il nécessite en effet de pouvoir moduler même sur la pile fonctionnant à haute puissance. Les problèmes mécaniques posés par cette opération peuvent être résolus assez simplement, mais la question des contraintes thermiques qu'une telle modulation en puissance entraine pour les éléments combustibles doit être examinée avec le plus grand soin. Une étude est actuellement en cours sur ce sujet ; une solution satisfaisante sera certainement mise au point dans un proche avenir.

NUCLEAR INSTRUMENTS AND METHODS 6 (1960) 94–95; NORTH-HOLLAND PUBLISHING CO.

A DIRECTIONAL SCINTILLATION COUNTER FOR NEUTRONS†

R. F. STETSON†† and S. BERKO†††

University of Virginia, Charlottesville, Virginia

Received 12 August 1959

A description of several models of a directional neutron counter constructed of plastic filaments is given. Ratios as high as 1000:1 have been obtained for the counting rate with filamental axis parallel to the neutron direction to the counting rate with filamental axis perpendicular to the neutron direction.

In order to improve further the techniques for counting neutrons in elastic scattering experiments, a scintillation counter has been developed, the efficiency of which is determined by the incident neutron direction. Similar counters have been constructed by Hill[1]), using thin sheets of scintillator material separated by glass spacers, and by Thompson[2]), using Pyrex capillary tubes filled with liquid scintillator.

The counter to be described is similar to these in that the forward-peaked angular distribution of protons from n–p collisions is utilized to achieve directional effects. An isotropic angular distribution (center-of-mass system) means that the differential cross section (lab system) for n–p scattering is proportional to $\cos\theta$, where θ is the lab scattering angle. The energy of the scattered proton is, of course, proportional to $\cos^2\theta$. Thus, the product of the number of protons scattered at θ and the range of those protons is proportional to $\cos^4\theta$, since the range varies approximately as the $\frac{3}{2}$ power of the energy. The strongly forward-peaked distribution and the increased energy loss of the proton near the end of its path suggest the possibility of a directional counter composed of cylindrical plastic filaments of diameter less than the proton range in the plastic.

† Supported in part by U. S. Army Office of Ordnance Research, and U.S.A.E.C.

†† Present address: University of Florida, Gainesville, Florida.

††† A. P. Sloan Research Fellow.

Scintillator arrays were assembled using thin plastic filaments of NE 102 phosphor, available from Nuclear Enterprises, Ltd. The arrays were designed for use with 14 MeV neutrons—the range in NE 102 of a 14 MeV proton being about 2.5 mm—and models were made with both 1 mm and 2 mm diameter filaments. The details of the various models are given in table 1;

Table 1

Details of filament counters.

Model	Number of filaments	Filament diameter (mm)	Minimum distance between centers of filaments (mm)	Pulse height (% solid chunk)
A	81	1	3.0	58
B	49	2	3.5	63
C	121	1	2.0	54

all were built in a square array. In Model A the distance between individual filaments was sufficiently large to prevent protons from one filament from reaching another. All the filaments were 25 mm long and were mounted in lucite holders, optical contact being provided by means of Dow Corning 200 fluid. The arrays were sealed in aluminum caps lined with aluminum foil for better light-reflecting properties, and the caps were then filled with Nujol, which

[1]) R. W. Hill, Phys. Rev. **109** (1958) 2105.

[2]) M. A. Thompson, Rev. Scient. Instr. **29** (1958) 1149.

acted as an absorber of protons. The caps were mounted on a RCA 6342 photomultiplier. The pulse heights for 14 MeV neutrons obtained with the filament counters are listed in table 1 as the percentage of the pulse heights obtained with a solid chunk of plastic.

All the models were tested for directionality with 14 MeV neutrons from the T (d,n) He^4 reaction, using the n–α coincidences as a means of defining the neutron beam. The ratio of the counting rate at 0° (neutron direction parallel to filamental axis) to that at 90° is shown in table 2 as a function of the integral bias setting of the scaler (expressed as the percentage of the maximum pulse height at 0°).

Table 2

Ratio of counting rates for 14 MeV neutrons

Discriminator setting (% max P. H.)		C. R. (0°) / C.R. (90°)
A	70	40
	80	100
	90	1000
B	80	2
	90	4
	97	13
C	70	11
	80	65
	90	300

The absolute efficiency of Model A is estimated to be $\approx 0.2\%$ for 14 MeV neutrons. Model A with the high bias setting yields a ratio of 1000:1, making the counter more directional than those of Hill[1]) and Thompson[2]) but still nearly as efficient. The pulse heights were also checked with the 0.662 MeV gamma ray from the decay of Cs^{137} and found to be approximately 50% that of the solid chunk.

NUCLEAR INSTRUMENTS AND METHODS 6 (1960) 96–100; NORTH-HOLLAND PUBLISHING CO.

ACCELERATORS IN BIOLOGY AND MEDICINE†

HOWARD L. ANDREWS

Radiation Branch, National Cancer Institute, National Institutes of Health, Public Health Service, Dept. of Health, Education and Welfare, Bethesda, Md.

Received 25 August 1959

With the passing of the first wave of enthusiasm, radiation biology has settled down to that slow and painful accumulation of information which characterizes most scientific fields. The hope of obtaining a quick and complete understanding of the biological action of radiation has vanished, as has the hope for a simple counteractant to be taken in the event of an overexposure. It is, then, a good time to consider some of the problems of radiation biology and therapeutic radiology from the standpoint of the equipment needed for a full scale attack on these problems.

In some ways, the problems ahead are simpler than those facing industrial radiography for example. In biology the microscopic makeup of the critical targets upon which radiation impinges may be unknown, but maximum size and chemical composition are well defined. Acceptance of man as the largest object of biological interest immediately fixes maximum field size and maximum target depth.

Consider first the matter of radiation quality, with particular emphasis on photon radiation. Here, rapid advances in technology have drastically altered the situation in the past few years, and today a wide range of photon energies are available. Recently a committee gave serious consideration to the feasibility of organizing a carefully conducted, definitive study of the relative merits of 250 kV X rays and "supervoltages" in the treatment of cancer. A truly balanced experiment was judged to be impossible since most of the radiologists having supervoltages available felt that they would prefer to use them. The same preference has been expressed by radiation biologists working with test objects as small as the mouse, or even with tissue cultures.

This preference for the higher photon energies does not arise from a qualitatively different biological action of the more energetic radiation. Much effort has gone into measuring the relative biological effectiveness, or RBE, of a wide variety of radiations using many different biological endpoints. This is a very complex field, and one in which great care must be taken to obtain meaningful results. It appears that RBE values depend primarily upon the linear energy transfer, or the LET of the radiation which is to say the density of ionization along the tracks of the charged particles set in motion by primary and secondary photons.

For photon energies above perhaps 200 kilovolts, the average value of LET does not change markedly, even up to the highest energies available. Any striking differences in biological effects, or effectiveness, must be sought at lower rather than at higher energies. High-energy beams can, of course, deliver relatively more energy at depth than is obtainable from lower-energy radiation, and this accounts in a large measure for the expressed preferences for the higher voltages.

Because of the relatively small variation in LET with energy, there seems to be no physical reason to prefer monoenergetic radiation to that obtained from a well-filtered X-ray tube. Individual requirements may strike different balances between the inherent simplicity of a

† Adapted from a paper presented at the 1958 Accelerator Conference, Cambridge, Mass.

gamma ray source and the flexibility of an accelerator, but there should be no detectable differences in the biological effects of the radiation from the two sources.

In spite of the relative independence of RBE and photon energy it would be highly desirable if some agreement could be reached to use only a few of the almost innumerable combinations of applied voltage, waveform, and filtration. Many of these combinations produce essentially equivalent radiation, but this equivalence is frequently not recognized by the biologist. Too often incompatible results are attributed to some mysterious differences in radiation quality, when more careful considerations would lead to other causes of the discrepancies.

Care must be taken to separate possible quality differences from differences in depth dose distributions. Thousands of "whole-body" irradiations have been done with little thought as to the actuality of the term. Bond *et al.*[1]) have called attention to this problem which is important even for small animals. Photons are considered to be penetrating radiation and the mouse is a small target but even here there may be a substantial decrease of dose with depth (fig. 1). A half value layer of 11 mm of lead as obtained with either Co-60 gamma rays, or a 2.5 MeV constant potential X-ray beam seems like penetrating radiation, but the dose may drop by 10 per cent at a depth of 2 cm. Obviously whole body exposure to even a hard photon beam does not insure truly whole body dosage.

The distribution curves of fig. 1 are strong arguments for using penetrating beams at large target distances, and these requirements force the use of high output machines if inconveniently long exposure times are to be avoided. Accelerators appear to be the source of choice for high output at large target distance because equivalent isotope sources become inconveniently large. Accelerator produced X-ray intensities of 1000 r/min at one meter are readily obtained and only target failures prevent still higher outputs. An almost identical depth dose distribution can be obtained with Co-60 gamma rays but a source of over 45 000 curies would be required to obtain an equal dose rate. With pulsed operation dose rates of 2×10^4 r/min at 1 meter have been obtained and this appears to be well above what can be reasonably obtained from radioactive sources.

Accelerator produced photons have a big intensity advantage over gamma radiation since it is difficult to take advantage of the isotropic distribution of gamma emission over the full 4π solid angle. On the other hand care must be taken to insure that accelerator outputs are uniform over the required field. At the higher voltages where bremstrahlung production becomes more efficient, forward photon production predominates, and field correcting filters become essential.

Fig. 2 shows the radiation fields obtained from a 3.5 MeV Van de Graaff generator with and without field correction. Routine operation is at 2.5 MeV and the field correcting filter was designed for this energy. At 3.5 MeV this filter

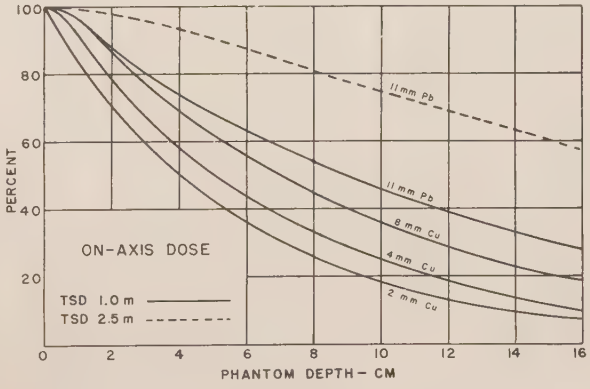

Fig. 1. On-axis depth dose in a unit density phantom for various values of HVL.

undercorrects because of the field constriction at the higher energies, but the field is still satisfactorily flat for many purposes.

Field correction becomes more difficult at the higher voltages as the beam intensity increas-

[1]) V. P. Bond, E. P. Cronkite, C. A. Sondhaus, G. Imirie, J. S. Robertson, and D. C. Borg. The Influence of Exposure Geometry on the Pattern of Radiation Dose Delivered to Large Animal Phantoms. Rad. Research, 6, 554–573, 1957.

ingly peaks in the forward direction. If only small objects are to be irradiated field correction can be made up to quite high energies. However, if the present interest in whole-body human irradiation continues there will be an increased demand for flat fields of 180 cm diameter. With fields of this size the maximum useful voltage is probably not over 5 MV.

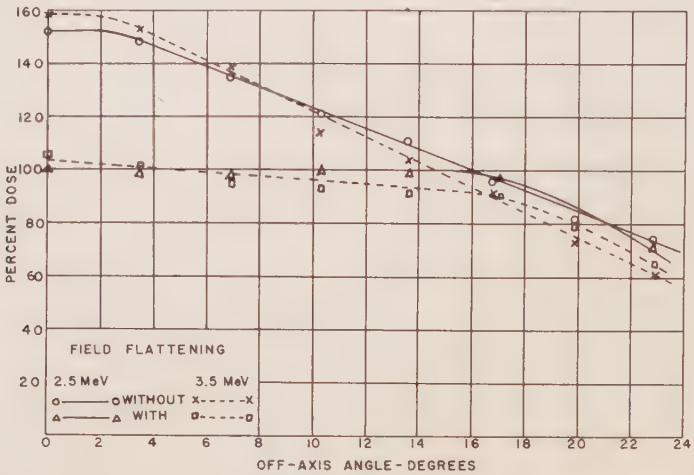

Fig. 2. Effect of field flattening filter on a constant potential X-ray beam.

Fig. 3 shows the on-axis depth dose in a unit density phantom using 2.5 MeV photons from a Van de Graaff generator. With two ports a dose uniform to $\pm$ 5 per cent can be achieved at a TSD of 2.5 meters and a dose rate of 150 r/min. A 180 cm field is flat within about the same limits and so truly whole body radiation can be delivered to an object as large as an adult human at a reasonable dose rate.

Many biological effects of radiation are strongly dose-dependent and considerable care must be given to dosimetry when accelerator-produced radiation is used. Even with voltage regulators, radiation output can be sufficiently variable to make dosimetry by time and meter settings of dubious value. We routinely use a thin transmission ionization chamber large enough to cover the entire useful beam close to the target, and connected to an electronic integrator. Our biological experiments have required the accurate administration of doses ranging from 25 to 100 000 roentgens and deflection type integrators have proved completely inadequate. A repetitive condenser-discharge circuit[2]) and glow-transfer tube counter has been in use for several years and has substantially improved the statistics from many biological experiments. The circuit can be standardized against a certified ionization chamber of convenient range, and then any desired dose can be preset on the counter with complete assurance of linearity.

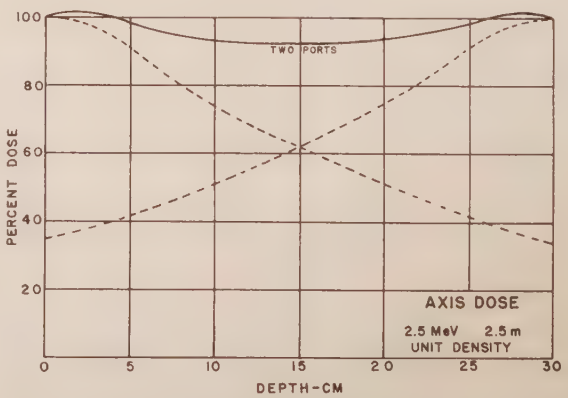

Fig. 3. On-axis depth dose in a unit density phantom. Effect of two entrance ports.

Biological effects of radiation appear to be independent of dose-rate over a wide range, but there may be a change in RBE at very low rates, below perhaps 1 r per minute. The

[2]) W. A. Higinbotham and S. Rankowitz, Rev. Sci. Inst. 22 (1951) 688–690.

obvious interpretation of this is that some repair mechanism becomes inoperative at the higher rates. At low dose rates irradiation times become long and gamma ray sources may be more satisfactory than accelerator-produced photons. A low dose rate does not, of course, obviate the need for maintaining uniform field conditions and a satisfactory depth dose distribution.

At exceedingly high dose rates some change in radiation effectiveness might be anticipated because of the overlapping of radiation products from adjacent ionization tracks. The dose rate at which this effect becomes appreciable is not known but it must be high because of the fleeting nature of the primary products. Mortality statistics from mice receiving pulsed X rays at 20 000 r per minute in the pulses were identical with those from mice receiving 200 r per minute. It is also known that the oxidation of ferrous sulphate solution shows no dose rate effect up to 10^{10} rad per second. It appears then that the dose rates needed to obtain overlapping can only be attained by direct irradiation with charged particles. Even in high energy pulses photon dose rates are some orders of magnitude too low to show any demonstrable effects due to overlapping.

Biological uses of charged-particle beams are increasing, but because of their penetration characteristics rather than their inherently high dose rate. This interest in particle beams is new and the extent of their usefulness is yet to be evaluated.

Proton beams, accelerated to energies of 100 MeV or more, have been used for ablating sharply defined portions of the central nervous system. The high energy provides sufficient penetration and the mass of the proton is sufficient to keep scatter low. For some purposes, the needle-sharp beams that can be achieved with protons or other heavy particles are most useful, but in other cases the very sharpness may be a drawback rather than an asset. If, for example, an infiltrating, expanding neoplasm is to be destroyed, total destruction must be obtained if regrowth is to be prevented. Exact knowledge of the extent of the neoplasm and its invasive processes is seldom available and a sharply defined beam may miss some of the malignant tissue. A more diffuse, scattered beam such as is obtained with electrons may well give better results in such situations.

Extremely high-energy, penetrating beams of electrons have been little used in biology and medicine, chiefly because few medical institutions have the necessary high-voltage accelerators. Experience with electron beams of 2–6 MeV is more extensive. The low penetration of such beams restricts their use to relatively superficial lesions which in some cases respond in dramatic fashion.

The potentialities of electron beam therapy are not completely known at present and more work is urgently needed. Three distinct methods for obtaining uniform fields are now in use. Electron scattering at some distance from the patient with field limitation by coning has been used for several years with good clinical results. Considerable work has been done with a linearly scanned beam which provides essentially monoenergetic electrons. More recently electron therapy has been carried out with a scattered beam sprayed into the treatment room at a distance of several feet from the patient.

Whatever the treatment method, it appears that machine-produced electrons are to be preferred to those obtained from radioactive isotopes, particularly if large areas of the body are to be treated. There are problems associated with electron beam therapy which have only been partially solved and an accelerator ideally suited for this work is not available. Improvements in electron-beam dosimetry are also needed if administered doses are to be properly characterized.

Serious biological consequences can follow an overdose of electrons, and great care must be taken to see that the desired dose is not exceeded. Beam controls, both on voltage and current, are highly desirable, and present methods leave something to be desired. Even in simpler electrical systems, the high-speed control of currents well below 1 microampere presents

some difficulties and these difficulties are increased when control of a high-energy beam is required.

The problems involved in developing an ideal accelerator for biological use become compounded since most machines must perform several functions. Few, if any, institutions can afford separate machines for each duty and so any equipment represents a compromise. Presently available accelerators are reliable and versatile but better equipment for biological applications can be built. It would be presumptuous to suggest design details, but perhaps not out of place to list some of the basic requirements in an ideal accelerator for biology and medicine. No distinction is made between a machine to be used for treatment, and one intended for research in radiolbiology.

Any list of desirable features may contain some inconsistencies or incompatabilities and no attempt is made here to resolve them. Thus a compromise must be made between flexibility and simplicity of operation, and no single machine can satisfy both extremes.

1. Voltage variable and capable of stabilization at any value from 1–6 MV.
2. Maximum beam current 5 mA.
3. Beam-current stabilization at any value from 10^{-9} amp. to maximum.
4. Preset X-ray dose integrator.
5. Beam focus and beam controls.
6. Two acceleration tubes, one for X-rays and one for electrons.
7. Provision for pulsed or continuous operation.
8. High-speed over-current protection.
9. Linear 24-inch scan on electron beam.
10. Trunnion-mounting for beam alignment.

A few comments on these requirements are in order. The upper limit of 6 MV is not set as a limit of desirability. It is, rather, what is probably the upper limit for a single machine. If only a single machine can be procured, one in the 1–6 MV range seems most useful. The double capability, photons and electrons, seems inevitable with the increasing demands for radiation-sterilization and processing. The requirement for two acceleration tubes is an important one. This feature permits a rapid change from photons to electrons,and equally important, permits pulsed operation over a wide range of conditions with a constant load on the generator. By properly dividing the load between the two tubes pulses can be delivered without changing the operating voltage of the machine.

No requirement for positive-ion operation was listed because it seems outside the efficient capability of a single machine. Even if an accelerator design permits polarity conversion, the process will probably be too complicated for routine operations, and so a separate positive-ion source will be required.

The positive-ion machines capable of producing beams of 100 MeV or more are expensive and highly specialized, and it seems unlikely that they will become generalyl available in the near future. An accelerator capable of providing a positive-ion beam of a few MeV energy is a most valuable adjunct to a biological laboratory. With such a machine, neutrons become available as bombarding particles, tracing experiments with short-lived isotopes become possible, and activation analyses can be done with prompt assays of induced activity. Few positive-ion machines are available primarily for biological use and the full capabilities in this field have not been determined.

Any list of desirable features, such as the one presented, comes primarily from personal experience, and it seems improbable that many will agree completely with it. It is even more improbable that a machine having all of the listed features will ever be built. However, some common factors may appear on a broad survey of requirements and these common factors may guide future designs toward more biologically useful machines.

NUCLEAR INSTRUMENTS AND METHODS 6 (1960) 101–102; NORTH-HOLLAND PUBLISHING CO.

LETTER TO THE EDITOR

STATISTICAL ERRORS IN PARTICLE POLARIZATION MEASUREMENTS

EDWARD J. BURGE

Wheatstone Laboratory, King's College, London

Received 22 August 1959

The accuracy of measurements of the polarizations of beams of particles, in double and triple scattering experiments, is limited in part by the low statistical weights associated with low beam intensities. It is common practice in double scattering experiments to locate counters in a scattering plane, containing the incident and scattered beams, which is perpendicular to the plane of polarization of the incident beam. For this arrangement the left-right asymmetry is a maximum and leads to the relation $P_1P_2 = (L - R)/(L + R)$ where P_1 is the polarization of the incident beam, P_2 is the polarization of an initially unpolarized beam after scattering from the second target, and L and R are the numbers scattered to left and right at the same scattering angle, θ.

If ϕ is the azimuthal angle between the plane of scattering and the plane of polarization of the incident beam, the number scattered into a given infinitesimal solid angle is given by $N = N_0 (1 + P_1P_2 \cos \phi)$, where N_0 is the number scattered under the same conditions when the incident beam is unpolarized. It will be shown that the fractional error in P_1P_2 depends markedly on the range of the angle ϕ accepted, for a given θ, and a range of $\phi = \pm 20°$ is suggested as a useful maximum.

From the equation for N given above, it can be shown that $(L - R)/(L + R) = (P \sin \phi)/\phi = P'$ where L and R now refer to the numbers scattered to left and right in a range from $-\phi$ to $+\phi$. The value of P' reduces to P for the small values of ϕ usually employed. The fractional error in P is clearly equal to the fractional error in P'. Let T be the total number scattered at an angle θ, i.e. for $\phi = 0 \to 2\pi$. Then the fractional error in P' (or P) is given by

$$f = \frac{1}{T^{\frac{1}{2}}} \left(\frac{\pi}{2\phi}\right)^{\frac{1}{2}} \left\{\frac{[1 + (P \sin \phi)^2/\phi^2]}{[P (\sin \phi)/\phi]^2}\right\}^{\frac{1}{2}}.$$

A plot of $fT^{\frac{1}{2}}$ as a function of ϕ for four values of P is shown in the figure. For $T =$ 10 000 counts the ordinates give the precentage errors directly.

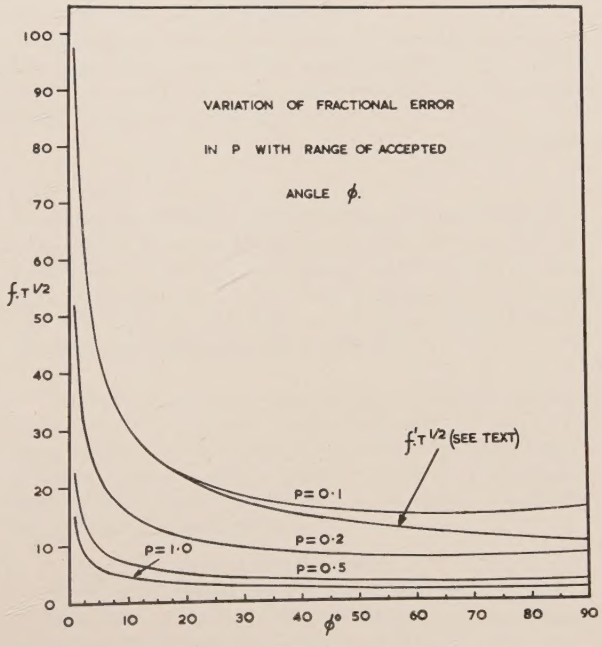

Fig. 1

The major contribution to the rapid decrease of f with ϕ, for small values of ϕ, arises simply from the increased numbers of particles counted. At larger values of ϕ this is offset by the decre-

asing asymmetry as ϕ approaches $\frac{1}{2}\pi$ and $\frac{3}{2}\pi$. The two contributions can be separated by calculating $fT^{\frac{1}{2}}$ for the hypothetical distribution $N = N_0 (N + P)$ for $\phi = -\frac{1}{2}\pi$ to $\frac{1}{2}\pi$ and $N = N_0 (1 - P)$ for $\phi = \frac{1}{2}\pi$ to $\frac{3}{2}\pi$. For comparison this is also plotted in the figure for $P = 0.1$, and labelled $f'T^{\frac{1}{2}}$. It can be easily shown that

$$f'T^{\frac{1}{2}} = (\pi/2\phi)^{\frac{1}{2}} [(1 + P^2)/P^2]^{\frac{1}{2}} .$$

Some practical difficulties may be encountered in using such a large range of ϕ. The target would need to be designed to avoid distortion of the $(1 + P_1P_2 \cos \phi)$ distribution over the range of ϕ used, otherwise uncertain corrections in the factor $(\sin \phi)/\phi$ might arise. If scintillation counters are used the ideal size and shape could be prohibitive. However, a compromise between the definition of θ and the range of ϕ would be possible. For a wide range of θ it would be inconvenient to use the ideal shape for each θ, and for forward angles the simplest arrangement would be to traverse the counters parallel to the incident beam. Most of these difficulties with counters could be easily overcome in experiments using nuclear emulsion detectors by choosing suitable acceptance criteria during scanning. Background could also be allowed for with greater certainty.

These calculations were originally made in connection with an experiment very similar to that of Feld and Maglić (1959)[1]), in which interactions with the nuclei in nuclear emulsions are used to measure the polarization of a beam of 150 MeV protons.

[1]) B. T. Feld and B. C. Maglić, Phys. Rev. Letters 1 (1958) 375.

BOOK REVIEWS

Energy levels of light Nuclei VI. F. AJZENBERG-SELOVE and T. LAURITSEN. North-Holland Publishing Co. 20 guilders.

This volume is a reprint from Nuclear Physics 11 (1959) pages 1–340. It is the sixth in a series of compilations summarizing information on nuclear energy levels from He^5 to Ne^{24}. The five precedent compilations were all published in Reviews of Modern Physics between 1948 and 1955. These papers are well known as the standard reference works in this field. The present extensive review has brought the compilation of data up to date and replaces the earlier articles. It contains complete information on experimental data for about 70 nucleids. There are more than 2000 references.

It is unnecessary to recommend this reprint to those who work in this field.

T. R. GERHOLM

Handbuch der Physik – Encyclopedia of Physics, (Editor S. FLÜGGE) Vol. 38-2. Springer-Verlag (Berlin-Göttingen-Heidelberg, 1959) 868 pages. Price DM 178: (Subscription DM 142.40).

The thirty-eighth volume, part two, of the Encyclopedia of Physics has now appeared under the title "Neutron and related Gamma Ray Problems". The section on neutron physics ("The production and slowing down of neutrons") occupies the major part of the volume, 659 out of the 817 pages of text. For this section the publisher has succeeded in securing the cooperation of a man, whose name is closely linked with neutron physics form its very early days, Edoardo Amaldi.

In his introductory chapter, Amaldi elucidates the description of the neutron as a fundamental particle with a very initiated historical account without thereby obscuring the most recent theories and results.

The second chapter is a systematic treatment of nuclear reactions accompanied by the emission of neutrons. The theoretical conditions for neutron emission are outlined, after which specific reactions are treated, with emphasis on those of practical importance. Here the work has a clearly encyclopedic character and should be of great value to anyone confronted with practical neutron source problems.

The following two chapters are devoted to the slowing down of neutrons. The presentation is the most logical one, which, for practical reasons, is rarely given in text-books on reactor physics, namely the one starting with the fundamental Boltzmann equation and working its way down to the various approximations. The slowing down of neutrons in the "chemical" region, i.e. with energies less than or of the order of one electron volt, is treated separately and in detail.

The last chapter deals with the diffusion of thermal neutrons. The author describes the elementary diffusion theory, which is subsequently identified with the P_1-approximation to transport theory. The methods of higher order transport theory approximations are discussed. A survey of experimental techniques for measuring diffusion parameters concludes the chapter.

It is commendable that, in spite of the fundamental approach, Amaldi in his nomenclature conforms to what might be called nuclear engineering practice. Thus, although the work is perhaps not suitable as an introductory text, it is extremely readable also for persons, whose interests lie on the practical side.

The second section of the volume, by U. Fano, L. V. Spencer and M. J. Berger, bears the title "Penetration and Diffusion of X-rays". (The term "X-rays" is understood to cover any electromagnetic radiation of energy higher than that of ultraviolet light.) There are several motivations for bringing the two sections together in the same volume, the primary one being the coupling that has long existed between the theories of X-ray and neutron diffusion. Further, the two sections may have equal bearings on the work of at least one category of scientists, namely those concerned with shielding problems.

Throughout the entire volume the theoretical presentations are interwoven with experimental results, which gives the reader a clear understanding of the present status of any one problem.

E. SOKOLOWSKI

Handbuch der Physik – Encyclopedia of Physics, (Herausgegeben von S. FLÜGGE. Mitherausgeber E. CREUTZ), Vol. 44, *Instrumentelle Hilfsmittel der KernphysikI.* Mit 225 Figuren. VIII, 473 Seiten Gr. — 8°. 1959. Ladenpreis: Ganzleinen DM 125. (Bei Verpflichtung zur Abnahme des ges. Handbuches Subskriptionspreis Gln. DM 100.—).

The latest volume of Handbuch der Physik has been given the title "Nuclear Instrumentation I" but could more adequately have been called Accelerator Techniques. It contains eight separate sections written by wellknown experts, each section treating in great detail one special type of particle accelerator.

E. Baldinger: Kaskadengeneratoren.

Raymond G. Herb: Van de Graaff Generators.

Bernard L. Cohen: Cyclotrons and Synchrocyclotrons.

Robert R. Wilson: Electron Synchrotrons.

Donald W. Kerst: The Betatron.

George Kenneth Green and Earnest D. Courant: The Proton Synchrotron.

Lloyd Smith: Linear Accelerators.

Donald James Hughes: Reactor Techniques (The reactor as a neutron source).

Each chapter is well illustrated and contains a comprehensive bibliography. The contributions were written at the end of 1957 which means that some of the most recent

achievements are not incorporated as for instance the development of the tandem Van de Graaff machines, which are only mentioned as a future possibility. B. Cohen's article on cyclotrons and synchrocyclotrons may be mentioned here in order to illustrate the range of information covered in the survey articles. It first contains a theoretical description of problems concerned with orbit stability, magnetic focussing and electric focussing effects. Some detailed discussion is concerned with the AVF-cyclotron (azimuthally varying field cyclotron) which is considered to be the most promising line of development of the cyclotron technique. The phase relations in conventional cyclotrons and in synchrocyclotrons are discussed as well as the initial motion of the ions near the ion source, a problem which is closely related to the sharp phase bunching of the beam. In the second part of Cohen's article the different components of a cyclotron are described. Magnets, radio-frequency systems, ion sources, beam deflection systems and targets are discussed without going too much into the details of construction.

A table showing operational data of existing cyclotrons and synchrocyclotrons is presented at the end of the article.

The book will be of great interest to all those who want to penetrate into calculations on a special type of accelerator or need information on recent development in accelerator techniques.

K. G. MALMFORS

SANBORN C. BROWN: *Basic Data of Plasma Physics*. The Technology Press of MIT and John Wiley and Sons, Inc. $ 6.50.

The research worker in the field of plasma physics needs a great number of basic data, such as cross sections for various types of collisions, Townsend coefficient, etc. However, the tremendous work done during several decades in this field is scattered among many papers in the litterature, and it is often quite difficult to find what one needs, expecially since now and then experiments are performed, showing that some cross sections are functions of the measuring apparatus. This is e.g. the case for many measurements of elastic collisions between ions and gas atoms.

Although earlier collections of cross section data have been found in e.g. the physical chemical tables by Landolt-Börnstein and in Electronic and Ionic Impact Phenomena by Massey and Burhop, the present contribution to these data collections is unique, most welcome and indeed needed, partly because so many improved measurements are made during the last few years. The Electronics Research Laboratory at MIT has in this respect made extremely important contributions by means of their most refined microwave technique, largely thanks to Professor Brown himself.

The present volume is a continuation in book form of the previously published MIT Research Laboratory of Electronics technical reports on Basic Data of Electrical Discharges. It cannot replace, but may serve as an excellent compliment to an ordinary text book on plasma physics or electrical discharges, and it is invaluable as a reference book for the research worker, mainly because it is not merely a collection of data but it also describes various methods of measurements and discusses their reliability.

The first two chapters deal more exclusively with various types of elastic cross sections. Then there is a chapter on diffusion and mobility. Probability data for inelastic collisions are then given, so that the first Townsend coefficient as a function of E/p can be presented. After, that various types of break down mechanisms are described, and this also requires data on electron attachment and secondary electron emission to be given. The book concludes with four chapters on corona-, glow-, microwave- and arc-discharges which in an excellent way give the physical essentials of the discharge mechanisms. As examples of the many characteristic discharge data given in these chapters we may mention normal cathode falls and thicknesses as functions of gas and cathode material, electron and gas temperatures etc.

The book was prepared for a summer course at MIT in 1959 on plasma dynamics and this is logically reflected in the disposition of the book. It contains very much instructive and important information and is of very high standard.

LARS BLOCK

ERRATUM

Arieh Fischmann Arbel, Precision Schmitt Trigger

Nuclear Instruments, Vol. 5, No. 1 (1959) p. 56

(1) page 57, second column, first line:

"... D_2 is conducting and no additional output is obtained..."

(2) page 60, second column, first line:

"...may be found by equalling the total voltage across R_{L1} owing to $i_1 + \Delta i$ to the corresponding total voltage across R_3, R_{L2} and r_{p3} owing to $i_2 - \Delta i$.